2

The
PHILOSOPHICAL
MAGAZINE

FIRST PUBLISHED IN 1798

UNIVERSITY OF HAWAII
LIBRARY
APR 21 '54

. 45 SEVENTH SERIES No. 360 January 1954

A Journal of
Theoretical Experimental
and Applied Physics

EDITOR
PROFESSOR N. F. MOTT, M.A., D.Sc., F.R.S.

EDITORIAL BOARD
SIR LAWRENCE BRAGG, O.B.E., M.C., M.A., D.Sc., F.R.S.
SIR GEORGE THOMSON, M.A., D.Sc., F.R.S.
PROFESSOR A. M. TYNDALL, C.B.E., D.Sc., F.R.S.

PRICE 15s. 0d.
Annual Subscription £8 0s. 0d. payable in advance

AND PUBLISHED BY TAYLOR & FRANCIS LTD., RED LION COURT, FLEET ST., LONDON, E.C.4.

ALERE FLAMMAM

THE MATHEMATICAL WORKS OF JOHN WALLIS, D.D., F.R.S.

by

J. F. SCOTT, Ph.D., B.A.

"His work will be indispensable to those interested in the early history of The Royal Society. I commend to all students of the Seventeenth Century, whether scientific or humane, this learned and lucid book."—Extract from foreword by Prof. E. N. da C. Andrade, D.Sc., Ph.D., F.R.S.

Recommended for publication by University of London

12/6 net

Printed and Published by

TAYLOR & FRANCIS, LTD.
RED LION COURT, FLEET STREET, LONDON, E.C.4.

DECADE 1941–50

We are requested by many of our clients overseas, to purchase on their behalf

PHILOSOPHICAL MAGAZINE

and all other important Scientific Journals for the years 1941–50 during which time, owing to war restrictions their supply was stopped.

YOUR OFFERS WILL BE APPRECIATED

Complete sets and longer runs also required by

THE SCIENTIFIC BOOK SUPPLY SERVICE
(T. FREDERICK DE LOCHE)
5 FETTER LANE, FLEET ST., LONDON, E.C.4.

All enquiries for Advertisements to:

ADVERTISEMENT MANAGER,
22a College Hill, Cannon Street,
London, E.C.4
Telephone: CITy 2381

THE
PHILOSOPHICAL MAGAZINE
A JOURNAL OF THEORETICAL EXPERIMENTAL
AND APPLIED PHYSICS
First published in 1798
[SEVENTH SERIES—VOL. 45]

I. *Boundary Layer Growth on a Spinning Body*

By C. R. Illingworth
Department of Mathematics, The University, Manchester *

[Received October 19, 1953]

Abstract

The skin frictional force is calculated for a body of revolution in the early stages of a suddenly initiated (and subsequently constant) screw motion about the axis of symmetry. In particular the effect of spin on the time of separation of the boundary layer of a sphere in such a motion is determined.

---

§ 1. Introduction

One question that naturally arises in considering the boundary layer of a body in a screw motion (i.e. moving forward in the direction of some axis and at the same time spinning about that axis) is : how does the spin influence the position of separation of the boundary layer ? Of course, one can immediately give a qualitative answer to this question. Since spin imparts a centrifugal acceleration to fluid elements near the surface of the body, it produces a favourable contribution to the pressure gradient upstream of the maximum section of the body and an adverse contribution to the gradient downstream of this section, so that the effect of increasing the spin is always to move the position of separation nearer to the maximum section of the body. To give a quantitative answer to the question when the flow is steady would require rather laborious although straightforward calculations involving the integration of a series of pairs of simultaneous ordinary differential equations of second and third order. It is easier to answer the question when the flow has just been started up, and the boundary layer is in the initial stages of its growth. These conditions are just those that apply to the initial motion of a projectile fired from a rifled projector. For one can suppose that at $t=0$, the moment of firing, the projectile, a body of revolution, is instantaneously given a forward velocity V and an angular velocity Ω. However, the speeds involved in this external ballistic problem are so high that compressibility effects would have to be taken into account in solving it. The problem that is investigated below is simpler than this: it is concerned with the case when V and Ω are sufficiently small for compressibility to be negligible. This type of investigation for a non-spinning body of revolution was originally carried out by Boltze (1908), and the present work is a simple extension of Boltze's.

---

* Communicated by M. J. Lighthill.

§ 2. BOUNDARY LAYER GROWTH FOR A GENERAL BODY OF REVOLUTION

The independent variables to be used are t, x and y, where t denotes time from the beginning of the motion, x distance from the nose of the body measured along a meridian curve whose orientation is fixed in space, and y distance along the normal to this curve. This means that the frame of reference moves forward with the body but does not rotate with it. The radius of the body at the station x will be denoted by $R(x)$. With u, v representing the x and y components of velocity, and w the transverse component due to the spin, the equations for incompressible flow in the boundary layer are

$$\frac{\partial}{\partial x}(Ru)+\frac{\partial}{\partial y}(Rv)=0, \quad \text{. . . . . (1)}$$

$$\frac{\partial u}{\partial t}+u\frac{\partial u}{\partial x}+v\frac{\partial u}{\partial y}-\frac{w^2}{R}\frac{dR}{dx}=U\frac{dU}{dx}+\nu\frac{\partial^2 u}{\partial y^2}, \quad \text{. . . (2)}$$

and

$$\frac{\partial w}{\partial t}+u\frac{\partial w}{\partial x}+v\frac{\partial w}{\partial y}+\frac{uw}{R}\frac{dR}{dx}=\nu\frac{\partial^2 w}{\partial y^2}, \quad \text{. . . . . . . (3)}$$

where $U(x)$ is the velocity of the main stream, and ν is the kinematic viscosity of the fluid.

It is supposed that the fluid motion is caused by suddenly starting the body to move at $t=0$ with constant linear velocity V in the direction of its axis and with constant angular velocity Ω about its axis. The quantity $U(x)$ is therefore the velocity the main stream would have at the station x if the body were fixed in a flow of constant velocity V. As Goldstein and Rosenhead (1936) explain in discussing boundary layer growth on a cylinder, the boundary layer is initially a vortex sheet which begins to thicken because of diffusion. Since the boundary layer growth is essentially a process of diffusion, the convection terms and the pressure gradient $U\,dU/dx$ can be neglected in (2) and (3) in the first place. Hence the first approximations u_1, v_1, w_1 to the velocity components satisfy

$$\frac{\partial}{\partial x}(Ru_1)+\frac{\partial}{\partial y}(Rv_1)=0, \quad \text{. . . . . (4)}$$

$$\frac{\partial u_1}{\partial t}=\nu\frac{\partial^2 u_1}{\partial y^2}, \quad \text{. . . . . . . (5)}$$

$$\frac{\partial w_1}{\partial t}=\nu\frac{\partial^2 w_1}{\partial y^2}. \quad \text{. . . . . . . (6)}$$

The required solutions of (5) and (6) are

$$u_1=UE, \tag{7}$$

$$w_1=\Omega R(1-E), \tag{8}$$

where $E=\operatorname{erf}\eta=2\alpha\int_0^\eta e^{-z^2}\,dz$, $\alpha=\pi^{-1/2}$ and $\eta=y/2(\nu t)^{1/2}$.

These satisfy $u_1=0$, $w_1=\Omega R$ at $y=0$, $t>0$ and $u_1=U$, $w_1=0$ for large values of y. From (4),

$$v_1=-2(\nu t)^{1/2}\frac{1}{R}\frac{d}{dx}(RU)F, \tag{9}$$

where $F=\int_0^\eta E(z)\,dz=\eta E-\alpha(1-e^{-\eta^2})$. Actually, (9) is not an entirely satisfactory expression for v_1 because it behaves like $-y\dfrac{1}{R}\dfrac{d}{dx}(RU)$ for large η instead of becoming very small. However, u_1 is practically equal to U and w_1 practically equal to 0 at moderate values of η, for which $v_1=O[(\nu t)^{1/2}]$.

The second approximate expressions for the velocity components are u_1+u_2, v_1+v_2, w_1+w_2, where u_2, v_2, w_2 satisfy

$$\frac{\partial}{\partial x}(Ru_2)+\frac{\partial}{\partial y}(Rv_2)=0, \tag{10}$$

$$\nu\frac{\partial^2 u_2}{\partial y^2}-\frac{\partial u_2}{\partial t}=u_1\frac{\partial u_1}{\partial x}+v_1\frac{\partial u_1}{\partial y}-\frac{w_1{}^2}{R}\frac{dR}{dx}-U\frac{dU}{dx}, \tag{11}$$

and

$$\nu\frac{\partial^2 w_2}{\partial y^2}-\frac{\partial w_2}{\partial t}=u_1\frac{\partial w_1}{\partial x}+v_1\frac{\partial w_1}{\partial y}+\frac{u_1w_1}{R}\frac{dR}{dx}. \tag{12}$$

The solutions of (11) and (12) may be written as

$$u_2=t\left(U\frac{dU}{dx}f_{21}+\frac{U^2}{R}\frac{dR}{dx}f_{22}+\Omega^2R\frac{dR}{dx}f_{23}\right),$$

$$w_2=t\left(\Omega R\frac{dU}{dx}g_{21}+\Omega U\frac{dR}{dx}g_{22}\right),$$

in which f_{2i}, g_{2i} are functions of η satisfying

$$\left.\begin{aligned} f_{2i}''+2\eta f_{2i}'-4f_{2i}&=4s_{2i},\\ f_{2i}(0)=f_{2i}(\infty)&=0,\end{aligned}\right\} \tag{13}$$

$$\left.\begin{aligned} g_{2i}''+2\eta g_{2i}'-4g_{2i}&=4t_{2i},\\ g_{2i}(0)=g_{2i}(\infty)&=0.\end{aligned}\right\} \tag{14}$$

Here dashes denote differentiation with respect to η, and

$$s_{21}=E^2-E'F-1,$$

$$s_{22}=-E'F,$$

$$s_{23}=-(1-E)^2,$$

and

$$t_{21}=E'F,$$

$$t_{22}=2E(1-E)+E'F.$$

Now, the two independent functions occurring in the complementary functions of eqns. (13) and (14) are

and

$$\left.\begin{aligned} j&=1+2\eta^2, \\ k&=(1+2\eta^2)E+\eta E'. \end{aligned}\right\} \quad . \ . \ . \ . \ . \ . \ . \ . \quad (15)$$

Also it is easy to verify that the particular integrals corresponding to the terms $1-E$, $(1-E)^2$ and $E'F$, of which the s_{2i} and t_{2i} are linear combinations, are respectively

$$\left.\begin{aligned} l&=E-1, \\ m&=2\eta^2E^2+2\eta EE'+\tfrac{1}{2}E'^2+2E-1, \\ n&=(\eta^2+\tfrac{1}{2})E^2+\tfrac{1}{2}\eta EE'+\tfrac{2}{3}\alpha E'. \end{aligned}\right\} \quad . \ . \ . \ . \ . \quad (16)$$

It follows that

$$\left.\begin{aligned} f_{21}&=-(1+\tfrac{2}{3}\alpha^2)j+(\tfrac{1}{2}+\tfrac{2}{3}\alpha^2)k-2l+m-n, \\ f_{22}&=\tfrac{4}{3}\alpha^2j+(\tfrac{1}{2}-\tfrac{4}{3}\alpha^2)k-n, \\ f_{23}&=-(1-2\alpha^2)j+(2-2\alpha^2)k-m, \\ &\text{and} \\ g_{21}&=-\tfrac{4}{3}\alpha^2j-(\tfrac{1}{2}-\tfrac{4}{3}\alpha^2)k+n, \\ g_{22}&=\tfrac{8}{3}\alpha^2j+(\tfrac{3}{2}-\tfrac{8}{3}\alpha^2)k+2l-2m+n. \end{aligned}\right\} \quad . \ . \ . \ . \quad (17)$$

Finally, from (10) we find

$$v_2=-2\nu^{1/2}t^{3/2}\left[U\frac{d^2U}{dx^2}h_{21}+\left(\frac{dU}{dx}\right)^2h_{21}+U\frac{dU}{dx}\frac{1}{R}\frac{dR}{dx}(h_{21}+2h_{22})\right.$$
$$\left.+U^2\frac{1}{R}\frac{d^2R}{dx^2}h_{22}+\Omega^2R\frac{d^2R}{dx^2}h_{23}+2\Omega^2\left(\frac{dR}{dx}\right)^2h_{23}\right],$$

where $h_{2i}(\eta)=\int_0^\eta f_{2i}(z)\,dz$.

In the third approximation (the last one we shall consider) the velocity components are $u_1+u_2+u_3$, $v_1+v_2+v_3$, $w_1+w_2+w_3$, where u_3 and w_3 satisfy

$$\nu\frac{\partial^2u_3}{\partial y^2}-\frac{\partial u_3}{\partial t}=u_1\frac{\partial u_2}{\partial x}+u_2\frac{\partial u_1}{\partial x}+v_1\frac{\partial u_2}{\partial y}+v_2\frac{\partial u_1}{\partial y}-2\frac{w_1w_2}{R}\frac{dR}{dx}, \quad . \ . \quad (18)$$

$$\nu\frac{\partial^2w_3}{\partial y^2}-\frac{\partial w_3}{\partial t}=u_1\frac{\partial w_2}{\partial x}+u_2\frac{\partial w_1}{\partial x}+v_1\frac{\partial w_2}{\partial y}+v_2\frac{\partial w_1}{\partial y}+\frac{u_1w_2+u_2w_1}{R}\frac{dR}{dx}. \quad (19)$$

The solutions of (18) and (19) are

$$u_3=t^2\left[U^2\frac{d^2U}{dx^2}f_{31}+U\left(\frac{dU}{dx}\right)^2f_{32}+U^2\frac{dU}{dx}\frac{1}{R}\frac{dR}{dx}f_{33}+U^3\frac{1}{R}\frac{d^2R}{dx^2}f_{34}\right.$$
$$\left.+U^3\frac{1}{R^2}\left(\frac{dR}{dx}\right)^2f_{35}+\Omega^2\frac{dU}{dx}R\frac{dR}{dx}f_{36}+\Omega^2UR\frac{d^2R}{dx^2}f_{37}+\Omega^2U\left(\frac{dR}{dx}\right)^2f_{38}\right],$$

$$w_3=t^2\left[\Omega U\frac{d^2U}{dx^2}Rg_{31}+\Omega\left(\frac{dU}{dx}\right)^2Rg_{32}+\Omega U\frac{dU}{dx}\frac{dR}{dx}g_{33}+\Omega U^2\frac{d^2R}{dx^2}g_{34}\right.$$
$$\left.+\Omega U^2\frac{1}{R}\left(\frac{dR}{dx}\right)^2g_{35}+\Omega^3R^2\frac{d^2R}{dx^2}g_{36}+\Omega^3R\left(\frac{dR}{dx}\right)^2g_{37}\right],$$

where

$$\left.\begin{aligned}f_{3i}''+2\eta f_{3i}'-8f_{3i}&=4s_{3i},\\ f_{3i}(0)=f_{3i}(\infty)&=0,\end{aligned}\right\}\quad\dots\dots\quad(20)$$

$$\left.\begin{aligned}g_{3i}''+2\eta g_{3i}'-8g_{3i}&=4t_{3i},\\ g_{3i}(0)=g_{3i}(\infty)&=0,\end{aligned}\right\}\quad\dots\dots\quad(21)$$

in which

$s_{31}=Ef_{21}-E'h_{21},$
$s_{32}=2Ef_{21}-Ff_{21}'-E'h_{21},$
$s_{33}=3Ef_{22}-F(f_{21}'+f_{22}')-E'(h_{21}+2h_{22}),$
$s_{34}=Ef_{22}-E'h_{22},$
$s_{35}=-Ef_{22}-Ff_{22}',$
$s_{36}=Ef_{23}-Ff_{23}'-2(1-E)g_{21},$
$s_{37}=Ef_{23}-E'h_{23},$
$s_{38}=Ef_{23}-Ff_{23}'-2E'h_{23}-2(1-E)g_{22},$

and

$t_{31}=Eg_{21}+E'h_{21},$
$t_{32}=-Fg_{21}'+E'h_{21},$
$t_{33}=2(1-E)f_{21}+E(2g_{21}+g_{22})-F(g_{21}'+g_{22}')+E'(h_{21}+2h_{22}),$
$t_{34}=Eg_{22}+E'h_{22},$
$t_{35}=2(1-E)f_{22}+Eg_{22}-Fg_{22}',$
$t_{36}=E'h_{23},$
$t_{37}=2(1-E)f_{23}+2E'h_{23}.$

The complementary functions of (20) and (21) contain the functions $p=3+12\eta^2+4\eta^4$ and $q=(3+12\eta^2+4\eta^4)E+(5\eta+2\eta^3)E'$, and so the solution of (20) is

$$f_{3i}=\frac{1}{12\alpha}\left[q\left\{\int_0^\infty e^{z^2}q(z)s_{3i}(z)\,dz-\int_\eta^\infty e^{z^2}p(z)s_{3i}(z)\,dz\right\}-p\int_0^\eta e^{z^2}q(z)s_{3i}(z)\,dz\right].$$

The corresponding formula for g_{3i} is obtained by substituting t_{3i} for s_{3i}. It would be rather laborious to evaluate the integrals involved in these expressions for f_{3i} and g_{3i}. However, we can determine the skin friction at the surface of the body with much less effort. For the longitudinal and transverse components of skin friction are given by

$$\tau_x=\mu\left(\frac{\partial u}{\partial y}\right)_{y=0}=\frac{1}{2}\left(\frac{\mu\rho}{t}\right)^{1/2}\left(\frac{\partial u}{\partial\eta}\right)_{\eta=0},$$

and
$$\tau_z=-\mu\left(\frac{\partial w}{\partial y}\right)_{y=0}=-\frac{1}{2}\left(\frac{\mu\rho}{t}\right)^{1/2}\left(\frac{\partial w}{\partial\eta}\right)_{\eta=0},$$

where μ, ρ are the viscosity and density of the fluid respectively. Clearly one does not need $f_{3i}(\eta)$, $g_{3i}(\eta)$ but only $f_{3i}'(0)$, $g_{3i}'(0)$ in order to obtain the skin friction. Now,

$$f_{3i}'(0)=G(s_{3i}),$$

$$g_{3i}'(0)=G(t_{3i}),$$

where

$$G(\phi)=\frac{4}{3}\int_0^\infty e^{z^2}\{q(z)-p(z)\}\phi(z)dz.$$

Since s_{3i} and t_{3i} are linear combinations of terms of the types f_{2i}, g_{2i}, Ef_{2i}, Eg_{2i}, Ff_{2i}', Fg_{2i}', $E'h_{2i}$, it is convenient to evaluate $G(f_{2i})$ etc. From these quantities we easily obtain :—

$$f_{31}'(0)=-\frac{7}{6}\alpha+\left(-\frac{11}{15}+\frac{9}{5}\sqrt{3}\right)\alpha^3+\frac{128}{45}\alpha^5,$$

$$f_{32}'(0)=\frac{11}{6}\alpha+\left(\frac{89}{15}-\frac{36}{5}\sqrt{3}\right)\alpha^3-\frac{256}{135}\alpha^5,$$

$$f_{33}'(0)=\frac{7}{6}\alpha+\left(-\frac{193}{9}+\frac{63}{5}\sqrt{3}\right)\alpha^3-\frac{1792}{135}\alpha^5,$$

$$f_{34}'(0)=-\frac{2}{9}\alpha+\left(\frac{154}{45}-\frac{3}{5}\sqrt{3}\right)\alpha^3-\frac{256}{45}\alpha^5,$$

$$f_{35}'(0)=\left(-\frac{220}{9}+9\sqrt{3}\right)\alpha^3+\frac{256}{9}\alpha^5,$$

$$f_{36}'(0)=\frac{13}{3}\alpha+(-56+18\sqrt{3})\alpha^3+\frac{896}{27}\alpha^5,$$

$$f_{37}'(0)=-\frac{1}{18}\alpha+\left(7-\frac{12}{5}\sqrt{3}\right)\alpha^3-\frac{128}{15}\alpha^5,$$

$$f_{38}'(0)=\left(-\frac{370}{9}+\frac{126}{5}\sqrt{3}\right)\alpha^3-\frac{1664}{135}\alpha^5,$$

and

$$g_{31}'(0)=\frac{23}{18}\alpha+\left(\frac{253}{45}-\frac{39}{5}\sqrt{3}\right)\alpha^3+\frac{512}{45}\alpha^5,$$

$$g_{32}'(0)=\frac{23}{18}\alpha+\left(\frac{451}{15}-\frac{84}{5}\sqrt{3}\right)\alpha^3-\frac{256}{15}\alpha^5,$$

$$g_{33}'(0)=\frac{1}{6}\alpha+\left(-\frac{491}{9}+\frac{117}{5}\sqrt{3}\right)\alpha^3+\frac{512}{35}\alpha^5,$$

$$g_{34}'(0)=2\alpha+\left(-\frac{914}{45}+\frac{63}{5}\sqrt{3}\right)\alpha^3-\frac{1024}{45}\alpha^5,$$

$$g_{35}'(0)=\frac{4}{3}\alpha+\left(-\frac{220}{3}+27\sqrt{3}\right)\alpha^3+\frac{1024}{27}\alpha^5,$$

$$g_{36}'(0)=\frac{35}{24}\alpha+\left(-\frac{57}{4}+\frac{63}{10}\sqrt{3}\right)\alpha^3-\frac{64}{15}\alpha^5,$$

$$g_{37}'(0)=\frac{13}{9}\alpha+\left(-\frac{58}{3}+\frac{24}{5}\sqrt{3}\right)\alpha^3+\frac{256}{15}\alpha^5.$$

Also, $E'(0)=2\alpha$ and, from (15), (16) and (17),

$$f_{21}'(0)=2\alpha+\frac{8}{3}\alpha^3,\qquad f_{22}'(0)=2\alpha-\frac{16}{3}\alpha^3,\qquad f_{23}'(0)=4\alpha-8\alpha^3,$$

and

$$g_{21}'(0)=-2\alpha+\frac{16}{3}\alpha^3,\qquad g_{22}'(0)=2\alpha-\frac{32}{3}\alpha^3.$$

We may now summarize our calculations in the following formulae for the skin friction components:—

$$\begin{aligned}\tau_x=0{\cdot}56419\left(\frac{\mu\rho}{t}\right)^{1/2}\Bigg[&U+\left\{1{\cdot}4244U\frac{dU}{dx}+0{\cdot}1512\frac{U^2}{R}\frac{dR}{dx}\right.\\&\left.+0{\cdot}72676\Omega^2R\frac{dR}{dx}\right\}t-\left\{0{\cdot}05975U^2\frac{d^2U}{dx^2}+0{\cdot}21987U\left(\frac{dU}{dx}\right)^2\right.\\&+0{\cdot}02876U^2\frac{dU}{dx}\frac{1}{R}\frac{dR}{dx}+0{\cdot}02005U^3\frac{1}{R}\frac{d^2R}{dx^2}-0{\cdot}03154U^3\frac{1}{R}\left(\frac{dR}{dx}\right)^2\\&+0{\cdot}102869\Omega^2\frac{dU}{dx}R\frac{dR}{dx}+0{\cdot}007592\Omega^2UR\frac{d^2R}{dx^2}\\&\left.+0{\cdot}220731\Omega^2U\left(\frac{dR}{dx}\right)^2\right\}t^2+\ldots\Bigg],\qquad(22)\end{aligned}$$

$$\begin{aligned}\tau_z=0{\cdot}56419\left(\frac{\mu\rho}{t}\right)^{1/2}\Bigg[&\Omega R+\left\{0{\cdot}1512\Omega R\frac{dU}{dx}+0{\cdot}6977\Omega U\frac{dR}{dx}\right\}t\\&+\left\{0{\cdot}0401\Omega U\frac{d^2U}{dx^2}R+0{\cdot}0716\Omega\left(\frac{dU}{dx}\right)^2R+1{\cdot}9568\Omega U\frac{dU}{dx}\frac{dR}{dx}\right.\\&-0{\cdot}0879\Omega U^2\frac{d^2R}{dx^2}+1{\cdot}6404\Omega U^2\frac{1}{R}\left(\frac{dR}{dx}\right)^2\\&\left.+0{\cdot}01826\Omega^3R^2\frac{d^2R}{dx^2}+0{\cdot}16698\Omega^3R\left(\frac{dR}{dx}\right)^2\right\}t^2+\ldots\Bigg].\qquad(23)\end{aligned}$$

§ 3. SKIN FRACTION ON A SPINNING SPHERE

We are now in a position to calculate from (22) and (23) the skin friction on any particular body of revolution. We choose the sphere as a convenient example. In the early stages of boundary layer growth, the velocity $U(x)$ must be the velocity of inviscid flow round the body concerned. Thus, for a sphere, $U(x)=\frac{3}{2}V\sin x/a$, where a is the radius of the sphere, this being the velocity at the surface in potential flow.

Also, $R(x)=a \sin x/a$. It follows that

$$\tau_x=0{\cdot}84628\left(\frac{\mu\rho}{t}\right)^{1/2} V \sin x/a[1+\{(2{\cdot}3634+0{\cdot}48451\beta)\cos x/a\}\xi$$
$$-\{-(0{\cdot}17955+0{\cdot}007592\beta)\sin^2 x/a$$
$$+(0{\cdot}48844+0{\cdot}323601\beta)\cos^2 x/a\}\xi^2+\ldots], \quad \ldots\ldots \quad (24)$$

and

$$\tau_z=0{\cdot}56419\left(\frac{\mu\rho}{t}\right)^{1/2} \Omega a \sin x/a[1+\{1{\cdot}2732 \cos x/a\}\xi$$
$$+\{(0{\cdot}1077-0{\cdot}01826\beta)\sin^2 x/a$$
$$+(8{\cdot}2548+0{\cdot}16698\beta)\cos^2 x/a\}\xi^2+\ldots], \quad \ldots\ldots \quad (25)$$

where $\beta=\Omega^2a^2/V^2$ and $\xi=Vt/a$.

The flow will separate from the surface along the circle of latitude at which $\tau_x=0$. If, in the first instance, we neglect the ξ^2 term in (24), we find that separation will first occur at $x=a\pi$, the rear stagnation point on the sphere, when

$$\xi=\xi_1=(2{\cdot}3634+0{\cdot}48451\beta)^{-1}.$$

Also, if we retain the ξ^2 term, we find that separation will still occur first at $x=a\pi$, when $\xi=\xi_2$, where ξ_2 is the positive root of

$$(0{\cdot}48844+0{\cdot}323601\beta)\xi^2+(2{\cdot}3634+0{\cdot}48451\beta)\xi-1=0.$$

Values of ξ_1 and ξ_2 for different β are as follows :—

β	ξ_1	ξ_2
0	0·423	0·391
0·1	0·415	0·383
1·0	0·351	0·322
10	0·139	0·130

The quantity ξ is of course the number of radii through which the sphere travels before separation, and, as separation occurs behind the maximum section of the sphere in this problem for a non-rotating sphere, we expect that it will occur sooner when spin is introduced. The table gives an indication of how much sooner for different values of the spin. It suggests too that the time of separation can be found to the second approximation, whatever the spin, by calculating it to the first approximation (ξ_1) and reducing the answer by about 7%. This does not mean that one can dispense with the quadratic terms in the series for τ_x and τ_z. Reference to (25) shows that the quadratic term in τ_z is of the same order of magnitude as the linear term when $\xi=\xi_1$.

REFERENCES

BOLTZE, E., 1908, *Göttingen Dissertation.*
GOLDSTEIN, S., and ROSENHEAD, L., 1936, *Proc. Camb. Phil. Soc.*, **32**, 392.

II. *On the Validity of Mott's Theory of the Beta-Flow in Polycrystals*

By Paul Feltham
Standard Telecommunication Laboratories, Enfield, Middlesex *

[Received November 3, 1953]

Summary

A survey is given of the experimental evidence about the activation energy for transient creep. It is concluded that, if the Andrade equation is written in the form $\epsilon^3 = At$, the dependence of A on stress and temperature is governed by the same constants as for steady state creep.

In a recent paper Mott (1953) proposed a statistical theory of the Andrade beta-flow. The theory postulates a hardening of the material during flow, in agreement with the ' lamellar break-down ' observed by Andrade (1914) in lead and subsequently studied by means of x-rays by Gibbs and Ramlal (1934) and other workers, and more recently by McLean (1953) in aluminium by optical means ; and, given this hardening, it is of a sufficiently general nature to be applicable to a wide range of crystalline and non-crystalline materials (e.g. celluloid, Jessop and Filon 1928) in which Andrade's relation between strain and the cube root of the time has been observed. The theory leads to the equation

$$\epsilon_{tr} = C\left(\frac{d\epsilon}{dt}t\right)^{1/3}, \qquad \qquad (1)$$

where C is a constant, independent of stress and temperature, ϵ_{tr} is the (transient) strain and $d\epsilon/dt$ the strain-rate of the steady, second-stage, flow.

The object of the present note is to present results of an investigation of the validity of this relation, based on data either published as such or derived from the flow-curves of a number of metals and alloys given in the literature.

From a detailed study of the flow under constant stress of high-purity copper (99·98%), aluminium (99·98%) and cadmium (99·99%), and of three grades of aluminium of commercial purity, all polycrystalline, in the temperature range −196° to 140°C, Wyatt (1953) concludes that at low temperatures the flow curves fitted

$$\epsilon_{tr} = \alpha \log t + c_1, \qquad \qquad (2)$$

and at higher temperatures

$$\epsilon_{tr} = \beta t^{1/3} + c_2, \qquad \qquad (3)$$

while in the intermediate range the curves fitted

$$\epsilon_{tr} = \alpha \log t + \beta t^{1/3} + c_3. \qquad \qquad (4)$$

The α-flow obeyed an equation of state

$$F(\sigma, \epsilon_\alpha, d\epsilon_\alpha/dt) = 0, \qquad \qquad (5)$$

---

* Communicated by the Author.

and was interpreted by him by an exhaustion mechanism ; the β-flow was related by him to a recovery process.

Although Wyatt did not specify the nature of this process, it appears to be associated with a capacity for inter-granular deformation, and β-flow practically free from the α-component would probably occur in metals only at temperatures (generally above about $\frac{1}{3}T_{\text{melt}}$ °K), and stresses outside the domain of ‘ equi-cohesion ’. The results for aluminium and magnesium at 20°C probably do not conform to these requirements ; they are given in the table alongside the remaining data for the sake of completeness.

The analysis upon which the determination of the results tabulated here was based depends on the assumption, verified experimentally in many cases (Novick and Machlin 1947, Fastov 1950, Johnson and Frost 1952, Feltham 1953, etc.) that the dependence on stress and temperature of the steady flow-rate can be represented by the formula

$$\frac{d\epsilon}{dt}=2A\exp(-H/kT)\sinh\left(\frac{q\sigma}{kT}\right), \quad \ldots\ldots \quad (6)$$

or, for stresses high enough to permit the replacement of $2\sinh(q\sigma/kT)$ by $\exp(q\sigma/kT)$, by

$$\frac{d\epsilon}{dt}=A\exp\left(\frac{-H+q\sigma}{kT}\right). \quad \ldots\ldots\ldots \quad (7)$$

Here σ is the applied tensile stress and A, H and q are constants. We write

$$-H+q\sigma=Q(\sigma) ;$$

in general, if the linear dependence of $\log\dot{\epsilon}$ on σ is not valid, we have

$$d\epsilon/dt=A\exp\{-Q(\sigma)/kT\}.$$

The validity of Mott's relation (eqn. (1)) then implies

$$\epsilon_{tr}=B\exp\{-Q_{tr}(\sigma)/kT\}t^m=\beta t^m, \quad \ldots\ldots \quad (8)$$

where

$$Q_{tr}/Q=H_{tr}/H=q_{tr}/q=m=\tfrac{1}{3}. \quad \ldots\ldots \quad (9)$$

With reference to the table, in which the above ratios and measured values of the exponent of time, m, are given for a number of pure metals and for some alloys, the following comments must be made :

(*a*) The assumption of the occurrence of stress fluctuations of random sign, of the type assumed by Mott in the derivation of eqn. (1), is probably nearest to the truth in the case of well annealed, pure polycrystals and homogeneous one-phase alloys. The results, given in the table, which relate to impure metals (i.e. steels) must therefore be accepted with reserve.

(*b*) According to Mott's theory the β-flow would be expected to go-over smoothly into the steady flow after a certain amount of hardening, determined by the magnitude of the stress and the temperature, has taken place. The transient part of the flow should therefore be the sole type of flow up to the point at which its rate becomes equal to that of the

Metal	Melting temp. °c	Flow temp. °c	m				Reference
			Experimental	Q_{tr}/Q	H_{tr}/H	q_{tr}/q	
Aluminium 99·995%	660	20	0·35–0·45	0·33–0·41	—	—	I
		150	0·50–0·55				
		200	0·18–0·65				
Al alloy RR 59	630	50–250	0·33	0·37	—	—	II
Copper 'pure'	1083	410	0·33	0·36	—	—	III
Lead 'pure'	327	17	0·33	0·37	—	—	III
Magnesium 99·8%	651	20	0·3	0·33–0·46	—	—	I
		150	0·42–0·45				
		200	0·75				
		270	0·39–0·85				
Iron (alpha) 'pure'	1535	444	0·33	0·36	—	—	III
Iron (gamma) 99·99%	1535	950–1270	0·33	—	≃ 0·5	≃ 0·7	IV
Steel, plain							
0·05%C	1530	950–1300	0·18–0·43	—	1·00	0·94	IV
0·23%C	1520	950–1350	0·33	—	0·42	0·38	V
0·44%C	1515	950–1300	0·26–0·44	—	0·45	0·53	IV
0·56%C	1510	950–1150	0·25–0·43	—	0·40	0·61	IV
0·79%C	1490	950–1220	0·39–0·65	—	0·48	0·53	IV
1·15%C	1475	950–1170	0·37–0·59	—	0·97	1·11	IV
Zinc 99·99%	419	20	—	0·42–0·63	—	—	I

I. Crussard 1946.
II. Johnson and Frost 1952. RR 59 contains from 1 to 2% each of Cu, Fe, Ni, Mg. Duration of tests up to 2000 hours.
III. Andrade 1914. Duration of tests : about half an hour.
IV. Feltham 1953 a. Duration of tests : one minute to one hour approximately.
V. Feltham 1953 b. Duration of tests : one minute to one hour approximately.

The 0·05%C steel was of the non-deoxidized basic open-hearth type ; the 0·79%C steel was a deoxidized acid open-hearth steel, the other steels were of the deoxidized basic open-hearth type.

steady flow. The initial, non-linear part of the flow should therefore be represented by eqn. (3) and not by the commonly adopted form

$$\epsilon=\epsilon_0+\beta t^{1/3}+\gamma t. \qquad \qquad (10)$$

In fact, if eqn. (10) is used, β sometimes appears to attain a constant 'saturation' value above a given stress, while γ continues to increase with stress. Now from eqns. (7), (8), (9):

$$\frac{\partial \log \beta/\partial\sigma}{\partial \log \gamma/\partial\sigma}=\frac{q_{tr}}{q}=m, \qquad \qquad (11)$$

and m could thus not remain constant if an increase in γ were not accompanied by a corresponding increase in β.

If β- and γ-values derived by Andrade (1914) for lead at 17°c, by the use of eqn. (10), are employed for the evaluation of m by means of eqn. (11), it is found to fall to zero at high stresses, while the measured exponent of the time maintains its value of approximately 1/3. However, if the total strain of the initial flow is plotted against $t^{1/3}$ (eqn. (3)), β-values are obtained which, substituted into (11), give a constant m-value of about 1/3 at all stresses used.

(*c*) Flow curves were not available for copper and alpha-iron, and consequently β and γ values determined only by means of (10) were available. The tabulated results for these metals were determined for stresses up to only 750 and 2150 kg/cm^2 respectively, for which the 'saturation' of β did not appear to have been attained.

(*d*) The measured m-values for aluminium and magnesium, given by Crussard (1946), are also based on the assumed validity of (10); the remaining results were obtained by the use of (3).

(*e*) The values of the parameters A, H and q (eqn. (6)) in the case of the aluminium alloy, determined by the method described by the author (Feltham 1953 a) from curves given in a paper by Johnson and Frost (1952), were found to be $A=0{\cdot}15$ per hour, $H=13{\cdot}9$ kcals/g atom, $q/k=2{\cdot}44$°K/kg/cm^2 which, except for the last, are different from those estimated by the authors of that paper.

If the qualifications relating to the results given in the table are taken into account, the data seem to point to the essential correctness of Mott's interpretation of the β-flow.

REFERENCES

ANDRADE, E. N. DA C., 1914, *Proc. Roy. Soc.* A, **90,** 329.
CRUSSARD, C., 1946, *Rev. Met.*, **43,** 307.
FASTOV, N. S., 1950, *J. Tech. Phys. USSR*, **20,** 543.
FELTHAM, P., 1953 a, *Proc. Phys. Soc.* B, **66,** 865; 1953 b, *Proceedings of the Second International Congress on Rheology* (London: Butterworth Ltd.).
GIBBS, R. L., and RAMLAL, N., 1934, *Phil. Mag.*, **18,** 949.
JESSOP, T. H., and FILON, L. N. G., 1928, *Phil. Trans. Roy. Soc.* A, **223,** 89.
JOHNSON, A. E., and FROST, N. E., 1952, *J. Inst. Met.*, **81,** 93.
MCLEAN, D., 1953, *J. Inst. Met.*, **81,** 287, 293.
MOTT, N. F., 1953, *Phil. Mag.*, **44,** 742.
NOVICK, A. S., and MACHLIN, E. S., 1947, *J. Appl. Phys.*, **18,** 79.
WYATT, O. H., 1953, *Proc. Phys. Soc.* B, **66,** 459.

III. *Analysis of V-Events*

By J. Podolanski and R. Armenteros*
The Physical Laboratories, University of Manchester†

[Received August 27, 1953]

Abstract

From the observed momenta and angles of decays in flight, variables are constructed which are better suited for the analysis than the measured quantities themselves. These variables are $1/P$, the reciprocal of the primary momentum, α, a combination of the longitudinal momenta of the secondaries, and either p_t, the transverse momentum, or the quantity $\epsilon = 2p_t/P$. The regularities in the distribution of the new variables, to be expected from a two-body decay, are discussed. The decay scheme may be derived by comparison with the experimental distributions.

Introduction

A method of analysing the dynamics of two-particle decays will be described here. The need for such a method was felt after the inhomogeneity of neutral V-particles had been discovered by the Pic du Midi group. In order to treat the experimental data it was essential to devise a method of separating the events into different decay schemes.

An examination of the energy released in the decay, the Q-value, is in general not sufficient for this purpose. This test can show up inconsistencies between the experimental data and the assumed decay schemes, but it cannot reveal the reasons for these inconsistencies. The Q-values, therefore, provide no clear indication as to how such a discrepancy can be removed.

A more detailed (graphical) representation of decays has been given by Blaton (1950), but it does not lend itself to a quantitative treatment as we shall see in § 3. The transformation of variables discussed in this paper provides a suitable approach. The first analysis based on the new variables was made by Armenteros *et al.* (1951). Some of the properties of the quantity α have been employed by Leighton *et al.* (1953) and Fretter *et al.* (1953) in the examination of their results, while a more extensive use of the new variables has been made to great advantage by Thompson *et al.* (1952, 1953).

It is essential to realize that the method is merely a convenient way of displaying experimental results. The analysis in terms of ϵ and α cannot reveal more than has been put into it: conservation of momentum and energy. Its superiority over the Q-value method derives from the fact that the latter checks energy conservation only.

---

* Now at the Laboratoire de l'Ecole Polytechnique, Paris.

† Communicated by Dr. G. D. Rochester.

I. THE DECAY SURFACE

§ 1. THE DECAY SURFACE IN TERMS OF TWO MOMENTA AND THE INCLUDED ANGLE

(i) *The Decay Relations*

We consider a decay $M \rightarrow m_1+m_2$. If the decay scheme is known, the momenta P, p_1, p_2 in the laboratory system (L.S.) and the angles included, ϕ_1, ϕ_2, $\phi=\phi_1+\phi_2$, are completely determined when β, the velocity of the primary, and θ, the angle of ejection in the centre of mass system (C.M.S.), are given. We assume that *three* quantities have been measured,† the momenta p_a, p_b of two particles and the angle ϕ_{ab} included. Here p_a and p_b stand for any pair of the three momenta P, p_1, p_2. As a decay is fixed by *two* parameters (β, θ), the measured quantities have to satisfy a relation of the form‡

Fig. 1

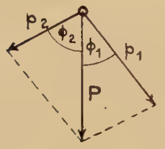

Decay in the laboratory system.

Fig. 2

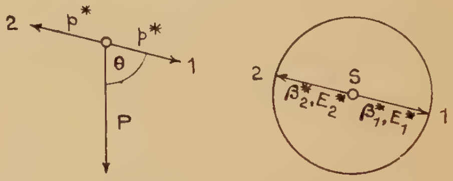

Decay in the centre of mass system.

$$E_aE_b-p_ap_b\cos\phi_{ab} = (m_a^2m_b^2+M^2p^{*2})^{\frac{1}{2}}, \quad . \quad . \quad . \quad . \quad . \quad (1)$$

with $E=(m^2+p^2)^{\frac{1}{2}}$. The constant on the r.h.s. is fixed by the decay scheme: M is the mass of the primary and p^* the momentum of the decay products in the C.M.S.:

$$p^* = \frac{1}{2M}[M^2-(m_1+m_2)^2]^{\frac{1}{2}}[M^2-(m_1-m_2)^2]^{\frac{1}{2}}. \quad . \quad . \quad . \quad (2)$$

Equation (1) stands for three ' decay relations ':

$$E_1E_2-p_1p_2\cos\phi = \tfrac{1}{2}(M^2-m_1^2-m_2^2), \quad . \quad . \quad . \quad (1\,a)$$

$$EE_1-Pp_1\cos\phi_1 = \tfrac{1}{2}(M^2+m_1^2-m_2^2), \quad . \quad . \quad . \quad (1\,b)$$

$$EE_2-Pp_2\cos\phi_2 = \tfrac{1}{2}(M^2-m_1^2+m_2^2). \quad . \quad . \quad . \quad (1\,c)$$

The first relation applies to a neutral, the other two to a charged, decay. In principle, three events—three sets of measurements p_a, p_b, ϕ_{ab}—should be sufficient to fix the parameters M, m_1, m_2 determining the form of the decay relation. Because of the errors of measurement, the decay scheme is, in practice, adjusted so that the decay relation is satisfied as well as possible.

---

† In § 7 (v) we deal with the case when only two angles are measured.

‡ Here, as elsewhere, masses and momenta are expressed in energy units. Velocities are referred to the velocity of light.

The decay relation may be visualized as a surface in the space of the three measured quantities p_a, p_b, ϕ_{ab}. The *decay surface* is fixed by the decay scheme. The parameters M, m_1, m_2 have to be chosen so that the points representing the decay events lie as close to the surface as possible. The decay surfaces in the space p_a, p_b, ϕ_{ab} are, however, intricate structures.† It is impossible to guess, from a series of observations, the parameters M, m_1, m_2 fixing the surface. The essence of the method to be proposed is the construction, from p_a, p_b, ϕ_{ab} (and *from these only*), of another set of three variables, in terms of which the decay surface becomes manageable. With the new variables, it will be possible to construct the decay surface directly from the observations, whereas using p_a, p_b, ϕ_{ab} one can only check the decay relations (1) *against an assumed decay scheme* (by examining the constancy of the Q-values).

(ii) *Statistical Distribution*

Momenta and angles in the L.S. can be expressed as functions

$$p_a(\beta, \theta), \qquad p_b(\beta, \theta), \qquad \phi_{ab}(\beta, \theta) \quad . \quad . \quad . \quad . \quad . \quad . \quad (3)$$

of β, the velocity of the decaying particle, and of θ, the angle of ejection in the C.M.S. The eqns. (3) are a parametric representation of the decay surface ; elimination of β and θ results in the decay relation (1).

From (3), the statistical distribution of events over the decay surface—corresponding to the (supposed) isotropy of decays—can be derived. The isotropic θ-distribution,

$$w(\theta)\,d\theta = \tfrac{1}{2}\sin\theta\,d\theta, \qquad (0 \leqslant \theta \leqslant 180^\circ), \quad . \quad . \quad . \quad . \quad (4)$$

gives, with (3), the distribution of decays along a line β=const on the surface.

Again, the distribution over the p_a, p_b, ϕ_{ab}-surface is much too complicated for a detailed comparison with experiment. In contradistinction, the theoretical distribution in terms of the new variables is simple enough to allow of a sensitive test for isotropy in the C.M.S.

§ 2. THE VARIABLES ϵ, α, $1/P$

The real trouble with the quantities p_a, p_b, ϕ_{ab} is that their values are determined primarily by β, the velocity of the decaying particle. Our aim is to *eliminate the dependence on* β, as far as it is feasible to do so *without any presumed knowledge of the decay scheme*. The dependence on M, m_1, m_2 and θ will then come to the fore, and this will make it easier both to design a decay scheme and to test the statistical distribution.

(i) A quantity well fitted for the purpose is the *transverse* momentum

$$p_t = p_1 \sin\phi_1 = p_2 \sin\phi_2. \quad . \quad . \quad . \quad . \quad . \quad . \quad . \quad (5)$$

This variable is not affected by the transformation to the L.S. and is therefore independent of β. It is obvious what information we expect to gain from p_t: its maximum value is the momentum p^* with which the secondaries are thrown out in the C.M.S. For the reasons presented in § 3 we shall use, besides p_t, the dimensionless variable

---

† A graphical representation of the surface (1 b) has been given by Stanton (1944). See also Butler (1951).

$$\epsilon = \frac{2p_t}{P} = \frac{2 \sin \phi_1 \sin \phi_2}{\sin \phi}. \quad . \quad . \quad . \quad . \quad . \quad . \quad (6)$$

(ii) The *longitudinal* components,

$$p_{1l} = p_1 \cos \phi_1, \qquad p_{2l} = p_2 \cos \phi_2,$$

contrariwise, take up the momentum of the primary completely ($P = p_{1l} + p_{2l}$) and thus depend strongly on β. The longitudinal components by themselves are, therefore, unsuited for the analysis, but they convey information about the masses of the secondaries by the way they share the incoming momentum. The heavier particle takes up, on the average, the greater part of P:

$$\overline{p_{1l}/P} = \tfrac{1}{2}(M^2 + m_1^2 - m_2^2)/M^2, \qquad \overline{p_{2l}/P} = \tfrac{1}{2}(M^2 - m_1^2 + m_2^2)/M^2.$$

For large momenta ($P \gg p^*$), the ratios p_{1l}/P and p_{2l}/P depend only slightly on β. We suggest as second variable

$$\alpha = \frac{p_{1l} - p_{2l}}{P} = \frac{p_1^2 - p_2^2}{P^2} = \frac{\sin(\phi_2 - \phi_1)}{\sin \phi}. \quad . \quad . \quad . \quad . \quad . \quad (7)$$

Its mean value is a measure of the mass difference of the decay products and should be equal to

$$\alpha^* = \frac{m_1^2 - m_2^2}{M^2}. \quad . \quad . \quad . \quad . \quad . \quad . \quad . \quad . \quad (8)$$

Depending on the angle of ejection, α will fluctuate about α^* with an amplitude which, for high energies, approaches

$$\epsilon^* = 2p^*/M. \quad . \quad . \quad . \quad . \quad . \quad . \quad . \quad . \quad . \quad (9)$$

(iii) As third variable, $1/P$, the reciprocal of the primary momentum, has proved to be a convenient choice.

Thus we propose to analyse decay data in terms of the variables

$$1/P, \qquad p_t, \qquad \alpha \quad . \quad . \quad . \quad . \quad . \quad . \quad . \quad (10\,a)$$

or

$$1/P, \qquad \epsilon, \qquad \alpha \quad . \quad . \quad . \quad . \quad . \quad . \quad . \quad . \quad (10\,b)$$

defined by (5), (6) and (7), instead of the directly measured ones p_1, p_2, ϕ (neutral decay) or P, p_1, ϕ_1 (charged decay).

The introduction of the set of variables (10) unifies the treatment of neutral and charged decays. The three decay relations (1) reduce to one, namely,

$$p_t^2 + \frac{1}{4(1/M^2 + 1/P^2)} \cdot (\alpha - \alpha^*)^2 = p^{*2}. \quad . \quad . \quad . \quad . \quad (11\,a)$$

or

$$\frac{\epsilon^2}{(M/P)^2} + \frac{(\alpha - \alpha^*)^2}{1 + (M/P)^2} = \epsilon^{*2}, \quad . \quad . \quad . \quad . \quad (11\,b)$$

with p^*, α^*, ϵ^* given by (2), (8), (9). The secondary masses m_1, m_2 enter through these quantities only. For the purpose of the proposed method it is therefore more natural to define the decay scheme by p^*, α^*, ϵ^* or M, α^*, ϵ^* rather than by M, m_1, m_2. We shall devote § 4 to a discussion of the first two sets of parameters, before we analyse, in §§ 5, 6 and 7, the distribution of events over the three projections of the decay surface (11).

But first of all, we wish to give another justification for the introduction of the new variables. We shall, in particular, see that the ϵ, α-projection of the decay surface (11 *b*) allows of a simple geometrical interpretation.

§ 3. THE DECAY ELLIPSE

In the C.M.S., the end-points of the secondary momenta move on a sphere of radius p^* and centre at the source S (fig. 2). The L.S. momenta $\mathbf{p}_1$, $\mathbf{p}_2$ are obtained, in a classical fashion, by vector addition of $m_1\mathbf{P}/M$ and $m_2\mathbf{P}/M$, respectively. For a given primary momentum $\mathbf{P}$, the end-points of $\mathbf{p}_1$, $\mathbf{p}_2$ move, therefore, in the plane of decay, on circles of radius p^*, but whose centres are now shifted from the source in the direction $\mathbf{P}$ by different amounts. To picture the decay in the L.S., one circle suffices, if the source is represented by two images S_1 and S_2, separated by $\mathbf{P}$. In figs. 3 and 4 the picture is corrected for relativity:

Fig. 3

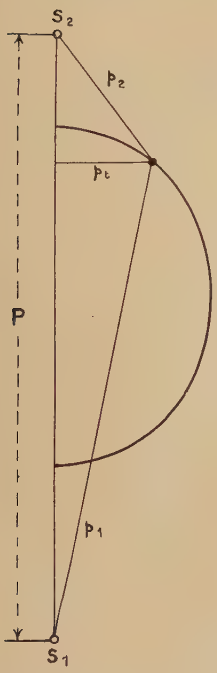

Decay in the L.S.

Fig. 4

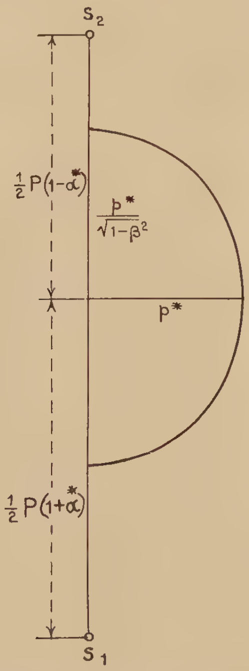
S_2
$\frac{1}{2}P(1-\alpha^*)$
$\frac{p^*}{\sqrt{1-\beta^2}}$
p^*
$\frac{1}{2}P(1+\alpha^*)$
S_1

Decay ellipse P=const.

Fig. 5

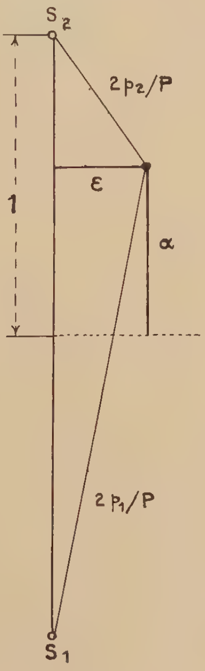

The plane ϵ, α.

the loci $P=$ const are *ellipses*[†] whose minor semi-axes are constant and equal to p^*. The centre of the ellipse divides S_1S_2 in the ratio

$$\frac{1+\alpha^*}{1-\alpha^*} \quad \text{with} \quad \alpha^* = \frac{m_1^2-m_2^2}{M^2}.$$

This ratio is at the same time the average value of p_{1l}/p_{2l}, for events on the upper half of the ellipse are as frequent as those on the lower half. The sources S_1 and S_2 will be outside the ellipse as long as β, the velocity of the primary, is greater than both β_1^* and β_2^*, the velocities of the secondaries in the C.M.S.

The advantages of such a method of visualizing the decays need not be stressed (Blaton 1950). However, for the display of decay data and their analysis the scheme is quite unsuited: if we fix, say, S_2, then S_1 and with it the ellipse recede from S_2 with increasing momentum P. Ellipses belonging to different momenta intersect. For a wide range of momenta, occurring in practice, the ellipses are elongated in one direction so much that, for the analysis, it is of no avail to know that they are ellipses.

The remedy is to fix the distance S_1S_2 by reducing the momentum scale of each event proportionally to $1/P$. We choose as scale factor $2/P$, fixing thus $S_1S_2=2$. From the centre of S_1S_2, which we make the origin, we have therefore to set out the vector

$$\frac{2}{P}(\mathbf{p}_1-\tfrac{1}{2}\mathbf{P}) = \frac{\mathbf{p}_1-\mathbf{p}_2}{P}.$$

The transverse and longitudinal components of this vector are just the variables ϵ and α, introduced in § 2. In the ϵ, α-plane (fig. 5) each decay is represented in its original shape, all angles being preserved. The momentum scale has been chosen so that all events have the same 'size'. The rather abstract concept of the decay surface acquires, in the variables ϵ, α, $1/P$, a concrete meaning: the planes $1/P=$const are faithful pictures of the decays, compatible with the P in question.

After this mapping, the ellipses $P=$const (see § 7 (iii) and fig. 13) are centred in a fixed point on S_1S_2 and are confocal with eccentricity $\epsilon^*=2p^*/M$. The axes decrease with increasing momentum, the vertical (major) axis as $1/P$, the horizontal axis as $1/\beta$.

These are the facts which make the analysis in the ϵ, α-plane so attractive, compared with the p_t, α-diagram.[‡]

§ 4. THE DECAY PARAMETERS p^*, ϵ^*, α^* AND M, ϵ^*, α^*

The mass M of the unstable particle is, of course, greater than the masses of the secondaries together: $M \geqslant m_1+m_2$. For most purposes we may, furthermore, restrict ourselves to $m_1 \geqslant m_2$.

[†] As a consequence of the convention to take p_t positive, the events $P=$const cover only the right half of the ellipse.

[‡] In this projection, used by Thompson *et al.* (1952, 1953), the decays are re-scaled only in the longitudinal direction.

(i) We denote quantities referring to the C.M.S. with an asterisk. The momenta and the energies of the secondaries are related to the masses by

$$p^* = \frac{1}{2M}[M^2-(m_1+m_2)^2]^{\frac{1}{2}}[M^2-(m_1-m_2)^2]^{\frac{1}{2}} \quad . \quad . \quad . \quad (12\,a)$$

$$E_1^* = \frac{1}{2M}(M^2+m_1^2-m_2^2) \quad . \quad . \quad . \quad . \quad . \quad . \quad . \quad . \quad . \quad (12\,b)$$

$$E_2^* = \frac{1}{2M}(M^2-m_1^2+m_2^2), \quad . \quad . \quad . \quad . \quad . \quad . \quad . \quad . \quad . \quad (12\,c)$$

and the velocities follow then from

$$\beta_1^*E_1^* = \beta_2^*E_2^* = p^*. \quad . \quad . \quad . \quad . \quad . \quad . \quad (13)$$

(ii) The essential features of a decay are shaped by the two dimensionless constants $\epsilon^*=2p^*/M$ and $\alpha^*=(E_1^*-E_2^*)/M$, which can be expressed by the mass ratios :

$$\epsilon^* = \left[1-\left(\frac{m_1+m_2}{M}\right)^2\right]^{\frac{1}{2}}\left[1-\left(\frac{m_1-m_2}{M}\right)^2\right]^{\frac{1}{2}} \quad . \quad . \quad (14\,a)$$

$$\alpha^* = \frac{m_1^2-m_2^2}{M^2} \quad . \quad . \quad . \quad . \quad . \quad . \quad . \quad . \quad . \quad . \quad . \quad . \quad . \quad (14\,b)$$

Fig. 6

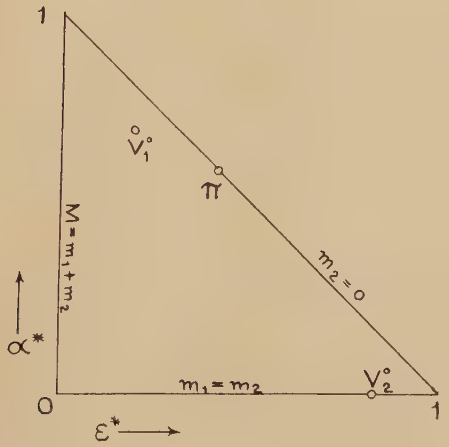

Classification of decays according to ϵ^*, α^*.

The parameters ϵ^*, α^* determine completely the relations connecting dimensionless decay quantities, e.g. the velocities and the angles in the L.S. The number ϵ^* is a measure of the *energy release*. No energy is freed if $\epsilon^*=0$. When ϵ^* reaches its maximum value 1, the whole rest mass of the primary is converted into kinetic energy. The parameter α^*, on the other hand, characterizes the *asymmetry* of the decay. It runs, for a fixed ϵ^*, from $\alpha^*=0$ (symmetric decay, $m_2=m_1$) to $\alpha^*=1-\epsilon^*$, when $m_2=0$. All decays with $m_1 \geqslant m_2$ can thus be located in the triangle of fig. 6, in which the positions of some two-body decays are indicated.

(iii) The knowledge of ϵ^* and α^* suffices for the calculation of the decay velocities in the C.M.S.:

$$\beta_1^* = \frac{\epsilon^*}{1+\alpha^*}, \qquad \beta_2^* = \frac{\epsilon^*}{1-\alpha^*}. \quad . \quad . \quad . \quad . \quad . \quad (15)$$

The *energy scale* is determined when, in addition, either M or p^* are given. Momenta and energies in the C.M.S. can then be calculated from M, ϵ^*, α^* or p^*, ϵ^*, α^*:

$$p^* = \frac{M}{2}\epsilon^* \quad . \quad . \quad . \quad . \quad . \quad . \quad . \quad . \quad . \quad . \quad . \quad . \quad . \quad (16\,a)$$

$$E_1^* = \frac{M}{2}(1+\alpha^*) = p^* . \frac{1+\alpha^*}{\epsilon^*} \quad . \quad . \quad . \quad . \quad . \quad . \quad (16\,b)$$

$$E_2^* = \frac{M}{2}(1-\alpha^*) = p^* . \frac{1-\alpha^*}{\epsilon^*}. \quad . \quad . \quad . \quad . \quad . \quad . \quad (16\,c)$$

These formulae are to be compared with (12), (13) which express the same quantities in terms of M, m_1, m_2.

(iv) The method proposed aims in the first instance at the determination of p^*, ϵ^*, α^* or M, ϵ^*, α^*. With either of these sets the masses involved in the decay can be calculated from

$$M = \qquad p^* . \frac{2}{\epsilon^*} \quad . \quad . \quad . \quad . \quad . \quad . \quad (17\,a)$$

$$m_1 = \frac{M}{2}[(1+\alpha^*)^2-\epsilon^{*2}]^{\frac{1}{2}} = p^*\left(\frac{1}{\beta_1^{*2}}-1\right)^{\frac{1}{2}} \quad . \quad . \quad (17\,b)$$

$$m_2 = \frac{M}{2}[(1-\alpha^*)^2-\epsilon^{*2}]^{\frac{1}{2}} = p^*\left(\frac{1}{\beta_2^{*2}}-1\right)^{\frac{1}{2}} \quad . \quad . \quad (17\,c)$$

with β_1^*, β_2^* from (15).

II. THE THREE PROJECTIONS OF THE DECAY SURFACE

§ 5. THE PROJECTIONS $1/P$, ϵ AND $1/P$, p_t

Determination of p^*

The projection $1/P$, ϵ is of interest only in combination with the ϵ, α-diagram and for visualizing the complete decay surface (fig. 11). Since

$$\epsilon = \frac{2p_t}{P} = \epsilon^* . \frac{M}{P} . \sin\theta, \qquad (0 \leqslant \theta \leqslant 180°)$$

the decay events will fill the region between the axis $\epsilon=0$ and a straight line of slope $2p^*$.

Here we consider the projection $1/P$, p_t, which leads to the determination of p^*, the C.M.S. momentum of the secondaries (fig. 7). Since

$$p_t = p^* \sin\theta, \qquad (0 \leqslant \theta \leqslant 180°)$$

the observed events should lie within the strip between $p_t=0$ and $p_t=p^*$. The distribution in the horizontal direction is given by the momentum spectrum of the decaying particles. In the vertical direction, the distribution, assuming isotropy in the C.M.S., is†

$$w(p_t)\,dp_t=\frac{p_t\,dp_t}{p^*(p^{*2}-p_t^2)^{\frac{1}{2}}}, \qquad \ldots\ldots \quad (18\,a)$$

which leads to an increasing number of events as p_t approaches p^*.

For the *determination of* p^* it may be better to use the integral probability distribution

$$W(p_t>p_t^0)=\left[1-\left(\frac{p_t^0}{p^*}\right)^2\right]^{\frac{1}{2}}. \qquad \ldots\ldots \quad (18\,b)$$

Fig. 7

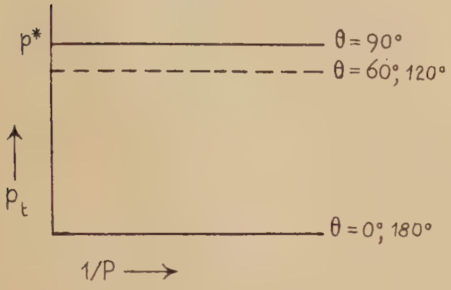

The projection $1/P$, p_t.

Fig. 8

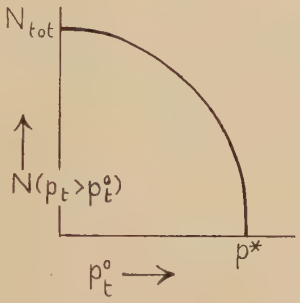

Number of decays with transverse momentum greater than p_t^0.

The number of particles with a transverse momentum greater than p_t^0, plotted against p_t^0, will lie on an ellipse (fig. 8) whose horizontal semi-axis is p^*. The broken line in fig. 7 corresponds to $W=\frac{1}{2}$ and divides the inhabited part of the plane into regions of equal population.

§ 6. The Projection $1/P$, α

(i) *The Limiting Hyperbola*

Remembering the definition

$$\alpha=\frac{p_{1l}-p_{2l}}{P}=\frac{\sin(\phi_2-\phi_1)}{\sin\phi}$$

one finds, by a Lorentz transformation,

$$\alpha=\alpha^*+\epsilon^*[1+(M/P)^2]^{\frac{1}{2}}\cos\theta \qquad \ldots\ldots \quad (19\,a)$$

with $\qquad \alpha^*=(m_1^2-m_2^2)/M^2, \qquad \epsilon^*=2p^*/M.$

The decays are distributed between the two branches ($\theta=0$, 180°)

$$\alpha=\alpha^*\pm\epsilon^*[1+(M/P)^2]^{\frac{1}{2}} \qquad \ldots\ldots \quad (19\,b)$$

of a hyperbola, drawn in fig. 12. The *position* of the limiting hyperbola is fixed by the difference in mass of the secondaries, since its axis of symmetry ($\theta=90°$) is given by $\alpha=\alpha^*$. About this axis the decays are uniformly distributed (see (ii)) with an amplitude increasing as $1/\beta$. The *shape* of the limiting hyperbola is determined by the energy release: the real semi-axis is equal to ϵ^*, and the slopes of the asymptotes are equal to $\pm 2p^*$.

---

† For the influence of experimental errors on the p_t distribution, see Barker (1953).

This slope is the same as that of the limiting line in the $1/P$, ϵ-diagram (fig. 11). The reason for this is clear: the space between the asymptotes is the region allowed by classical mechanics. The broadening to a hyperbola is a relativistic effect. According to classical mechanics the events with $P=\infty$ are concentrated in the point $\alpha=\alpha^*$ of the vertical axis, whilst, in fact, they extend over the segment F_1F_2. The transverse component, ϵ, however, does not undergo a Lorentz dilatation. In classical mechanics, the decay ellipses of § 3 are circles and the decay surface is (half) a circular cone, whose contours are given by the limiting line in fig. 11 and the asymptotes in fig. 12. This cone is, by relativity, deformed into the surface described in § 7 (v).

(ii) *Statistics. Determination of α^* and ϵ^**

The assumption of isotropy in the C.M.S. leads to two consequences regarding the distribution of α-values for a given primary momentum P, i.e. in the $1/P, \alpha$-diagram, the distribution of decays along a vertical strip: (*a*) For any P, the distribution is symmetric about a fixed value α^*. (*b*) The distribution is rectangular with a width ϵ^*/β. Both these inferences can be checked independently and enable α^* and ϵ^* to be calculated:

$$\alpha^* = \bar{\alpha} \quad . \quad . \quad . \quad . \quad . \quad . \quad . \quad (20)$$

$$\tfrac{1}{3}\epsilon^{*2}+\alpha^{*2} = \overline{\alpha^2}-\tfrac{1}{3}\overline{(2p^*/P)^2}. \quad . \quad . \quad . \quad . \quad . \quad (21)$$

Comparison of these averages for different ranges of the primary momentum provides a check for isotropy. In (21) p^* is assumed to be known from inspection of the $1/P$, p_t-diagram.† The corresponding eqn. (25) of the next section is probably more useful.

The over-all distribution of α is flat between $\alpha^*-\epsilon^*$ and $\alpha^*+\epsilon^*$ and tails off in a way determined only by the momentum spectra of the decaying particles.

In principle, thus, the three decay parameters p^*, α^*, ϵ^* have been derived from the distribution of events in the planes $1/P$, p_t and $1/P$, α. In § 8, we shall indicate how the limitations of this procedure, due to experimental errors, can be overcome.

An assumed decay scheme may be checked in the $1/P, \alpha$-plane by comparing the measured p_t-values with those to be expected from the decay scheme. For this purpose one draws the curves $\theta=$const which, according to (19 *a*), are hyperbolae. Since $p_t=p^* \sin\theta$, they are also the loci of constant p_t corresponding to the assumed decay scheme. Alternatively, the check may be done by means of the curves p_1, p_2 or

---

† Another method of finding ϵ^*, when p^* and α^* are known, is described in § 9.

ϕ=const. Methods of constructing these loci are not too difficult to design. Other ways of examining a decay scheme will be described in § 9.

(iii) *The Events* S_1, S_2

These are the 'sources' of § 3, projected on to the decay surface. They are the points $\alpha=\mp 1$ of the limiting hyperbola (fig. 12) and represent decays in which one of the secondaries is at rest in the L.S. ($p_1=0$ or $p_2=0$). This can happen only when the primary has a velocity equal to the velocity of the secondary in the C.M.S. ($\beta=\beta_1{}^*$ or $\beta=\beta_2{}^*$) *and* when the secondary is ejected in a direction opposite to the primary momentum ($\theta=180°$ or $\theta=0$):

$$\left.\begin{array}{llll} S_1: & \beta=\beta_1{}^*, & p_1=0, & p_2=P=Mp^*/m_1 \\ S_2: & \beta=\beta_2{}^*, & p_2=0, & p_1=P=Mp^*/m_2. \end{array}\right\} \qquad (22\,a)$$

The secondary which does not come to rest emerges in the L.S. with the velocity

$$\frac{1}{\beta_{2,1}}=\left[1+\left(\frac{m_1m_2}{Mp^*}\right)^2\right]^{\frac{1}{2}}=\frac{M^2-m_1{}^2-m_2{}^2}{2Mp^*}. \quad . \quad . \quad . \quad . \quad (22\,b)$$

The points S_1, S_2 are important for many constructions. Some of their properties are summarized here (and in § 7 (iii)):

The loci ϕ_1=const start from S_1, the loci ϕ_2=const from S_2. The horizontal lines through S_2 and S_1 enclose the region where both secondaries are, in the L.S., ejected in the forward direction. Above S_2, particle 2, and below S_1, particle 1, is thrown backwards. The probability of finding particle 1 or 2 ejected in the backward direction is, for a fixed velocity β of the primary, given by $\frac{1}{2}(1-\beta/\beta_1{}^*)$ and $\frac{1}{2}(1-\beta/\beta_2{}^*)$, respectively. For primary velocities† greater than $\beta_2{}^*$, i.e. to the left of S_2, both ϕ_2 and $\phi=\phi_1+\phi_2$ go through a maximum. To the right of S_1, the angle ϕ has a minimum. The loci ϕ=const connect S_1 and S_2.

Furthermore, the points S_1, S_2 play a rôle in the construction of the curves p_1=const and p_2=const.

§ 7. THE PROJECTION ϵ, α

(i) The third projection, already discussed in § 3, has as coordinates the dimensionless quantities‡

$$\left.\begin{array}{l} \epsilon=\dfrac{2p_t}{P}=\dfrac{2\sin\phi_1\sin\phi_2}{\sin\phi} \\[2ex] \alpha=\dfrac{p_{1l}-p_{2l}}{P}=\dfrac{\sin(\phi_2-\phi_1)}{\sin\phi} \end{array}\right\} \quad . \quad . \quad . \quad . \quad . \quad (23)$$

The events fill the whole of the half-plane $\epsilon\geqslant 0$. Energetic events will be found near the segment F_1F_2 which represents, as in the $1/P$, α-diagram, decays with $P=\infty$. For low energies of the primary the events recede to a distance $\gtrsim M/P \gtrsim 1/\beta$ from the centre of F_1F_2.

---

† S_2 is to the left of S_1, i.e. $\beta_2{}^*\geqslant\beta_1{}^*$, because of $m_1\geqslant m_2$.

‡ An alternative is the plot p_t, α, used by Thompson *et al.* (1952, 1953).

The position of an event in the ϵ, α-plane is, according to (23), determined *by the angles only*. This representation is therefore the appropriate choice when the momenta are not known, but two angles are measured. (In (iv) more attention will be given to this case.)

Also, if only one angle is measured (together with the momenta), this projection possesses one striking virtue when the errors of measurement are taken into account: the position of an event is much better defined than in the other planes. The errors in the angle are usually negligible compared with the momentum errors. The event is, therefore, bound to lie on a line $\phi=\text{const}$ (or $\phi_1=\text{const}$, $\phi_2=\text{const}$), i.e. on a circle through S_1 and S_2 (or on a straight line through S_1 or S_2) as is evident from fig. 9. Because of the momentum errors, the event will be represented by a segment of this line. In the other projections a decay event will be spread, by the momentum errors, over a quadrangle.

Fig. 9

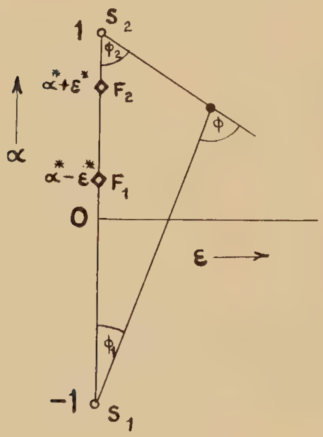

The projection ϵ, α.

Fig. 10

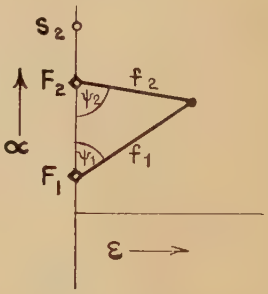

Calculation of the momenta from the angles ϕ_1, ϕ_2.

In the ϵ, α-projection—and only in this projection—the loci of constant ϕ_1, ϕ_2 or ϕ are independent of the decay scheme. The same is true for any dimensionless combination of measured quantities, e.g. p_1/P, p_2/P, p_1/p_2 which are constant along semi-circles.

(ii) *Determination of α^* and ϵ^**

The distribution of events over the ϵ, α-plane yields, as does the $1/P, \alpha$-projection, the dimensionless decay parameters α^*, ϵ^*:

$$\alpha^* = \overline{\alpha} \qquad (24)$$

$$\tfrac{1}{3}\epsilon^{*2}+\alpha^{*2} = \overline{\alpha^2-\epsilon^2}. \qquad (25)$$

Compared with (21), formula (25) has the advantage of referring to the plots in the ϵ, α-plane only. Application of (21), employing the $1/P, \alpha$-plane, depends on the previous scrutiny of the $1/P, p_t$-diagram and is sensitive to errors in the determination of p^*.

In order to check an assumed decay scheme, the measured values of both P and p_t may be compared with those expected. The curves P=const and p_t=const, corresponding to the assumed decay scheme, serve this purpose. These loci are constructed below. They can, of course, also be used to *evaluate*, from the decay scheme, the momenta if these are not known. This will be done, however, in a more efficient way in (iv).

(iii) *P=const and θ=const* (fig. 13)

The lines P=const,

$$\frac{(\alpha-\alpha^*)^2}{1+(M/P)^2}+\frac{\epsilon^2}{(M/P)^2}=\epsilon^{*2}, \quad . \quad . \quad . \quad . \quad . \quad . \quad (26)$$

are confocal ellipses with foci F_1, F_2 and eccentricity $\epsilon^*=2p^*/M$. The major (vertical) and minor (horizontal) semi-axes are given by

$$\epsilon^*/\beta=\epsilon^* . [1+(M/P)^2]^{\frac{1}{2}} \qquad \text{and} \qquad 2p^*/P=\epsilon^* . M/P\,;$$

the ratio of their lengths is $\gamma=(1-\beta^2)^{-\frac{1}{2}}$.

The curves P=const of fig. 13, together with fig. 9, make it possible to follow the behaviour of the angles ϕ_1, ϕ_2, ϕ for a given P. This behaviour will be different depending on whether the sources S_1, S_2 are outside or inside the ellipse P=const. This happens when $\beta>\beta_2{}^*$ and when $\beta<\beta_1{}^*$, respectively, where $\beta_1{}^*$, $\beta_2{}^*$ are the C.M.S. velocities of the secondaries (see footnote, page 23). The maxima of ϕ_1 and ϕ_2 are found by drawing the tangents from S_1 and S_2 on to the ellipse. Similarly, $\phi_{\max}$ and $\phi_{\min}$ are found by constructing the circle(s) through S_1 and S_2 tangential to the ellipse P=const. The points where, in the ϵ, α-diagram, ϕ_1 reaches a maximum lie on a semi-circle through S_1 and the point $\alpha=\alpha^*-\epsilon^*\beta_1{}^*$ on the α-axis (S_2 and $\alpha^*+\epsilon^*/\beta_2{}^*$ for ϕ_2).†

Since $p_t=p^* \sin\theta$, the curves p_t=const coincide with θ=const. They constitute a set of confocal hyperbolae,

$$\frac{(\alpha-\alpha^*)^2}{\cos^2\theta}-\frac{\epsilon^2}{\sin^2\theta}=\epsilon^{*2}, \quad . \quad . \quad . \quad . \quad . \quad . \quad . \quad (27)$$

with the same foci as the ellipses P=const, which they intersect at right angles. The asymptote of the hyperbola branch θ=const makes an angle θ with the positive direction of the α-axis. The loci θ=const can be used for testing the isotropy in the C.M.S. For instance, half the decays should fall between the two branches $\theta=60°$ and $\theta=120°$ of a hyperbola (fig. 13).

---

† The corresponding curves in the $1/P, \alpha$-diagram are parabolae through the same points, with vertex on the α-axis.

(iv) *Momenta from Angles and Decay Scheme*

When the angles ϕ_1, ϕ_2 are measured, the momenta p_1, p_2, P can be derived if a decay scheme is assumed, i.e. if p^*, α^* and ϵ^* are known.

Figs. 11, 12, 13

The three projections of the decay surface with lines P=const and θ=const. The statistical distribution of decays for constant P is indicated.

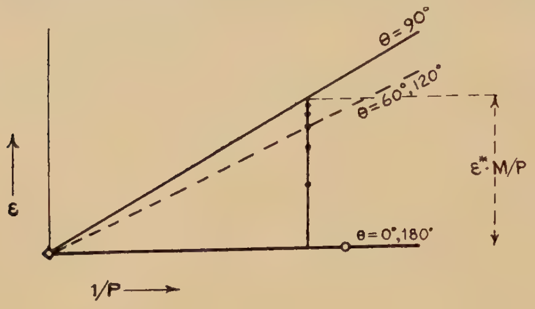

Projection $1/P$, ϵ. The decays are contained within the sector between the $1/P$-axis and the straight line θ=90°. Half of the events (population I) lie above, the other half (population II) below, the broken line.

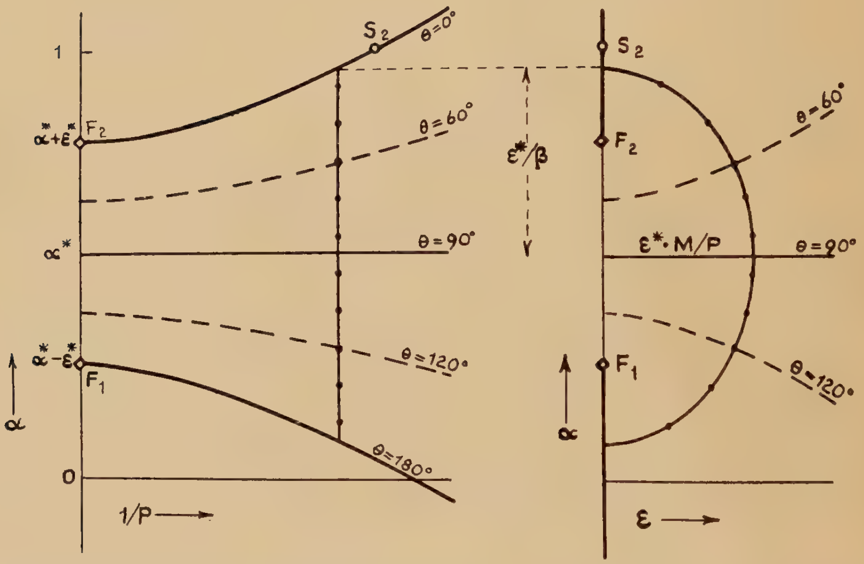

Projection $1/P$, α. The decays are contained between the two branches (θ=0, 180°) of a hyperbola. Population I of fig. 11 is to be found between the broken lines θ=60° and θ=120°, while population II is equally divided between the two marginal regions.

Projection ϵ, α. Population I is again contained between the lines θ=60° and θ=120°; population II is distributed over the rest of the half-plane.

We give below both a graphical and an analytical method of evaluating the primary velocity β and the ejection angle θ. Once, β and θ have been found from (28) or (29), the momenta follow from

$$p_1 \sin \phi_1 = p_2 \sin \phi_2 = P \,.\, \frac{\sin \phi_1 \sin \phi_2}{\sin \phi} = p^* \sin \theta.$$

For the *graphical* construction (fig. 10) one measures the distances f_1, f_2 of the event from the points F_1 and F_2 and finds β and θ by means of

$$\frac{1}{\beta}=\frac{f_1+f_2}{2\epsilon^*}, \qquad \cos\theta=\frac{f_1-f_2}{2\epsilon^*}. \quad . \quad . \quad . \quad (28)$$

To follow this construction *analytically*,† first the angles ψ_1, ψ_2 are calculated :

$$\left.\begin{aligned} \cot\psi_1 &= \frac{(1-\alpha^*)+\epsilon^*}{2}\,.\cot\phi_1-\frac{(1+\alpha^*)-\epsilon^*}{2}\,.\cot\phi_2 \\ \cot\psi_2 &= \frac{(1+\alpha^*)+\epsilon^*}{2}\,.\cot\phi_2-\frac{(1-\alpha^*)-\epsilon^*}{2}\,.\cot\phi_1. \end{aligned}\right\} \quad . \quad (29\,a)$$

Then β and θ are obtained from

$$\frac{1}{\beta}=\frac{\cos\frac{1}{2}(\psi_2-\psi_1)}{\cos\frac{1}{2}(\psi_2+\psi_1)}, \qquad \cos\theta=\frac{\sin\frac{1}{2}(\psi_2-\psi_1)}{\sin\frac{1}{2}(\psi_2+\psi_1)} \quad . \quad (29\,b)$$

or $\beta\gamma=P/M$ and θ from

$$\frac{M}{P}=\frac{(\sin\psi_1\sin\psi_2)^{\frac{1}{2}}}{\cos\frac{1}{2}(\psi_2+\psi_1)}, \qquad \sin\theta=\frac{(\sin\psi_1\sin\psi_2)^{\frac{1}{2}}}{\sin\frac{1}{2}(\psi_2+\psi_1)}. \quad (29\,c)$$

The problem just treated arises when the momenta have not been measured, but when the origin of a neutral V-event has been located. In this case, however, it may be impossible to distinguish between the particles 1 and 2 ; the sign of α is then undetermined. Evaluation of β and θ, according to (28) or (29), gives two different answers, but often one of them can be discarded.

(v) *The Decay Surface*

The three projections of the decay surface in the space‡ $1/P$, α, ϵ are shown in figs. 11, 12, 13. The surface constitutes half an elliptical cone with axis parallel to the $1/P$-axis. Towards $1/P=0$ the semi-ellipses contract into a straight line. Hence the surface develops into a wedge whose thin end is formed by the segment F_1F_2 of the α-axis. Towards low momenta the cross section changes into a semi-circle, and the decay surface approaches the 'classical' cone of § 6 (i).

III. DETERMINATION OF THE DECAY SCHEME

§ 8. THE DECAY SCHEME

In principle, the parameters p^*, α^*, ϵ^* can be derived from the distribution of the decay events in the three projections, and thus the decay scheme determined from the observations without any preconceptions : the $1/P$, p_t-plane gives p^*, the $1/P$, α or the ϵ, α yields α^* and ϵ^*. This method, however, is only feasible with very good experimental material.

---

† Equivalent expressions have been obtained by M. M. May (Fretter 1953) ; formulae (29) are however simpler.

‡ Thompson *et al.* (1953) have also pointed out the usefulness of plotting the decay events three-dimensionally, in the space $1/P$, α, p_t.

In practice, with not very accurate, or a limited amount of, data, only the parameters p^* and α^* may be expected to be determined with reasonable accuracy. To fix the decay scheme, further information must be invoked. This is provided by assuming the masses of two of the particles to be known.

Together with p^*, α^*, this additional information over-determines the decay scheme. Fixing two masses leads thus to a relation between p^* and α^*. This relation may be used to check the evaluation of p^* and α^*, and enables the values of all decay parameters to be adjusted within narrow limits. For decays into a proton and a π-meson, the relation between p^* and α^* is illustrated in fig. 14. Besides α^*, the energy release Q and the quantity $\alpha^*+\epsilon^*$ are plotted against p^*.

Fig. 14

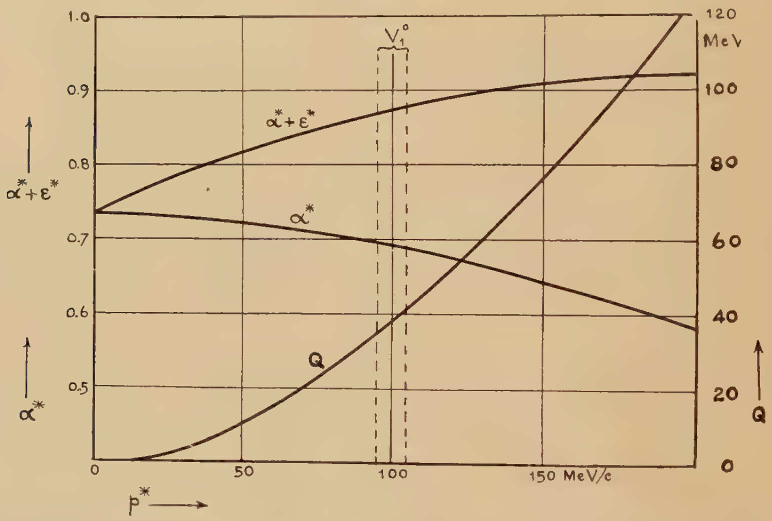

Relation between the decay parameters for decays into a proton and a π-meson.

The following procedure has been found to be very convenient for calculating the curves exemplified by fig. 14. The decay quantities are expressed in terms of *two* angles ρ and σ:

$$\left.\begin{aligned} \alpha^* &= \cos\rho\cos\sigma \\ \epsilon^* &= \sin\rho\sin\sigma \\ p^* &= \tfrac{1}{2}(m_1+m_2)\sin\rho\tan\sigma = \tfrac{1}{2}M\sin\rho\sin\sigma \\ Q &= (m_1+m_2)\tan\sigma\tan\tfrac{1}{2}\sigma = 2M\sin^2\tfrac{1}{2}\sigma. \end{aligned}\right\} \quad . \quad (30)$$

With two of the masses given, ρ and σ are connected by one of the following equalities:

$$\cos\rho = \frac{m_1+m_2}{m_1-m_2}\,.\cos\sigma = \frac{2m_1}{M} - \cos\sigma = \cos\sigma - \frac{2m_2}{M}. \quad . \quad (31)$$

For a range of σ-values, ρ is calculated from (31) and then the decay parameters from (30). For each value of σ, one obtains a set of decay parameters compatible with the assumed mass values.

§ 9. CHECK OF THE DECAY SCHEME

(i) A method of checking the decay events individually against an assumed decay scheme has been described in §§ 6 and 7. The measured values of p_t and P are compared with those expected from the assumed decay scheme. For this comparison one draws the curves p_t=const in the $1/P$, α-projection or the curves p_t=const and P=const in the ϵ, α-diagram.

(ii) Another test consists in taking two of the decay parameters as known and evaluating the third one for each event separately. This method can be applied in different ways :

(*a*) Starting from the assumption that two masses are known, the third mass is calculated by means of the decay relation (1). This is the usual check for the constancy of the Q-values.

(*b*) Alternatively one may start from p^*, α^*, calculate $\epsilon^*=2p^*/M$, and check against the value obtained, e.g. by the method of § 8. The calculation of ϵ^* from the observed values of p_t, α and P of a single decay is conveniently done in two steps :

$$\sin\theta = p_t/p^* \qquad \text{(32 } a\text{)}$$

$$\epsilon^{*2} = \left(\frac{\alpha-\alpha^*}{\cos\theta}\right)^2 - \left(\frac{2p^*}{P}\right)^2 . \qquad \text{(32 } b\text{)}$$

This test is, however, better performed graphically in the $1/P$, α-projection. With θ from (32 *a*), one plots

$$\left|\frac{\alpha-\alpha^*}{\cos\theta}\right| \quad \text{against} \quad \frac{1}{P} . \qquad (33)$$

The event is thereby shifted on to the upper branch of the limiting hyperbola (cf. (32 *b*) and (19 *b*)). To the points (33), therefore, a hyperbola has to be fitted with an asymptote whose slope ($2p^*$) is fixed from the outset. The value of ϵ^* is given by the length of the semi-axis.

(*c*) Finally one may start by assuming M and α^* to be known and again check the value of ϵ^* (Thompson, see Barker (1953)). By plotting

$$\frac{\alpha-\alpha^*}{(1+M^2/P^2)^{\frac{1}{2}}} \quad \text{against} \quad \frac{\epsilon}{M/P} \qquad (34)$$

the events are shifted, in the ϵ, α-plane, on to a semi-circle of radius ϵ^* (cf. (11 *b*)).

We have, however, a preference for the graph (33). It has the advantage of giving to the high energy events the greater weight† they carry in the determination of ϵ^*. But, more important, method (b) is still applicable if no assumptions regarding the masses are made: only the values of p^* and α^*, available directly from the analysis, are needed for the construction.

---

† Low momenta reveal, indeed, the value of p^* only—at least from momenta measurements. In the $1/P$, α-graph this shows up in the fact that, for small P, the branches of the limiting hyperbola are widely apart : the ordinate of an event is of little help in determining the length ϵ^* of the semi-axis. The better position, in this respect, of the high energy events may be counteracted by the greater errors in the momenta.

(d) The method (b) can be exploited in another way by plotting

$$\left(\frac{\alpha-\alpha^*}{\cos\theta}\right)^2 \quad \text{against} \quad \left(\frac{2p^*}{P}\right)^2 \quad . \quad . \quad . \quad (35)$$

and fitting to the points a straight line of slope 1. This intersects the ordinate axis at a distance ϵ^{*2} from the origin.

ACKNOWLEDGMENT

One of the authors (R. A.) would like to express his gratitude to his colleagues of the Pic du Midi group, who, by freeing him of some of the more onerous tasks, made possible his collaboration in this work.

In preparing this paper, we were fortunate to profit by Dr. G. D. Rochester's stimulating suggestions and his competent advice; we like to thank him very warmly. We recollect with pleasure the many discussions we had with our colleagues of the Manchester mountain teams and an animating encounter with Professor R. W. Thompson. The encouragement of Professor P. M. S. Blackett and Professor L. Rosenfeld has been of great value to us.

REFERENCES

ARMENTEROS, R., BARKER, K. H., BUTLER, C. C., and CACHON, A., 1951, *Phil. Mag.* [7], **62,** 1113.

BARKER, K. H., 1953, *Proc. Roy. Soc.* A (to be published).

BLATON, J., 1950, *Dan. Mat. Fys. Medd.*, **24,** No. 20.

BUTLER, C. C., 1951, *Progress in Cosmic Ray Physics* (Amsterdam: North Holland Publishing Company), p. 63.

FRETTER, W. B., MAY, M. M., and NAKADA, M. P., 1953, *Phys. Rev.*, **89,** 168.

LEIGHTON, R. B., WANLASS, S. D., and ANDERSON, C. D., 1953, *Phys. Rev.*, **89,** 148.

STANTON, H. E., 1944, *Phys. Rev.*, **66,** 48.

THOMPSON, R. W., 1952, *Proceedings of the Third Rochester Conference*, p. 39.

THOMPSON, R. W., BUSKIRK, A. V., ETTER, L. R., KARZMARK, C. J., and REDIKER, R. H., 1953, *Phys. Rev.*, **90,** 329.

IV. *Radioactivity of Neutron Excess Iridium Isotopes*

By F. D. S. Butement and A. J. Poë
Atomic Energy Research Establishment, Harwell, Berks.*

[Received October 15, 1953]

Abstract

The half-lives, mass assignments and radiation characteristics of the neutron excess iridium isotopes have been determined as follows :

	^{194m}Ir	^{195}Ir	^{196}Ir	^{197}Ir	^{198}Ir
Half-life	7·3 sec	140 min	9·7 days	7 min	50 sec
β-energy (Mev)	—	2·1, 1·25	0·08	1·6	3·6
γ-energy (Mev)	5·6, 0·125	0·42, 0·66, 0·81, $>$1·0	0·58, 0·76, $\sim$1·0	1·8	0·78

The gamma-ray energies of 19-hour ^{194}Ir have also been examined.

The 7-second ^{194m}Ir isomer is either a 125 kev E3 transition followed by the 5·6 Mev gamma-ray or possibly a 5·6 Mev M6, E6 or E7 transition followed by a 125 kev M1, E2 or E3 gamma-ray. The latter alternative would be the highest spin-change gamma-decaying isomer yet discovered and both are unusual in the very high energy transition involved.

§ 1. Introduction

With the partial exception of 19-hour ^{194}Ir the neutron excess isotopes of iridium have not previously been accurately characterized. Butement (1951) found evidence for ^{195}Ir or ^{197}Ir with a half-life of somewhat above one hour, produced by a (γ, p) reaction on platinum, using 23 Mev x-rays ; but the very low source intensity prevented any accurate study. While the work described below was in progress Christian, Mitchell and Martin (1952) found a 140-minute and a 7-minute iridium activity, the maximum beta-energy of the former being given as about one Mev and the activities being assigned to ^{195}Ir and to ^{195}Ir or ^{197}Ir respectively. This paper describes the production and characterization of the iridium isotopes of mass 194 to 198 inclusive.

§ 2. Experimental Techniques

The techniques for preparing the isotopes and studying their radiations were similar to those previously described (Butement and Shillito 1952). The isotopes were prepared by (n, p), (n, pn) and (γ, p) reactions on platinum using neutrons of energies up to 48 Mev and 28 Mev x-rays from a synchrotron. For half-lives so short that no chemical separation of the iridium was possible, discs of platinum metal were irradiated. For intermediate half-lives platinum chloride, and for long half-lives finely divided platinum metal, were irradiated, chemical separation of the iridium using an inactive carrier then being possible by standard methods.

---

* Communicated by the Authors.

§ 3. Results

(i) *Half-lives and Mass Assignments*

(n, p) and (n, pn) reactions in the cyclotron together produced activities with half-lives of 50 seconds, 7 minutes, 140 minutes, 19 hours, 9·7 days and 70 days in both beta- and gamma-decay, while a 7-second activity was observed in gamma-decay only. (n, p) reactions alone produced all the above activities except the 7-minute. (γ, p) reactions produced the 7-minute, 140-minute and 19-hour activities but the 50-second, 9·7-day and 70-day activities were not detected. All activities except the 7-second and 50-second were radiochemically identified as iridium. The 19-hour and 70-day activities correspond to the well known ^{194}Ir and ^{192}Ir. Of the remaining activities the 140-minute and 7-minute can be unambiguously assigned to ^{195}Ir and ^{197}Ir respectively while the 9·7-day and 50-second activities are most probably associated with ^{196}Ir and ^{198}Ir respectively. The approximate yields of the 19-hour, 140-minute and 7-minute isotopes from (γ, p) reactions on platinum were in the ratio 8 : 4 : 1 as compared with the relative abundances of the ^{195}Pt, ^{196}Pt and ^{198}Pt isotopes of 4·7 : 3·5 : 1 and to the yield ratio 5·3 : 3·7 : 1 obtained by Christian, Mitchell and Martin (1952).

The 7-second gamma-decay was also observed when ‘ Specpure ’ iridium metal was irradiated in the cyclotron by neutrons of energy $\gtrsim$15 Mev and it must therefore be associated with ^{190}Ir, ^{192}Ir or ^{194}Ir. The yields of the 7-second and 50-second isotopes after (n, p) reactions on platinum were about the same, so that the 7-second decay cannot be assigned to ^{190}Ir, which would be formed from the very scarce ^{190}Pt. It is therefore either ^{192}Ir or ^{194}Ir. Theoretical consideration of the radiation characteristics supports an assignment to ^{194}Ir (see below).

(ii) *Radiations*

(*a*) 50-*second* ^{198}Ir. The maximum beta-energy was found from the aluminium absorber curves to be 3·6±0·3 Mev, using Behrens' nomogram (1950). Each point on the curve (fig. 1) was found from a separate irradiation. The gamma-ray energy was measured by the photographic scintillation spectrometer which showed one 0·78 Mev gamma-ray decaying with about the right half-life. Knowing the efficiencies of the counters, the ratio of beta- to gamma-transitions was found to be 1 : 1, and the gamma-rays were found to be in coincidence with the beta-particles.

The decay scheme is therefore simply a 3·6 Mev beta-transition followed by a 0·78 Mev gamma-ray. The total decay energy of 4·4 Mev supports the assignment of this activity to ^{198}Ir, for which the decay energy calculated from the semi-empirical mass tables of Metropolis and Reitwiesner (1950) is 3·3 MeV.

(*b*) 7-*minute* ^{197}Ir. The aluminium absorber curve found as the result of several runs indicated a maximum beta-particle energy of 1·6±0·2 MeV, the shape of the curve indicating one or more lower energy beta-transitions. Aluminium absorption of beta-particles in coincidence with gamma-rays showed that the higher energy beta-decay does not go to the ground state of the daughter nucleus. The gamma-ray spectrum was examined photographically and a gamma-ray of 1·8 MeV was found.

Fig. 1

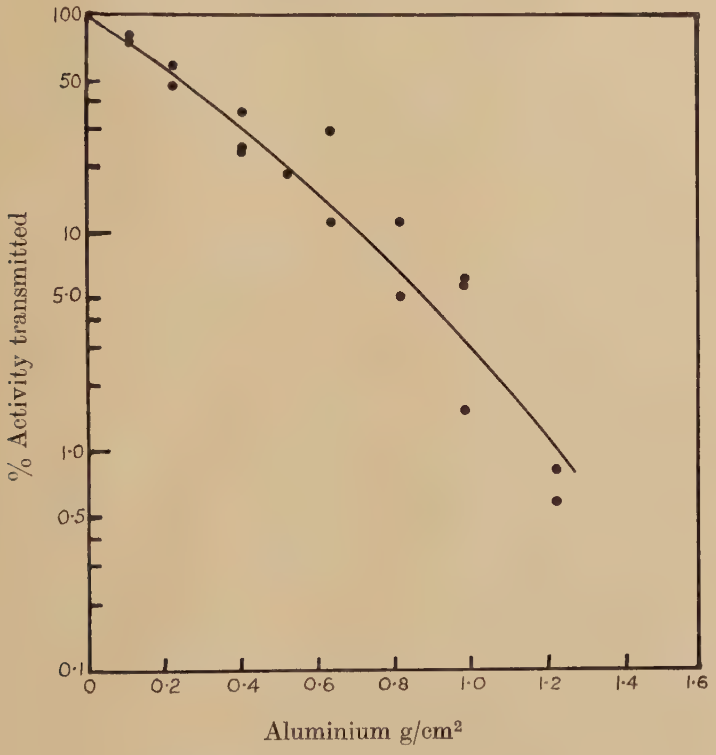

Absorption of radiation from 50 sec ^{198}Ir

Any other gamma-ray energies were not resolvable from the large amount of gamma-rays from the 140-minute and 19-hour activities present.

(*c*) 9·7-*day* ^{196}Ir. Aluminium absorption of the beta-particles from the mixture of this and the 70-day isotope indicated two beta-transitions of energy 80±20 kev and 0·67 MeV. Beta-activity passing through 12 mg/cm^2 of aluminium decayed with a 70-day half-life. The principal beta-energy of the 9·7-day isotope is therefore 80 kev, though there may be up to about 5% of a higher energy beta-transition which would not have shown up in the decay through 12 mg/cm² of aluminium. An accurate absorption curve for the 9·7-day isotope was not obtained because the corrections for the 70-day background were large.

Examination of the gamma-ray spectrum was effected using a scintillation spectrometer and single channel pulse analyser. Gamma-ray energies of 0·58 and 0·76 Mev were observed, the latter probably being two unresolved gamma-rays of similar energy. There were also some unresolved gamma-rays of about one Mev energy. The 0·58 Mev gamma-ray was resolved from a ^{192}Ir gamma-ray of similar energy by following its decay relative to the 0·31 and 0·47 Mev ^{192}Ir gamma-rays. 0·80 and 0·94 Mev gamma-rays from ^{192}Ir were also observed in fair agreement with observations by Roulston and Pringle (1952) of 0·775 and 0·870 Mev.

The ratio of beta- to gamma-counts and the beta- and gamma-counting efficiencies, as measured by coincidence counting techniques, indicated that there are relatively more beta-particles than gamma-rays and the decay scheme is therefore complex, some at least of the apparent beta-particles probably being conversion electrons.

The assignment of the 9·7-day activity to ^{196}Ir is plausible but not certain.

(*d*) 140-*minute* ^{195}Ir. Absorption of beta-particles indicated a beta-transition of 2·1±0·1 Mev energy together with a lower energy component. Absorption of beta-particles coincident with gamma-rays, however, indicated a beta-transition of energy 1·25±0·10 Mev, a softer component again being present (fig. 2). The 2·1 Mev beta-transition therefore goes to the ground state of the daughter nucleus.

The activity of this isotope obtained for the investigation of the gamma-ray spectrum was rather low for examination with the pulse analyser, but gamma-rays of energy 0·42, 0·66 and 0·81 Mev were indicated together with a 70 kev component, presumably an x-ray, and other unresolved gamma-rays of low intensity above one Mev. The 0·66 Mev gamma-ray was resolved from a ^{194}Ir gamma-ray of similar energy by following the decay. The 126 and 97 kev gamma-rays known to be associated with the ^{195}Pt nucleus, following the decay of ^{195}Au, were not observed. However, they would not follow directly after a beta-transition, as no high energy beta-disintegration followed by a low energy gamma-ray occurs and gamma-transitions from higher energy levels would not necessarily go via these low lying levels.

The total decay energy of 2·1 Mev is considerably higher than the theoretical prediction of 1·0 Mev based on the tables of Metropolis and Reitwiesner (1950).

(*e*) 19-*hour* ^{194}Ir. The gamma-rays from this isotope were examined using the pulse analyser scintillation spectrometer and gamma-rays of energy 0·32, 0·61, 1·18, 1·45 and ~1·8 Mev were detected, the approximate intensities being in the ratio 100 : 22 : 10 : 5 : 1·2 respectively. The 0·61 and 1·18 Mev gamma-rays have not previously been reported.

Sources for these experiments were obtained both by pile irradiation of 'Specpure' iridium and by cyclotron irradiations of platinum.

(*f*) 7-*second* ^{194m}Ir. This was prepared by the irradiation of platinum or iridium by fast neutrons in the cyclotron, the samples being transferred to the counter within ten seconds of the end of the irradiation. The gamma-rays of this isomer were examined with the photographic scintillation spectrometer and found to have energies of 125 kev and 5·6±0·2 Mev, the latter being compared with the 4·45 Mev gamma-ray from a polonium–beryllium source, and measurements being made both on the peak due to pair production in the NaI crystal and on that due to pair production with one annihilation quantum absorbed. The iridium K x-ray was also present in slightly greater intensity than the 125 kev gamma-ray.

Fig. 2

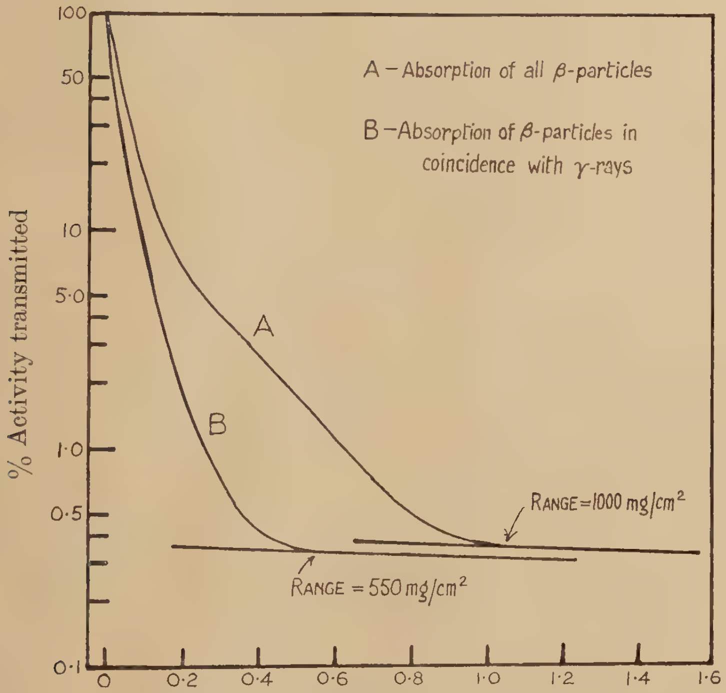

Aluminium g/cm²

Absorption of radiation from 140 min ^{195}Ir

The half-life of the isomer was found to be 7·3±0·1 seconds by using a fast tape recorder and applying a discriminator bias to the counter so that only the 5·6 Mev gamma-rays were counted. The 125 kev gamma-ray and the x-ray were also found to decay with a 7-second half-life, using a differential bias discriminator.

Applying Weisskopf's equations (1952) relating transition probability for gamma-ray emission with nuclear mass, spin change and energy the half-life of a 5·6 Mev isomeric transition in ^{192}Ir or ^{194}Ir (internal conversion being negligible at such high energy) will be as follows, using Goldhaber and Sunyar's classification (1951) :

Transition Type	E	M	E	M	E	M
Spin change	5	5	6	6	7	7
Parity change	Yes	No	No	Yes	Yes	No
Half-life (seconds)	6×10^{-6}	10^{-3}	2×10^{-2}	3·5	92	$1{\cdot}6\times10^{4}$

Similarly the half-life of a 125 kev transition (making no correction for internal conversion) will be :

Transition Type	M	E	M	E
Spin change	2	3	3	4
Parity change	Yes	Yes	No	No
Half-life (seconds)	$2{\cdot}3\times10^{-5}$	0·32	56·2	$2{\cdot}7\times10^{6}$

The K conversion ratio of the 125 kev transition, as measured by the ratio of the intensities of the X- and gamma-rays in the spectrometer oscilloscope photographs and in pulse-analyser experiments, is about 1·5. From the calculations of Rose *et al.* (1951) this defines the 125 kev gamma-ray as an E2, E3 or M1 transition. The K/L conversion ratio for the E3 transition obtained from the graphs of Goldhaber and Sunyar (1951) is ~0·2. The calculated half-life of the 125 kev E3 transition, correcting the value obtained above for internal conversion, is therefore $0{\cdot}32\ (1+1{\cdot}5+5\times1{\cdot}5)=3{\cdot}2$ seconds.

The decay from the metastable state may therefore occur in one of two ways :

(*a*) A 7-second half-life, 5·6 Mev transition of type E6, M6 or E7 followed by a 125 kev, partly converted, gamma-ray of type M1, E2 or E3.

(*b*) A 7-second half-life, 125 kev transition of type E3 followed by a 5·6 Mev gamma-ray of unknown type.

The isomer cannot be assigned to ^{192}Ir which is known to have a metastable state of spin 3 above the ground state and it must therefore be ^{194m}Ir.

It is not found possible to detect this isomer after irradiation of iridium with thermal neutrons in the pile or with neutrons of energy less than about 15 Mev in the cyclotron. Since ^{193}Ir has a spin of 3/2 (Bene *et al.* 1949) this indicates that the metastable ^{194m}Ir has a fairly high spin, being formed only via a high spin compound nucleus resulting from capture of a neutron carrying high angular momentum. This is only possible with relatively high energy neutrons and this is why the cross section for the reaction increases with energy in spite of the increasing probability of a neutron being re-emitted instead of being captured.

^{194}Ir is an odd–odd nucleus with 77 protons and 117 neutrons. Several shell model interpretations of the above decay schemes can be formulated. For example, shell theory suggests that the odd proton will be in the $d_{3/2}$ level and the odd neutron in the $p_{1/2}$ level. A ground level state of spin 1 and odd parity can be obtained by the subtraction of these spins, and a first excited level of spin 2 and odd parity by their addition. A higher level of spin 8 and even parity from the addition of the $d_{3/2}$ proton spin and an $i_{13/2}$ neutron spin would then give a consistent interpretation of decay scheme (*a*), the 5·6 MEV rate-determining transition being M6 and the 125 kev transition M1. At such high energies, however, the shell model is probably not strictly applicable and multiple excitation of both a neutron and a proton may well occur.

The occurrence of a high energy and high spin change transition as in decay scheme (*a*) would be very surprising in a heavy odd–odd nucleus where the many combinations of neutron and proton spins would be expected to give several levels of intermediate energy and spin, so that cascade emission could occur. In decay scheme (*b*) the energy, spin and parity of levels up to 5·6 MEV must be limited in such a way that the probability of transitions to them from the meta-stable level is less than the probability of the 125 kev transition, as well as in such a way that the 5·6 MEV transition is preferred to a cascade.

ACKNOWLEDGMENTS

Acknowledgment is gratefully made to Mr. R. B. Owen for carrying out some of the measurements of gamma-ray energies, to Mr. E. J. Jones for carrying out synchrotron irradiations, to the members of the cyclotron group for carrying out irradiations, to Mr. B. H. Flowers for helpful discussions and advice and to the Director, Atomic Energy Research Establishment, for permission to publish these results.

REFERENCES

BEHRENS, D. J., 1950, A.E.R.E. Report T/M. 6.
BENE, J. G., DENIS, P. M., and EXTERMAN, R. C., 1949, *Helv. Phys. Acta*, **22,** 606.
BUTEMENT, F. D. S., 1951, *Proc. Phys. Soc.* A, **64,** 395.
BUTEMENT, F. D. S., and SHILLITO, R., 1952, *Proc. Phys. Soc.* A, **65,** 945.
CHRISTIAN, D., MITCHELL, R. F., and MARTIN, D. S., 1952, *Phys. Rev.*, **86,** 946.
GOLDHABER, M., and SUNYAR, A. W., 1951, *Phys. Rev.*, **83,** 906.
METROPOLIS, N., and REITWIESNER, G., 1950, United States A.E.C. Report, NP. 1980.
ROSE, M. E., GOERTZEL, G. H., and SPINRAD, B. I., 1951, *Phys. Rev.*, **83,** 79.
ROULSTON, K. I., and PRINGLE, R. W., 1952, *Phys. Rev.*, **87,** 930.
WEISSKOPF, V. F., 1951, *Phys. Rev.*, **83,** 1073.

V. *The Mean Lifetime of the* V_1^0*-Particles*

By D. I. Page and J. A. Newth
The Physical Laboratories, The University, Manchester*

[Received October 21, 1953]

Abstract

The mean lifetime of V_1^0-particles has been determined from measurements on 26 selected V-decays observed in a large cloud chamber. The chief criterion for selection was that the momentum of the positive secondary particle should be at least three times as great as that of the negative particle. It is shown that this selects events which are predominantly V_1^0-decays. The decay scheme of the particles is assumed to be

$$V_1^0 \rightarrow P^+ + \pi^- + \sim 37 \text{ Mev.}$$

The result of the analysis gives a value of $(3{\cdot}7\,^{+3\cdot9}_{-1\cdot3}) \times 10^{-10}$ sec for the mean lifetime. Combining this with other published values, it is concluded that the lifetime is probably between 3·0 and $4{\cdot}5 \times 10^{-10}$ sec.

§ 1. Introduction

About 200 neutral V-particle decays have been observed in an experiment carried out at the Jungfraujoch (3580 m). Half the decays were observed in a cloud chamber that has been described previously (Astbury *et al.* 1952). The remainder occurred in a new, deeper chamber with an illuminated volume measuring 55 cm × 55 cm × 16 cm situated in a magnetic field of 5200 gauss. The V-particles came from nuclear interactions in lead placed above the cloud chamber.

An outstanding feature of the V-particle decays is their lack of symmetry. In the majority of the events the momentum of the positively charged secondary particle is much greater than that of the negative particle; events for which the converse is true are rare. This asymmetry is readily explained if a large proportion of the V-particles decay into a proton and a negative π-meson. This mode of decay was suggested by Armenteros *et al.* (1951) and further evidence for its correctness has come from the work of Leighton *et al.* (1953), Bridge *et al.* (1953) and Millar and Page (1953). The decay scheme that is deduced for these particles is

$$V_1^0 \rightarrow P^+ + \pi^- + \sim 37 \text{ Mev.} \qquad \qquad (1)$$

The asymmetry of their mode of decay has been used to separate V_1^0-decays from other neutral V-decays. From these events the mean lifetime of the V_1^0-particles has been estimated. The details of the separation and the analysis are discussed in § 2 and § 3 below.

---

* Communicated by Professor P. M. S. Blackett, F.R.S.

§ 2. SELECTION OF V_1^0-PARTICLES

The separation of V_1^0-particles is most easily described by reference to a study by Podolanski and Armenteros (1954) of the dynamics of two-body decay processes. They introduce a dimensionless parameter (α) which is related to the masses (M, m_+, m_-) and momenta (P, p_+, p_-) of the primary and secondary particles by the equations

$$\alpha = \frac{p_+^2 - p_-^2}{P^2} = \frac{m_+^2 - m_-^2}{M^2} + 2p^* \cos\theta^* \left(\frac{1}{M^2} + \frac{1}{P^2}\right)^{1/2} \quad . \quad . \quad (2)$$

where p^* is the momentum of either secondary particle in the centre of mass frame of reference and θ^* is, in the same frame of reference, the angle of emission of the positive secondary particle measured from the direction of flight of the primary particle.

Since the direction of decay in the centre of mass system is expected to be randomly orientated the average value of $\cos\theta^*$ for a number of decays will be zero. The average value of α for particles with the same mode of decay is thus

$$\alpha^* = \frac{m_+^2 - m_-^2}{M^2}.$$

For the V_1^0-particles α^* has the value 0·69 while for any decay scheme in which $m_+ = m_-$ the value of α^* is zero.

The range of the allowed values of α increases as P decreases. This is displayed in the figure where α is plotted against $1/P$. The region within which α must lie for a particular mode of decay is bounded by the hyperbolae (2) with $\cos\theta^* = \pm 1$. In the figure these boundaries are shown for the V_1^0-decay scheme and for the suggested scheme $V_2^0 \rightarrow \pi^+ + \pi^- + \sim 210$ MEV (Armenteros *et al.* 1951, Thompson *et al.* 1953).

Equation (2) reveals a property of α which is important in a statistical treatment of V-decays. If the decay process is isotropic in the centre of mass frame of reference the distribution of values of $\cos\theta^*$ is rectangular between ± 1. This means that the α-values obtained from V-decays should be uniformly distributed between the limits shown in the figure. (The distribution is only uniform along lines of constant momentum; along the $1/P$ axis it is determined by the spectrum of the decaying particles.)

Most of the V-particles observed to decay in our experiment had momenta greater than 10^9 ev/c. The figure shows that α is greater than 0·5 for nearly all V_1^0-particles with momenta in this range. Moreover, only about 25% of V_2^0-particles have $\alpha > 0{\cdot}5$.

Rather than use α itself, the ratio p_+/p_- can be used to select decays with large values of α. If ϕ is the angle between the trajectories of the secondary particles in the cloud chamber

$$P^2 = p_+^2 + p_-^2 + 2p_+p_- \cos\phi \leqslant (p_+ + p_-)^2.$$

From (2)

$$\alpha = \frac{p_+^2 - p_-^2}{P^2} \geqslant \frac{p_+ - p_-}{p_+ + p_-}.$$

This shows that events for which $p_+ > 3p_-$ necessarily satisfy the condition $\alpha > 0{\cdot}5$.

The three conditions satisfied by the events selected for analysis were

(*a*) the measurable track of each secondary particle was at least 10 cm long,

(*b*) the ratio p_+/p_- obtained by measuring 10 cm lengths of the tracks was greater than 3 and

(*c*) the values of p_+, p_-, ϕ and the ionization densities of the tracks were consistent with the event being a $V_1{}^0$-decay.

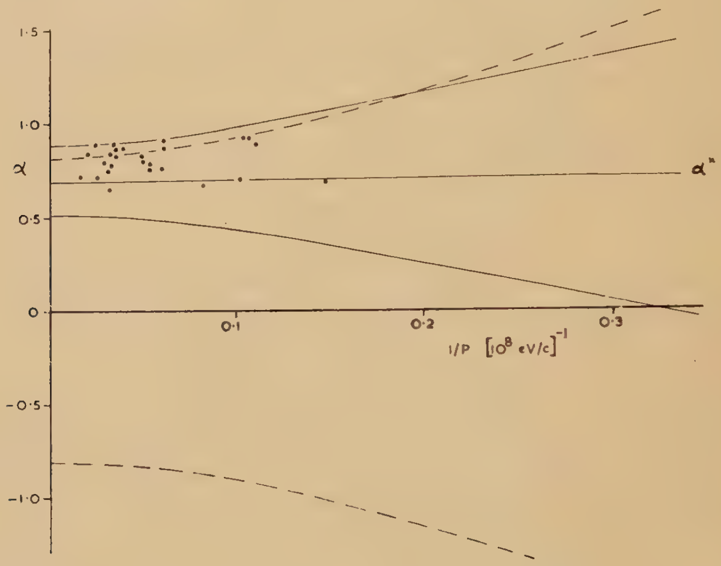

Diagram showing the allowed values of α as a function of $1/P$. The solid lines correspond to the decay scheme of the $V_1{}^0$-particles with a Q-value of 37 Mev and the interrupted lines are for $V_2{}^0$-particles decaying into two π-mesons with a Q-value of 210 Mev.

The points on the diagram represent the 26 events referred to in the text and the values of α have been calculated *on the assumption* that the events are $V_1{}^0$-decays.

The upper limit of momentum measurement on tracks 10 cm long is $1{\cdot}5 \times 10^9$ ev/c so that condition (*b*) selected, in general, events with $p_- \leqslant 5 \times 10^8$ ev/c. However, for three events there was an evident origin for the V-particle and condition (*b*) was satisfied by angle measurements using the fact that $p_+/p_- = \sin\theta_-/\sin\theta_+$ where θ_+ and θ_- are the angles the secondary tracks make with the line of flight of the primary.

§ 3. Measurements and Analysis

For each of the 26 selected events the momenta p_+ and p_- were derived from the track curvatures. Frequently only a lower limit could be put to p_+. However, by assuming the decay scheme (1) the values of p_+

and P were found from the more accurate measurements of p_- and ϕ. The possible error introduced by this procedure is discussed in § 4.

The events were reprojected stereoscopically and the angle (ϕ) between the secondary tracks was measured. The line of flight of the V-particle was determined and the distance (l) between the point of decay and the point where the V-particle entered the illuminated volume of the chamber was measured. In addition, the potential path (L) inside the chamber was found. This potential path is the distance between the extreme positions on the V-particle's trajectory where the decay would have satisfied the conditions given in § 2. This meant that every point where the decay would have produced secondary tracks 10 cm long was included in the potential path.

Table 1. Time of Flight Observations on V_1^0-Particles

Event	P (10^8 ev/c)	l (cm)	L (cm)	t (10^{-10} sec)	T (10^{-10} sec)
JB 85	18·2	0·6	35·9	0·1	8·2
LG 96	9·5	1·8	2·5	0·7	1·0
NC 79	37·0	28·2	36·6	2·5	3·3
NJ 97	9·5	2·6	6·1	1·0	2·4
NR 14	30·4	15·5	32·0	1·8	3·8
NU 178	31·0	1·2	32·2	0·1	3·9
NW 35	15·8	11·0	18·5	2·5	4·2
NY 21	58·5	26·0	28·0	1·6	1·7
NZ 49	27·5	21·5	32·0	2·8	4·2
OC 64	28·1	16·7	37·5	2·2	4·9
OD 555	19·5	10·0	33·2	1·9	6·3
OE 119	18·2	2·0	8·4	0·4	1·3
PB 150	9·7	13·6	37·0	5·2	14·1
PB 206	47·5*	15·5	18·5	1·2	1·5
PC 151	25·2	10·5	34·0	1·6	5·1
PE 346	16·0	16·4	23·8	3·8	5·5
PF 27	30·5*	30·0	35·5	3·6	4·3
PH 449	33·8	2·2	35·6	0·2	3·9
PK 28	20·0	2·6	35·6	0·5	6·8
QI 575	12·0	4·5	33·0	1·4	10·4
QJ 118	29·2	25·6	39·7	3·3	5·2
QJ 176	28·8	12·0	37·0	1·6	4·8
QL 46	6·7	2·2	6·4	1·2	3·5
QL 272	16·5	10·0	15·3	2·2	3·4
QL 329	8·9	0·2	3·0	0·1	1·3
QL 759	39·0	1·8	35·0	0·1	3·2

Details of the 26 events analysed in the experiment. P is the momentum of the neutral V-particle, l and L are the length of the trajectory in the chamber before decay and the potential length respectively. t and T are the corresponding proper times of flight.

The times of flight (t, T) corresponding to the distances l and L were then obtained from the relation $t = l \times M/P$. These times are given in table 1 together with the values of l, L and P for the 26 events.

Bartlett (1953 a) has described in detail how a maximum likelihood estimate of the mean lifetime (τ) can be obtained from a set of values (t_i, T_i). He shows that the statistical error in the estimate of the decay constant $(1/\tau)$ is approximately symmetrical and gives an interpolation procedure for finding the best value and standard error of $1/\tau$.

This procedure, when applied to the times of flight listed in table 1, leads to the result that

$$1/\tau = (0{\cdot}27 \pm 0{\cdot}14) \times 10^{10}\ \mathrm{sec}^{-1}$$

corresponding to
$$\tau = (3{\cdot}7^{+3{\cdot}9}_{-1{\cdot}3}) \times 10^{-10}\ \mathrm{sec}$$

where only the statistical error is quoted. Other sources of error are discussed in § 4.

From the measured values of p_- and the derived values of p_+ and P the values of α for the decays were calculated. The results are displayed in the figure. The fact that all the values of α are greater than 0·6 means only that the selection of events with $p_+/p_- > 3$ was over-cautious. If the events are $V_1{}^0$-decays the ratio p_+/p_- is greater than 4 in every case. It must be emphasized that the points in the figure do *not* represent measured values of α; they are calculated on the assumption that the events were $V_1{}^0$-decays.

§ 4. NON-STATISTICAL ERRORS

There are two important sources of error in the above result that have to be considered. The first is the presence among the selected events of decays not due to $V_1{}^0$-particles and the second is the uncertainty in determining the momenta P from the measured values of p_- and ϕ. By comparison, the errors involved in measuring l and L are trivial. The energy release in the decay of $V_1{}^0$-particles may well be greater than the value of 37 MEV that we have assumed (Armenteros *et al.* 1953 give a value of 40 to 45 MEV) but this uncertainty has only a small effect on the derived lifetime.

The number of particles erroneously classified as $V_1{}^0$-particles can be estimated if the α-values for all other V-decays are symmetrically distributed about $\alpha = 0$. This is true of the decay into two π-mesons suggested for $V_2{}^0$-particles and would also hold for a decay into a heavy and a light meson (Leighton *et al.* 1953) unless the heavy meson were preferentially positively charged.

Only three of the 200 V-decays examined have $\alpha < -0{\cdot}5$ and would satisfy the selection conditions of § 2 if the signs of the decay products were reversed. From the symmetry assumed for the α-values we expect three events which are not $V_1{}^0$-decays to have been included among the

26 events analysed.† The bias due to this dilution of the V_1^0-decays is certainly small—especially since the lifetime estimated for the V_2^0-particles is of the same order of size as that of the V_1^0-particles (Fretter *et al.* 1953, Bridge *et al.* 1953).

An error arises in the determination of P from p_- and ϕ since, for given values of p_- and ϕ, P is double-valued. In many cases one of the possible values can be excluded by measurement of p_+ but for some events values of P differing by a factor of two would fit the measurements equally well. In these cases (marked by an asterisk in table 1) the higher of the two values of P was used in the analysis. Fortunately, the events for which this uncertainty arises contribute very little to the final value of τ.

Apart from this ambiguity there is a random error of ~25% in the values of P arising directly from the errors in p_- and ϕ. The effect of this error is much smaller than the present statistical error in τ.

§ 5. DISCUSSION

The result quoted in § 3 can be compared with several other reported values for the mean lifetime. These are set out in table 2.

Table 2. Estimates of the Mean Lifetime of V_1^0-Particles

Authors	Number of events	Mean Lifetime (10^{-10} sec)
Fretter *et al.* (1953)	22	10 ± 7
Alford and Leighton (1953)	74	$2{\cdot}5 \pm 0{\cdot}7$
,, ,, (' High Q ' events)	20	$1{\cdot}3 \pm 0{\cdot}5$
,, ,, (' Low Q ' events)	37	$2{\cdot}9 \pm 0{\cdot}8$
Bridge *et al.* (1953)	21	$3{\cdot}5 \pm 1{\cdot}2$
Deutschmann (1953, unpublished)	22	$4{\cdot}8^{+2{\cdot}6}_{-1{\cdot}3}$
Gayther (1953, unpublished)	21	$4{\cdot}0^{+3{\cdot}1}_{-1{\cdot}2}$
Present paper	26	$3{\cdot}7^{+3{\cdot}9}_{-1{\cdot}3}$

The values of the mean lifetime of V_1^0-particles obtained in six different experiments. The results of Alford and Leighton and that reported in this paper were obtained from V-decays observed in magnet cloud chambers. The other four results have been obtained from multiplate cloud chamber experiments.

The various results are discussed briefly in § 5.

---

† Newth and James (1953) concluded that only about 50% of the fast V-decays observed in these experiments were V_1^0-decays. If the remainder are V_2^0-decays inspection of figure shows that a quarter of them (i.e. 12% of all V-decays) will have $\alpha > 0{\cdot}5$. This leads to the conclusion that 80% of the decays *with* $\alpha > 0{\cdot}5$ are V_1^0-decays. The proportion of V_1^0-decays is thought to be higher among the 26 events reported here partly because the value of α was not the only criterion of selection and partly because Newth and James considered V-particles with momenta above 10^9 ev/c only—for lower momenta the proportion of V_1^0-particles may well be higher than 50%.

The result of Fretter and his collaborators may be biased since they disregarded the presence of the lead plates in their cloud chamber when analysing their measurements. They state that if the plates are evenly spaced ignoring their presence introduces no bias in the result. This is certainly true if the plates are sufficiently thin. However, if the time spent by a V-particle in such an unobservable region of the cloud chamber is comparable with its mean life this fact must be taken into account in the analysis. If it is ignored a bias tending to increase the derived lifetime is introduced. How important this bias is in any particular experiment is difficult to assess but Bridge *et al.* (1953) have shown how the bias may be avoided and Bartlett (1953 b) has extended his estimation equations to deal with this kind of experiment. The published data of Fretter *et al.* are not sufficiently detailed for an unbiased estimate to be made from them. In addition, since the statistical error in the result depends upon the potential times of flight in a rather complicated way, ignoring the lead plates which obscure about 20% of the trajectories of their particles has led Fretter *et al.* to underestimate the error in their result.

Alford and Leighton have analysed by far the largest number of V-decays and have estimated lifetimes from the maximum likelihood equation. They use an approximate formula for the statistical error which gives a result symmetrical in τ. The classification of their V-particles is based on the work of Leighton *et al.* (1953) who state that only 20% or less of their V-decays could be of the V_2^0 type where the secondaries are of equal mass. Nearly all the remainder are consistent with decay into a proton and a π^--meson with a measured energy release varying from 10 to 100 MeV. This wide spread in Q-values leads Alford and Leighton to make tentative lifetime estimates for the 'low Q' events and the 'high Q' events, the division being made at a Q-value of 50 MeV. The results of these separate estimates are given in table 2.

There is no difficulty in identifying the 'low Q' decays with the V_1^0-decay scheme (1) but Leighton *et al.* consider it 'quite unlikely' that the whole spread in Q-values is due solely to errors in measurement. It seems possible to us that some of the 'high Q' events are, in fact, V_2^0-decays. This interpretation would reduce the discrepancy between the small number of V_2^0-decays found by Leighton *et al.* and the larger proportion found by Newth and James (1953) and by Thompson *et al.* (1953) in similar experiments. It would also account for the shorter lifetime of the 'high Q' events since the lifetime of the V_2^0-particles is shorter than that of the V_1^0-particles (Fretter *et al.* 1953, Bridge *et al.* 1953, Astbury 1953). However, the 'high Q' events with identified proton secondaries could not be explained in this way and the scarcity of decays with negative α-values found by Leighton *et al.* would have to be regarded as an unlikely statistical fluctuation. It is clear that further experimental evidence is necessary before these difficulties can be resolved.

Bridge *et al.*, Deutschmann, and Gayther observed their *V*-decays in multiplate cloud chambers. In each experiment the measurements have been analysed to avoid the bias referred to in connection with the result of Fretter *et al.* Bridge *et al.* consider that their result can best be expressed in the form

$$1/\tau=(0{\cdot}29\pm0{\cdot}11)\times10^{10}\ \mathrm{sec}^{-1}$$

or

$$\tau=(3{\cdot}5^{+2{\cdot}1}_{-1{\cdot}0})\times10^{-10}\ \mathrm{sec}$$

to take account of the asymmetry of the error in τ.

These workers also state that they have made no allowance for the nuclear interaction of the *V*-particles in the lead plates of their cloud chamber. If the cross section for nuclear absorption were appreciable their estimate of the lifetime would be biased to a low value. A very rough calculation of this effect using their data and assuming an absorption length of 150 g/cm^2 for *V*-particles in lead gives a bias of less than 5%. It is clear that the determination of the nuclear interaction of *V*-particles from lifetime measurements made in chambers with and without lead plates is a very remote possibility.

§ 6. CONCLUSIONS

The values for the mean lifetime given in table 2 can be combined together to give a weighted mean value. This has been done by weighting the separate values of $1/\tau$ inversely as their variance and then finding the weighted mean value and standard error in $1/\tau$. This procedure is justifiable since the errors in the separate results are largely statistical and the values of $1/\tau$ are expected to be approximately normally distributed.

The result of Fretter *et al.* has been excluded since it may contain a large bias. The result obtained by Alford and Leighton for their ‘ low *Q* ’ events has been used in view of the admitted uncertainty about the homogeneity of the events included in their main analysis. The fractional error in τ quoted for their result by Alford and Leighton has been transferred directly to the $1/\tau$ scale.

With these restrictions the weighted mean lifetime is found to be given by

$$1/\tau=(0{\cdot}27\pm0{\cdot}05)\times10^{10}\ \mathrm{sec}^{-1}$$

or

$$\tau=(3{\cdot}7^{+0{\cdot}8}_{-0{\cdot}6})\times10^{-10}\ \mathrm{sec}.$$

The agreement between the results obtained by workers with different types of apparatus observing *V*-particles of different energy is extremely satisfactory. The error in the ‘ best value ’ given above is still mainly the inherent statistical error. Since this value is derived from measurements on 127 events it is clear that many hundreds of events will be required before the statistical uncertainty in the lifetime can be made as small as the error due to our ignorance of the exact *Q*-value of the V_1^0-particles.

ACKNOWLEDGMENTS

The events discussed in this paper were recorded at the Jungfraujoch Research Station in Switzerland. We are grateful to the Administration of the Station and to the manager, Mr. Hans Wiederkehr, for making our work there possible.

Several colleagues in Manchester have cooperated in the maintenance of the cloud chamber and in interpreting the results. In particular, Dr. J. P. Astbury made many calculations and measurements that we have used.

Dr. M. Deutschmann and Mr. D. B. Gayther have very kindly allowed us to quote their conclusions before publication. Dr. R. Safford of the Massachusetts Institute of Technology and Professor M. S. Bartlett in Manchester have been most helpful in discussing the results of experiments with multiplate cloud chambers.

We have profited greatly from the advice of Professor P. M. S. Blackett and are grateful to him for supporting our work. One of us (D. I. P.) has received a grant from the Department of Scientific and Industrial Research during the course of this work.

REFERENCES

ALFORD, W. L., and LEIGHTON, R. B., 1953, *Phys. Rev.*, **90**, 622.

ARMENTEROS, R., BARKER, K. H., BUTLER, C. C., and CACHON, A., 1951, *Phil. Mag.*, **42**, 1113.

ARMENTEROS, R., BARKER, K. H., BUTLER, C. C., COATES, M. S., and SOWERBY, M. G., 1953, *Phil. Mag.*, **44**, 861.

ASTBURY, J. P., 1953, *Report of the Bagnères Conference on Cosmic Radiation.*

ASTBURY, J. P., CHIPPINDALE, P., MILLAR, D. D., NEWTH, J. A., PAGE, D. I., RYTZ, A., and SAHIAR, A. B., 1952, *Phil. Mag.*, **43**, 1283.

BARTLETT, M. S., 1953 a, *Phil. Mag.*, **44**, 249 ; 1953 b, *Ibid.*, **44**, 1407.

BRIDGE, H. S., PEYROU, C., ROSSI, B., and SAFFORD, R., 1953, *Phys. Rev.*, **91**, 362.

FRETTER, W. B., MAY, M. M., and NAKADA, M. P., 1953, *Phys. Rev.*, **89**, 168.

LEIGHTON, R. B., WANLASS, S. D., and ANDERSON, C. D., 1953, *Phys. Rev.*, **89**, 148.

MILLAR, D. D., and PAGE, D. I., 1953, *Phil. Mag.*, **44**, 1049.

NEWTH, J. A., and JAMES, G. D., 1953, *Report of the Bagnères Conference on Cosmic Radiation.*

PODOLANSKI, J., and ARMENTEROS, R., 1954, *Phil. Mag.*, **45**, 13.

THOMPSON, R. W., BUSKIRK, A. V., ETTER, L. R., KARZMARK, C. J., and REDIKER, R. H., 1953, *Phys. Rev.*, **90**, 329.

VI. *Angular and Energy Distributions in Energetic Pion Interactions with Nuclei*

By A. H. Morrish
Radiation Laboratory, McGill University, Montreal, Canada*

[Received September 7, 1953]

Abstract

A total of 405 events due to the interaction of 210 ± 20 Mev π^--mesons with the nuclei of photographic emulsion are analysed. Angular and energy distributions of the charged reaction products are interpreted as giving evidence of a cascade process for those events in which the meson survives. The characteristics of the remaining events, in which the meson is either absorbed or undergoes charge exchange, are primarily determined by the evaporation process.

§ 1. Introduction

Photographic emulsions, exposed to a beam of 210 ± 20 Mev π^--mesons, have been searched for events which have either at least one grey track produced by a proton ($200 > E > 30$ Mev), or at least one black prong ($E < 30$ Mev). The large number of events found now permits reliable studies of angular and energy distributions of the charged reaction products to be made. Such studies can, in principle, give evidence for or against the existence of a cascade process inside the target nucleus. There have been several papers on evidence for cascades produced by high energy protons in nuclei. (Bernardini *et al.* 1952 a, b, Randle *et al.* 1952, Hofman and Strauch 1953, Nelson *et al.* 1952, Fishman and Perry 1952.) However, this is the first detailed experiment using energetic mesons.

Goldberger (1948) has developed a model for the behaviour of a fast nucleon inside a nucleus. He represents a heavy nucleus as a Fermi gas of nucleons, and considers the incoming energetic nucleon to interact with this gas by a series of single nucleon–nucleon scatterings. The recoil nucleons in such a process, are assumed to interact in a like manner with other nucleons in the gas, and in this way the cascade develops. Some of the fast nucleons escape from the nucleus almost immediately. Finally, the remaining excited nucleus ejects some slow particles in accordance with the evaporation theory. (Weisskopf 1937.) Goldberger retained the statistical fluctuations which occur for each interaction in the cascade by using the Monte Carlo method (Ulam and Von Neumann

---

* Communicated by the Author.

1947), when carrying out calculations for 90 MeV neutrons interacting with Pb nuclei. Bernardini *et al.* (1952 b) subsequently made calculations for 300–400 MeV protons interacting with nuclei with $A \sim 100$. This value of A was chosen since it had been found that 80% of the stars produced by 300–400 MeV protons in emulsions were due to collisions with Ag and Br nuclei. Experimental results with emulsions supported the theory.

In the above calculations, the experimentally determined free nucleon–nucleon cross sections were employed. A similar calculation for meson interactions with nuclei could be made if the appropriate meson cross sections are known. Differential cross sections for elastic π^--meson–proton collisions and charge exchange interactions in hydrogen have been determined at 120 and 144 MeV by Anderson *et al.* (1953), and further work at 227 MeV is in progress now (Anderson 1953) at Chicago. There is almost no data available regarding the absorption of a fast π^--meson in a nucleus. While Goldberger type calculations of meson-nucleonic cascades in nuclei cannot be made at the time of writing, they may be possible in the near future. In this work the conclusions drawn from the data are essentially qualitative.

§ 2. EXPERIMENTAL METHOD

Electron sensitive Ilford G5 emulsions, 400 microns thick, were exposed to the 227 MeV π^--meson beam from the University of Chicago synchrocyclotron, and suitably processed. Considerations of energy loss by ionization in the stack of plates and measurements using the multiple scattering technique led to the conclusion that the average pion energy was about 210 ± 20 MeV. Further, a scan for tracks of about minimum ionization perpendicular to the pion beam direction showed that less than 2% of the tracks were due to energetic cosmic ray particles. About 5% of the tracks were produced by μ-mesons which resulted from π–μ decays in flight.

Previously, values of cross sections for various types of interactions of 210 MeV π^--mesons with the nuclei of photographic emulsions were determined in this laboratory (Morrish 1953 a), by scanning along individual tracks. Because this method is arduous and tedious, only 2823 cm of pion track were followed. Since that time, the number of events has been greatly increased by ‘ volume ’ or ‘ area ’ scanning using a high power (×53) oil objective. However, even with this great magnification, certain types of events are missed. These are ‘ stop ’ events, in which the meson disappears in flight with no visible disintegration products, and ‘ elastic scattering ’ events, in which the meson is scattered through an angle greater than 5° with a grain density change of less than 4%, again not accompanied by any visible disintegration products. There is also evidence that a few events of other types are missed ; but in general this is not serious. This loss will be discussed in the next section.

The following classification of the remaining events was adopted:

Type 1. *Stars.* Events in which the π^--meson disappears and produces a nuclear disintegration with one or more black prongs. ($E<30$ MeV.)

Type 2. *Inelastic scatterings.* Events in which the meson survives,* and is also accompanied by one or more black prongs. ($E<30$ MeV.) Such events with no black prongs were missed in the 'volume' scan.

Type 3. *Stars with one or two fast protons.* Stars accompanied, in addition, by one or two grey tracks produced by protons. ($E>30$ MeV.)

Type 4. *Uncertain events.* Either inelastic scatterings or stars accompanied by a fast proton.

Type 5. *Inelastic scatterings with a fast proton.* Inelastic scatterings, accompanied by a grey track produced by a proton. ($E>30$ MeV.)

Black prongs were usually identified visually. If of sufficient length, tracks of fast protons or of inelastically scattered mesons were identified by multiple scattering and grain density measurements.

Identification of short grey tracks as pions was made if (*a*) the grain density indicated the particle, if a proton, had an energy higher than the total energy of the incoming meson, or (*b*) the grain density indicated the particle, if a proton, had an energy greater than the kinetic energy, but less than the total energy of the incoming meson. The latter is believed to be an improbable process in negative meson absorption. Unambiguous identification was not possible for other short grey tracks; such events are listed as uncertain.

Also, it should be noted that determinations of the energy of the pions, on the basis of grain density measurements alone, are subject to large errors at energies above 100 MeV. This is because of the small change in grain density in this region (between 117 and 222 MeV the change is only about 6·5%; Morrish 1953 b) and because of the relatively large statistical fluctuations which exist for short tracks.

It is very difficult to discriminate between slow protons, deuterons, tritons and alpha particles in electron sensitive emulsions. It appears that most of the black prongs were due to protons, but no detailed classification of origin of the black prongs has been attempted.

§ 3. Mean Free Paths for Interactions

A total of 405 events of the type listed in the previous section were found. Of these, 74 had been observed in the previous 'along the track' scan, the remainder were found in the 'volume' scan. Table 1 records the frequency of events found as a function of the number of black prongs.

The relative frequency distributions for stars and inelastic scatterings for the two methods of scanning were compared, and, within the statistical limits, were found to be the same. In addition, the relative numbers of events of types 1, 2, 3 and 4 were the same in both scans. However, there was a definite loss of type 5 events (about 75–80%) accompanied by no black prongs in the volume scan. This is not too unexpected, since usually all tracks in such events have fairly low grain density.

---

* This assumes that the number of 'double charge exchange' events ($\pi^- \rightarrow \pi^\circ \rightarrow \pi^+$) is small.

The total track length in the volume scan was determined by considering the track length in numerous small sample volumes. From this, the mean free path for the type 1–5 interactions was determined to be 47 cm. The corresponding 'along the track' scan value was 38·2 cm. If the type 5 events with zero black prongs are excluded, the m.f.p.'s are 47·5 and 40·4 cm respectively. In other words, there is a 17% difference. Probable errors are about 7% and 8% respectively, where errors in the determination of the total track length for the volume scan are included. There is, therefore, some indication that a small percentage of other events have been missed, probably primarily those with only one black prong, and then most often when the prong is roughly perpendicular to the emulsion plane. The considerations of the previous paragraph however, seem to indicate that the total loss of events of type 1–4 is less than 10%. One has considerable confidence that such a small loss will not appreciably affect the angular and energy distribution data.

Table 1. Frequency Distribution of Events

Number of black prongs	0	1	2	3	4	5	6	7	Total
Stars	—	28	57	63	55	30	11	5	249
Inelastic scatterings	—	41	23	11	12	2	0	0	89
Stars with one fast proton	2	7	5	5	6	1	0	0	26
Stars with two fast protons	0	0	2	0	0	0	0	0	2
Uncertain events: stars with a fast proton or inelastic scatterings	1	11	7	5	2	2	0	0	28
Inelastic scatterings with a fast proton	7	2	0	1	0	1	0	0	11
Total									405

Previously, comparison with results obtained with 50–100 MEV π^--mesons at Columbia University showed that the number of black prongs per event increased at our energy, as expected (Morrish 1953 a). From table 1, it is seen that the stars have more black prongs per event than the inelastic scatterings. The stars represent interactions where either the incoming meson has been absorbed or has undergone charge exchange, and emerged as a neutral meson. It is clear therefore, that the increase in the number of black prongs in the stars is primarily due to the additional meson rest mass energy available in an absorption. Indeed, the distributions suggest that the absorption process may predominate over the charge exchange process. If it is assumed that, for the 7 prong stars, all the energy available is transferred as excitation energy, it follows that the average energy per black prong is about 50 Mev. Bernardini *et al.* (1952 a) obtained a similar figure in their work with protons.

The fact that there were 89 inelastic scatterings found as compared to 28 stars accompanied by a fast proton, suggests that the majority of the uncertain events were actually inelastic scatterings. Arguments concerning the frequency distributions are not conclusive, but comparison of the angular distributions strongly supports the suggestion. We will not discuss the uncertain events further in this work.

Table 2. Geometrical Mean Free Paths for Emulsion

<table>
<tr><th>Element</th><th>Ag</th><th>Br</th><th>I</th><th>C</th><th>H</th><th>O</th><th>S</th><th>N</th></tr>
<tr><td>$\left\{N\pi\hbar^2\left(\frac{A^{1/3}}{\mu c}\right)^2\right\}^{-1}$ (cm)</td><td>71·5</td><td>86·9</td><td>5820</td><td>236</td><td>498</td><td>261</td><td>8850</td><td>1010</td></tr>
<tr><td colspan="4">m.f.p. heavy nuclei : 39·2 cm</td><td colspan="5">m.f.p. light nuclei : 89·4 cm
m.f.p. light nuclei excluding hydrogen : 109 cm</td></tr>
<tr><td colspan="9">m.f.p. all nuclei : 27·25 cm
m.f.p. all nuclei, excluding hydrogen : 28·8 cm</td></tr>
</table>

Table 2 records the ‘ geometrical ’ mean free paths for the constituents of G5 emulsions assuming the nuclear radius to be equal to $\hbar A^{1/3}/\mu c$, where μ is the mass of the π^--meson. If the cross sections for 210 Mev π^--meson interactions with emulsion nuclei are roughly proportional to the geometrical one, then it follows that about 70% of our events occur in Ag, Br, or I nuclei. Further, elastic pion–proton events can be distinguished. If we neglect the hydrogen of the emulsion, this figure is raised to about 74%. It is reasonable to assume that the great majority of the interactions are with the heavier nuclei.

It would be of value, however, to determine the precise contribution that the light elements play on the results reported in this paper. Therefore, further experiments along the lines of this investigation using either sandwich or diluted emulsions would be worthwhile.

§ 4. ANGULAR AND ENERGY DISTRIBUTIONS

The angle of the prongs, relative to the incident pion direction, was calculated from measurements of the prongs' projected and ' dip ' angles, taking into account the shrinkage factor of the emulsion. The results for the black prongs occurring in the stars, and in the stars accompanied by a fast proton, are shown by the histogram of fig. 1. The results are considered per equal solid angles by plotting them in equal cosine intervals. Separate histograms were also plotted for stars with the same black prong size, and also for those accompanied by a fast proton. Each, within the statistics available, showed the same general shape as the one of fig. 1.

Fig. 1

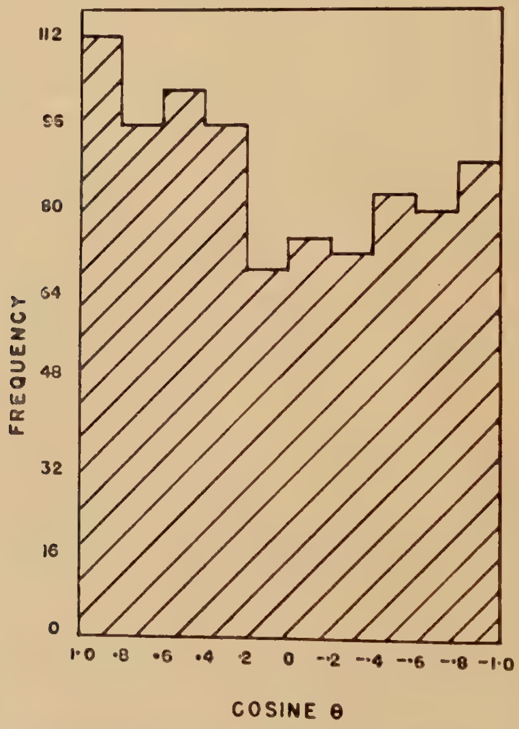

Histogram of the angles of the black prongs ($E < 30$ MEV) in stars.

Figure 2 illustrates the black prong angular distribution for the inelastic scatterings. Also, separate histograms for events with equal numbers of black prongs were very similar in shape to fig. 2. It is immediately obvious that there is a considerable difference between the distributions in figs. 1 and 2. Theory predicts that the particles emitted during the evaporation process are isotropic in direction. The work with fast protons, previously referred to, showed a preferential emission of slow

Fig. 2

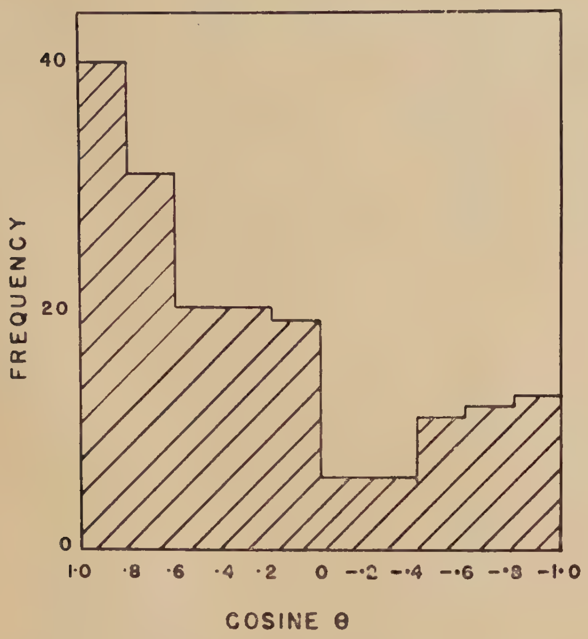

Angles of black prongs, relative to the incident pion direction, for inelastic scattering events.

Fig. 3

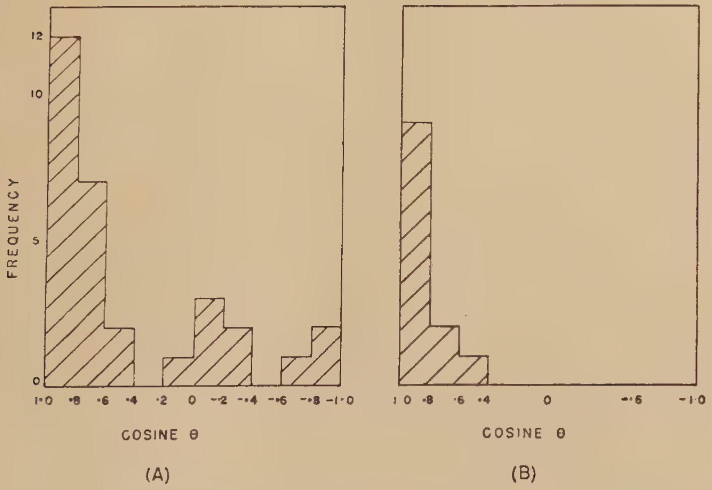

(A)

(B)

Fast proton angular distribution from (*a*) stars, and (*b*) inelastic scatterings.

protons in the forward direction. This is predicted by the Goldberger calculations, and is due to a ‘ knock on ’ process resulting from the nucleon cascade. It seems likely, therefore, that the distribution of

Table 3. Angular Distribution of Emergent Pions

Type	Pion energy MeV	Angular intervals											
		0°–37°	37°–53°	53°–66·5°	66·5°–78·5°	78·5°–90°	Total 0°–90°	90°–101·5°	101·5°–113·5°	113·5°–127°	127°–143°	143°–180°	Total 90°–180°
Inelastic scattering events	0– 64	2	3	4	0	7	16	4	6	4	5	7	26
	65–109	2	5	0	4	1	12	2	2	1	3	6	14
	110–230	6	4	0	1	1	12	0	1	5	1	2	9
	Total						40						49
Inelastic scattering plus fast proton events	All energies, when with a fast proton	0	0	0	0	1	1	1	0	3	4	2	10

fig. 2 is mainly due to a cascade process, generated by the incoming meson. The distribution of fig. 1 is much more isotropic in nature, but even here there is a tendency for an increase in the number of particles ejected forwards. It is tempting to consider this distribution to be made up of two parts ; one part, a cascade type of distribution which may be due to either the charge exchange events or to those absorption events in which one or two fast nucleons are produced which initiate a cascade. The other part, which appears to predominate, may be due to those interactions in which the meson is absorbed by a group of nucleons, with the result that the nucleus is left with a certain amount of excitation energy. The amount of this energy depends upon the number and energy of the fast neutrons which escape almost immediately, apparently without initiating a cascade. The presence of one or more fast neutrons coming from the majority of these stars is inferred by the conservation of energy principle.

Fig. 4

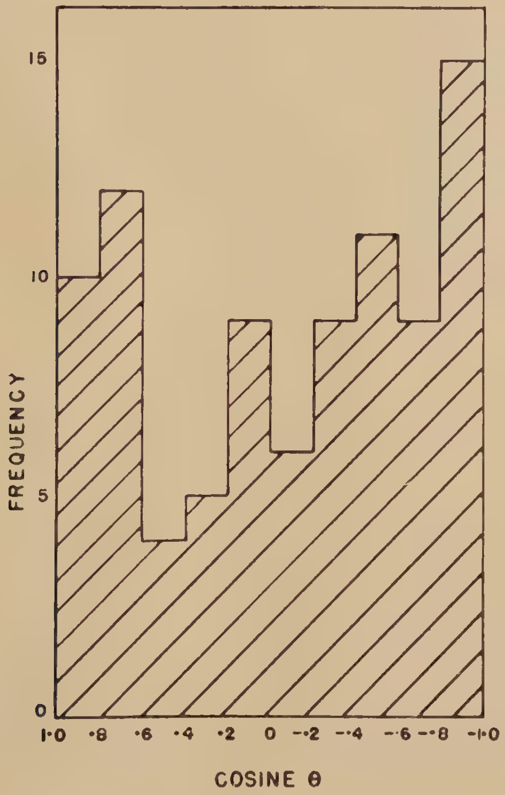

Angular distribution of pions emerging after a nuclear interaction.

It is unfortunate that in this type of experiment these neutrons cannot be detected and analysed. Instead, we will now consider those few events which are accompanied by a fast proton. Histograms of the angular distribution of fast protons associated with (*a*) stars, and (*b*) inelastic scatterings, are shown in fig. 3. It is interesting to note that none of the fast protons of the inelastic scattering events emerge in the backward direction in the laboratory system, whereas, for the stars, more than 25% emerge in the backward direction. This appears to give evidence that the former events may be due to a quasi-single pion–proton elastic scattering inside the nucleus. The argument is supported also by the observation, as shown in table 3, that these pions usually emerge in the backward direction. The fast protons ejected from stars in he backward direction could again be explained as meson absorption by a group (two or more) of nucleons in a nucleus. The limited statistics available here show the desirability of extending this type of experiment using energetic π^+-mesons.

Table 4. Energy Distribution of Emergent Pions and Fast Protons

Energy MEV	0–30	30–60	60–90	90–120	120–150	150–180	180–210	over 210
Pions from inelastic scattering events	5	31	26	7	7	3	8	2
Pions from inelastic scattering plus a fast proton event	1	4	4	1	1	0	0	0
Fast protons from stars	—	5	11	10	3	0	1	0
Fast protons from inelastic scatterings	—	1	4	6	0	0	0	0

Figure 4 is a histogram of the angular distribution of the ejected pions of the inelastic scattering events. There is some indication of a minimum at about 60°, and a slight increase at about 160°. A little more than half (49 of the 89 pions) are emitted at angles greater than 90°. However, when the angular distribution is considered for different energy groups a new feature becomes apparent. As shown by the results in table 3, the lower energy pions tend to be ejected backwards, while those of higher energy tend to be in the forward direction in the laboratory system. Table 4 records the energy distribution of the emerging π^--mesons; the great majority have an energy less than 90 MEV. Since the maximum energy a 215 MEV π^--meson can lose in an elastic single nucleon collision is about 135 MeV, it is clear that these results indicate these mesons usually undergo more than one nucleon collision inside the Ag or Br nucleus.

Finally, the energy distribution of the fast protons from stars and inelastic scatterings is tabulated in table 4.

§ 5. Conclusions

The observations have shown a striking difference between the angular distributions of the black prongs from stars and inelastic scatterings. The latter distribution appears to imply that cascade generation in the nucleus determines the main characteristics of the star, rather than the evaporation process. On the other hand, the black prong distribution for the stars appears to be primarily due to evaporation.

On the basis of earlier cosmic ray work, it has been the fashion to conclude that such black prongs are almost entirely due to the evaporation process. The present results, together with those of Bernardini *et al.* (1952 b), now provide ample evidence that this conclusion is not true in general.

The emulsions were exposed to the University of Chicago synchrocyclotron through the kind cooperation of H. L. Anderson.

References

Anderson, H. L., 1953, private communication.
Anderson, H. L., Fermi, E., Martin, R. L., and Nagle, D. E., 1953, *Phys. Rev.*, **91,** 155.
Bernardini, G., Booth, E. T., and Lindenbaum, S. J., 1952 a, *Phys. Rev.*, **85,** 826; 1952 b, *Ibid.*, **88,** 1017.
Fishman, U., and Perry, A. M., 1952, *Phys. Rev.*, **86,** 167.
Goldberger, M. L., 1948, *Phys. Rev.*, **74,** 1268.
Hofmann, J. A., and Strauch, K., 1953, *Phys. Rev.*, **90,** 449.
Morrish, A. H., 1953 a, *Phys. Rev.*, **90,** 674; 1953 b, *Ibid.*, **91,** 423.
Nelson, B. K., Guernsey, G., and Mott, G., 1952, *Phys. Rev.*, **88,** 1.
Randle, T. C., Cassels, J. M., Pickavance T. G., and Taylor, A. E., 1952, *Phil. Mag.*, **44,** 425.
Ulam, S., and von Neumann, J., 1947, *Bull. Amer. Maths. Soc.*, **53,** 1120.
Weisskopf, V., 1937, *Phys. Rev.*, **52,** 295.

VII. *Gamma Radiation from the Decay of* $^{228}_{90}$Th

By J. O. Newton and B. Rose
Atomic Energy Research Establishment, Harwell *

[Received October 1, 1953]

Abstract

The energies and relative intensities of the γ-rays following the α-particle decay of ^{228}Th have been investigated with proportional counters. Lines were observed at $84{\cdot}4 \pm 0{\cdot}2$, $132{\cdot}3 \pm 1{\cdot}3$, 167 ± 2 and 214 ± 3 kev. The multipolarity of some of the γ-ray transitions is discussed, and two possible decay schemes are presented.

The gamma radiation which follows the α-particle decay of radiothorium has been investigated in the range 30–220 kev using krypton and xenon filled proportional counters. When this work was begun, the only gamma radiation reported from this isotope was a line at 84·3 kev (Rosenblum *et al.* 1952) which had previously been interpreted as a doublet (Surugue and Tsien 1941). The resolution obtainable with the proportional counters would allow confirmation of this result.

The ^{228}Th was obtained by extraction from a pure ($<10^{-6}$ MsTh) solution of radiothorium chloride in equilibrium with its decay products. Two different samples of radiothorium solution were obtained from the Radio Chemical Centre, Amersham, and two different separation procedures were adopted during the course of the work; these gave similar results.

The first separation involved the precipitation of the daughters as sulphides and sulphates (Beling 1951). In the second separation the ^{228}Th as nitrate was extracted by washing with ethyl acetate (Bock 1950).

The energy measurements were made using the 59·78 kev γ-ray from the decay of ^{241}Am (Browne 1952) as a standard, other work having shown that the pulse height output of the detection system was linear with γ-ray energy to $\pm 0{\cdot}5\%$ up to 200 kev. The spectrum was measured at intervals up to 24 hours after the separation of each source in order to decide whether an observed line was due to ^{228}Th or to one of its decay products. The principal γ-activity from the decay products is due to ThB and subsequent members of the chain. A gamma ray from an early member of the chain will build up with the half-life of ThX, namely 3 days, whilst activities due to ThB or later members will remain low for the first 10 hours (the half-life of ThB) and then increase with the half-life of ThX. A gamma ray from ^{228}Th ($T\frac{1}{2} = 1{\cdot}9$ years) will of course remain

---

* Communicated by the Authors.

constant during this period of measurement. Typical curves taken with a xenon filled counter at 1 hour and 7 hours after the source separation are shown in fig. 1 (A and B).

In this way it was possible to ascribe to the decay of ^{228}Th lines at 84·4±0·2 kev, 132·3±1·3 kev, 167±2 kev and 214±3 kev. The energy of 84·4 kev is to be compared with that of 84·3 kev obtained by Rosenblum, Valladares and Guillot (1952). The line width we obtain supports their conclusions that this is a single γ-ray and not a double line as had been proposed by earlier work (Surugue and Tsien 1941). The gamma radiation from the decay of ^{228}Th has also been investigated by Boussières *et al.* (1953) using a sodium iodide crystal. Their interpretation of their curves is in fair agreement with our work.

Fig. 1

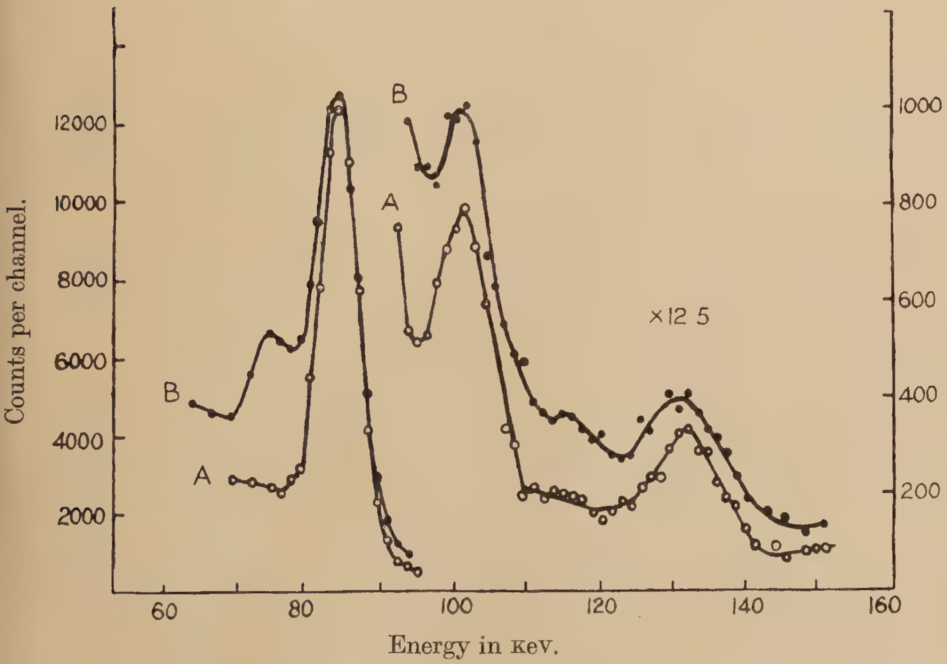

Curves taken with a xenon counter (A) 1 hour and (B) 7 hours after separation. The peak at 102 kev is the escape peak of the 132 kev line. The line at 75 kev in (B) is attributed to bismuth K radiation from ThB decay.

The counters used had an internal diameter of 5 cm and were filled to a gas pressure of ~60 cm. The proportion of photoelectrons produced in the counter gas which lose all their energy in it becomes small as the range of the photoelectron approaches the radius of the counter. It is not therefore possible to infer the relative intensities of gamma rays directly from a knowledge of the intensities of their photo peaks and corresponding mass absorption coefficients in the counter gas when this situation occurs, i.e. for gamma rays of energy greater than ~60 kev in our case. Correction curves for this effect published by West (1952) do not cover the energy range in which we were concerned. We were able to show (Newton and Rose 1953) that it was possible to obtain the necessary correction factor by observation of the change of counter efficiency with applied longitudinal magnetic field. The electron tracks are curled up by the field, thus increasing the number which lose all their energy in the counter gas. In the case of the krypton filled counter, a longitudinal field of ~2700 gauss was used in order to get peaks for the 167 kev and 214 kev radiation.

The relative intensities of the lines which we attribute to the decay of ^{228}Th are shown in the table.

Energies and Relative Intensities of the Gamma Rays from the Decay of Radiothorium

Radiation Energy in kev	$84{\cdot}4 \pm 0{\cdot}2$	$132{\cdot}3 \pm 1{\cdot}3$	167 ± 2	214 ± 3
Relative Intensity	1	$0{\cdot}105 \pm 0{\cdot}01$	$0{\cdot}058 \pm 0{\cdot}012$	$0{\cdot}18 \pm 0{\cdot}05$

We were also able to set an upper limit of 5×10^{-2} to the relative intensity of ThX K-radiation, which is sufficient to rule out the possibility that any of the three higher energy transitions is predominantly magnetic.

The α-fine structure of ^{228}Th as measured by Rosenblum, Valadares and Perey (1949) shows groups α_0 and α_1 corresponding to transitions to the ground and first excited states of ThX respectively, and also a group which he interpreted as being due to the α_2 group from the decay of ThX (Rosenblum *et al.* 1949) which was present as a contaminant. However, the intensity of this group seems too large for this interpretation and it could also be due to the group α_2 from radiothorium corresponding to an excited state in ThX at about 218 kev.

In view of this evidence and also of the fact that there is no indication from Rosenblum's data (Rosenblum, Valadares and Perey 1949) of an alpha particle group corresponding to an excited state in ThX at 167 kev, the two most likely decay schemes are those shown in fig. 2 (*a*) and (*b*). The Bohr–Mottelson collective excitation theory (1953) predicts levels of a rotational character in even–even nuclei far removed from closed shells with energies E, spins J and even parity given by

$E=\frac{\hbar^2}{2I}J(J+1)$ where $J=0, 2, 4 \ldots$ and I is an effective moment of inertia.

These states decay by cascade E2 transitions with energy ratios of 3 : 7 : 11 . . . . The first excited state of ThX is known to have spin 2 and even parity (Rosenblum *et al.* 1952) so that if the simple rule above is followed exactly we should expect a level of spin 4 and even parity at 282 kev. In fact, deviations from this simple rule are expected as a closed shell is approached, in such a way as to depress the higher levels proportionately more than the lower ones. In view of these considerations and also of the fact that rotational levels are found to exist in other nuclei it is tempting to assume that scheme (*a*) is the correct one and that the level at 252 kev is the second rotational state. Further work is however required to establish this point.

The 217 kev level in both schemes can be either 1− or 2+ ; spin values ⩾3− are excluded because the ground state gamma ray transition is observed to have the same order of intensity as that to the first excited state, and other values are excluded by the rules for angular momentum and parity.

Fig. 2

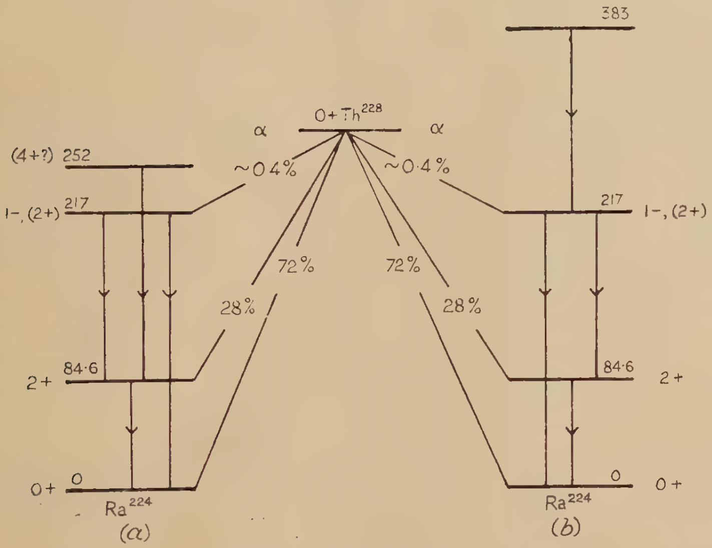

Possible schemes for the decay of ^{228}Th. The intensity of the α-particle group leading to the 217 kev state is estimated from the curves of Rosenblum, Valadares and Perey(1949).

By extrapolation from the tables of Rose *et al.* (1951) it is possible to estimate the amount of K radiation from the various transitions. This gives a relative intensity of $(2{\cdot}1 \pm 0{\cdot}4)10^{-2}$ for the combined 132 and 214 kev transitions if both are E1, and $(7{\cdot}2 \pm 0{\cdot}8)10^{-2}$ if both are E2. This is to be compared with the upper limit of 5×10^{-2} obtained experimentally for the total K radiation. This evidence suggests that the transition is E1 and therefore that the state at 217 kev is 1− ; but it cannot be considered conclusive since the K conversion coefficients are not known accurately. The intensity ratio between the '214' and 132 kev gamma rays calculated from Weisskopf's formula is 4·5 if both radiations are E1, and 11 if both are E2 whilst the observed ratio is $1{\cdot}8 \pm 0{\cdot}5$. This again agrees rather better when both transitions are E1.

After this study had been completed we received a report of some work done by Asaro (1953) on this problem ; he reached similar conclusions to those reported above.

We should like to express our gratitude to K. L. Wilkinson and J. Waldron of the Chemistry Division at Harwell who carried out the separations. We also thank the Director, A.E.R.E. Harwell, for permission to publish.

REFERENCES

ASARO, F., 1953, *Thesis.* U.C.R.L. Report No. 2180.
BELING, J. K., 1951, *Thesis*, M.I.T.
BOCK, R., 1950, *Zeitschrift für Anorganische und Allgemeine Chemie*, **263,** 146.
BOHR, A., and MOTTELSON, B. R., 1953, *Kongelige Danske Viderslabernes Selskab. Mat. Fys. Medd.*, **27,** No. 16.
BOUSSIÈRRES, G., FALK-VARIART, P., RIOU, M., TEILLAC, J., and VICTOR, C., 1953, *Comptes Rendus* (*Paris*), **256,**, 1874.
BROWNE, C. I., 1952, U.C.R.L. Report No. 1764.
NEWTON, J. O., and ROSE, B., 1953, to be published.
ROSE, M. E., GOERTZEL, G. H., and SPINRAD, B. I., 1951, *Phys. Rev.*, **83,** 79.
ROSENBLUM, S., VALADARES, M., and PEREY, M., 1949, *Comptes Rendus* (*Paris*), **228,** 385.
ROSENBLUM, S., VALADARES, M., PEREY, M., and VIAL, J., 1949, *Comptes Rendus* (*Paris*), **229,** 1009.
ROSENBLUM, S., VALADARES, M., and GUILLOT, M., 1952, *Comptes Rendus* (*Paris*), **235,** 238.
SURUGUE, J., and SAN-TSIANG TSIEN, 1941, *Comptes Rendus* (*Paris*), **213,** 172.
WEST, D., DAWSON, J. K., and MANDLEBURG, C. J., 1952, *Phil. Mag.*, **43,** 875.

VIII. *The Brownian Movement of Linear and Non-Linear Systems*

By D. K. C. MacDonald
Division of Physics, National Research Council, Ottawa*

[Received July 10, 1953]

Abstract

It has not so far proved possible to extend the conventional Brownian movement analysis to a system with an intrinsically non-linear relaxation mechanism (e.g. viscosity or electrical conductivity). In this paper a new statistical hypothesis is proposed which for the ideally *linear* circuit yields results in agreement with those already accepted and enables a calculation to be made of the Brownian movement (and corresponding frequency-spectrum) of a *non-linear* system.

The results may be of interest in a number of practical problems, particularly in relation to proposals for the use of electrical ' noise ' as an absolute thermometer at high temperatures.

§ 1. Introduction

Since the first classic treatment of the Brownian motion by Einstein (1905, 1906), the problem has been treated by many writers on the basis of various assumptions. The analysis of Langevin (1908) is in its essentials frequently followed today (cf. e.g. Uhlenbeck and Ornstein 1930) ; therein the equation of motion of classical mechanics for a free particle of mass m, in a fluid of viscosity coefficient, f, say

$$m\frac{du}{dt}=-fu, \qquad (1)$$

is replaced by

$$m\frac{du}{dt}=-fu+F(t), \qquad (2)$$

where u is the velocity of the particle ($\equiv dx/dt$). To quote Uhlenbeck and Ornstein : " . . . Characteristically of this equation, the influence of the surrounding medium is split into two parts :

(1) a systematic part $-fu$, which causes the friction

(2) a fluctuating part $F(t)$ . . . ".

More or less detailed (but very reasonable) statistical assumptions about the character of this semi-molecular force are then made to enable (2) to be ' solved ', yielding statistical parameters susceptible to experimental observations, such as $\bar{u}$, $\overline{x^2}$, etc. The average may either be one over an ensemble of similar individual systems, or be a time-average for a single (typical) system.

---

* Communicated by the Author.

This type of analysis has since been applied to many kinds of system—mechanical, electrical, and acoustical, for example—but it has generally been assumed that it is adequate to specify the frictional ' force ' as ideally linear in the velocity—i.e. that f in eqn. (2) is a *constant*. It is true that Kramers (1940) has pointed out that " . . . other laws of friction should also be possible . . . ", saying " . . . I do not know if the more complicated cases might have some physical application ". However, in his actual analysis (using the model of a particle under the influence of Brownian movement to discuss the rate of chemical reactions) he says " . . . we will restrict ourselves to the simple Einstein case " (i.e. of a linear friction).

It appears to us that in electrical circuits, for example, which may involve essentially non-linear elements such as crystal rectifiers, an analysis embracing a non-linear resistance (i.e. friction) is now very desirable on many grounds ; the more so in view of proposals to use electrical ' noise ' of thermal origin as an absolute thermometer for high temperatures. Also in problems involving radiative equilibrium of a body, it is evident that the radiative component of thermal conductance is intrinsically non-linear as a consequence of the quartic dependence on temperature (Stefan's Law).

It appears, however, that an extension of the analysis starting from eqn. (2) with $-fu$ replaced by a more general function of velocity is rather intractable. We therefore propose a new statistical hypothesis of a non-molecular character ; if applied to an ideally linear system this yields immediately the usually accepted results, while in the *non-linear* problem it enables us to derive closed expressions for the Brownian movement (and the corresponding frequency-spectrum). The degree of validity of the hypothesis must naturally depend on future experiments, but it appears already clear how we may expect a non-linear viscous force to influence the character of the Brownian movement.

§ 2. ANALYSIS

Let us deal, for the sake of definiteness, with a simple electrical circuit (see figure) of capacity C, and resistance R, whose thermodynamic state

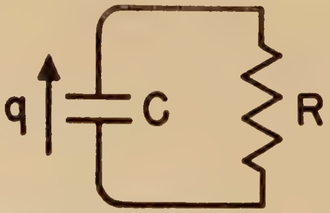

is defined by the parameter q (the charge on the condenser at any time t). Now let us consider the fluctuating quantity $\overline{\{q(t)-q(0)\}^2} \equiv \overline{\Delta q_t^2}$, where the bar denotes an average over similar time-intervals, t, for a single circuit or over an ensemble of similar circuits during the same time-interval, t.* Then

$$\overline{\Delta q_t^2}=\overline{q(t)^2}+\overline{q(0)^2}-\overline{2q(t)q(0)}. \qquad (3)$$

In statistical equilibrium, the first two terms on the right-hand side are equal and independent of t. Such terms can readily be evaluated quite generally if we accept, following Einstein (1906), that for a physical system placed in a 'heat-bath' at temperature T, the probability that certain observable parameters—such as the displacement of a particle, or the electric charge in a circuit—lie between, say, α and $\alpha+d\alpha$ is given by

$$p(\alpha)\, d\alpha=A\epsilon^{-\Phi(\alpha)/kT}d\alpha, \qquad (4)$$

where $\Phi(\alpha)$ is the potential energy necessary to displace the coordinate α from its thermodynamic equilibrium value.†

In order to deal with the time-dependent term (involving $\overline{q(t)q(0)}$ which remains in (3), we now propose the following *general hypothesis*:

The *average* charge in an assembly of similar circuits subject to thermal fluctuations, all having a given initial charge (say $q(0)$), is governed by the same differential equation of 'relaxation' as holds for a single circuit in the *absence* of spontaneous fluctuations.

Hence for an assembly of conventional *linear* circuits we have

$$\frac{d\bar{q}}{dt}+\frac{\bar{q}}{RC}=0, \qquad (5)$$

therefore

$$\overline{q(t)}=q(0)\exp(-t/RC),$$

and

$$\overline{q(t)q(0)}=\overline{q(0)^2}\exp(-t/RC).$$

Thus

$$\overline{\Delta q_t^2}=2\overline{q^2}[1-\exp(-t/RC)]. \qquad (6)$$

But now from (4), since the thermodynamic equilibrium value of q is zero, we have $\Phi(q)=q^2/2C$, and therefore

$$\overline{q^2}=\int_{-\infty}^{\infty}\exp(-q^2/2CkT)q^2\,dq\Big/\int_{-\infty}^{\infty}\exp(-q^2/2CkT)\,dq=kTC. \qquad (7)$$

Hence

$$\overline{\Delta q_t^2}=2kTC[1-\exp(-t/RC)]. \qquad (8)$$

For $t\ll RC$, this gives

$$\overline{\Delta q_t^2}=\frac{2kT}{R}t, \qquad (8\,a)$$

---

* The equality of such averages is essentially the assumption of the 'ergodic hypothesis'.

† This equation, although *apparently* closely related to the basic equation of statistical mechanics, presents certain difficulties in its derivation and application which will not be discussed here.

which is simply the well-known 'Brownian movement' equation of Einstein when applied to electricity.

Further now consider

$$\frac{d}{dt}\overline{\Delta q_t^2} \equiv \dot{\overline{\Delta q_t^2}} = \frac{2kT}{R}\exp(-t/RC). \quad . \quad . \quad . \quad . \quad . \quad (9)$$

A transform theorem, derived earlier by the writer (MacDonald 1949) enables us then immediately to derive the power spectrum $W(f)$, (or $\overline{i_f^2}$) of the current fluctuation; in fact

$$W(f)=4\pi f\int_0^\infty \dot{\overline{\Delta q_t^2}}\sin 2\pi ft\,dt, \quad . \quad . \quad . \quad . \quad . \quad . \quad (10\,a)$$

which, on inserting (9), gives

$$W(f)=\frac{4kT}{R}\left\{\frac{(2\pi fCR)^2}{1+(2\pi fCR)^2}\right\}. \quad . \quad . \quad . \quad . \quad . \quad . \quad (10\,b)$$

The spectrum of the *charge*-fluctuations is then given by

$$\begin{aligned}\overline{q_f^2}&=(1/2\pi f)^2W(f)\\ &=4RkTC^2/\{1+(2\pi fCR)^2\}, \quad . \quad . \quad . \quad . \quad . \quad (10\,c)\end{aligned}$$

and we may check immediately that the *total* fluctuation of charge

$$\overline{q^2}\left(=\int_0^\infty \overline{q_f^2}\,df\right)=kTC. \quad . \quad .$$

Corresponding to (10 *b*), the *voltage*-fluctuations are given by

$$\overline{V_f^2}=\overline{q_f^2}/C^2=\frac{4RkT}{1+(2\pi fCR)^2}, \quad . \quad . \quad . \quad . \quad . \quad . \quad (11\,a)$$

which for $f \ll 1/CR$ gives simply

$$\overline{V_f^2}=4RkT \quad . \quad . \quad . \quad . \quad . \quad . \quad . \quad . \quad . \quad (11\,b)$$

usually known as Nyquist's theorem.

§ 3. THE NON-LINEAR PROBLEM

Let us now generalize our circuit so that the electrical conductance, G, is no longer a *constant* but a function of the voltage across it and, therefore, of the charge $q(t)$ on the condenser. Let us assume $G(q)=\alpha+\gamma q^2$. Returning to eqn. (3) we may now write

$$\overline{\Delta q_t^2}=2\overline{q^2}-2\overline{\overline{q(t)q(0)}^i}, \quad . \quad . \quad . \quad . \quad . \quad . \quad . \quad (12)$$

where the symbol $\overline{\qquad}^i$ signifies an average first over a sub-assembly of similar circuits which all have initially charge $q(0)=q_i$. The upper bar then denotes the final average over all sub-assemblies.

Now in general, following our hypothesis,

$$\frac{d\bar{q}}{dt}+\frac{\overline{q(t)}\,.\,G(\bar{q})}{C}=0 \quad . \quad . \quad . \quad . \quad . \quad . \quad . \quad (13)$$

(in place of eqn. (5) for a linear circuit); whence, solving with $G(q)=\alpha+\gamma q^2$ and $q(0)=q_i$ we have

$$q(t)=\frac{q_i \exp(-\alpha t/C)}{(1+Bq_i^2)^{1/2}}$$

where $B=(\gamma/\alpha)[1-\exp(-2\alpha t/C)]$. Hence

$$\overline{\Delta q_t^2}=2\left(kTC-\overline{\left(\frac{q_i^2 \exp(-\alpha t/C)}{(1+Bq_i^2)^{1/2}}\right)}\right)$$

$$=2\left\{kTC-\exp(-\alpha t/C)\int_{-\infty}^{\infty}\frac{\exp(-q^2/kTC)q^2\,dq}{(1+Bq^2)^{1/2}}\right\}. \quad . \quad . \quad (14\,a)$$

The upper integral may be evaluated in terms of the Bessel functions K_ν and we have

$$\overline{\Delta q_t^2}=2kTC\left\{1-\exp(-\alpha t/C)\frac{a^3}{\sqrt{\pi}}\exp(a^2/2)\left[\frac{a^2}{2}(K_2-K_0)-(K_1+K_0)\right]\right\}, \quad . \quad . \quad . \quad . \quad . \quad (14\,b)$$

where $a^2=\{2kTC(\gamma/\alpha)[1-\exp(-2\alpha t/C)]\}^{-1}$ and the Bessel function argument is $a^2/2$ throughout.

We may now consider the behaviour of $\overline{\Delta q_t^2}$ for small and large values of a^2 either by use of appropriate expansions of the Bessel functions or by direct approximation to the integral in eqn. (14 *a*) above. If we recall that $G(q)=\alpha+\gamma q^2$ and therefore $\overline{G(q)}=\alpha+\gamma\overline{q^2}=\alpha[1+(\gamma/\alpha)kTC]$, we see that the non-linearity will be small or large according as $(\gamma/\alpha)kTC$ is small or large compared with unity.

If now $2(\gamma/\alpha)kTC\ll 1$, then a^2 is large for *all* values of t. Hence

$$\overline{\Delta q_t^2}\doteq 2kTC\left\{1-\frac{2}{\sqrt{\pi}}\exp(-\alpha t/C)\int_{-\infty}^{\infty}\exp(-x^2)x^2\left(1-\frac{x^2}{2a^2}\right)dx\right\}$$

$$=2kTC\left\{1-\exp(-\alpha t/C)\left[1-\frac{3}{2}kTC\frac{\gamma}{\alpha}[1-\exp(-2\alpha t/C)]\right]\right\}. \quad (15)$$

Evidently, as we expect, in the limit $\gamma/\alpha=0$ (i.e. zero non-linearity), $\overline{\Delta q_t^2}=2kTC[1-\exp(-\alpha t/C)]$, in agreement with (8) above, setting $R=1/\alpha$. More generally,

$$\overline{\Delta \dot{q}_t^2}=2\alpha kT\left\{\left(1-\frac{3}{2}kTC\frac{\gamma}{\alpha}\right)\exp(-\alpha t/C)+\frac{9}{2}kTC\frac{\gamma}{\alpha}\exp(-3\alpha t/C)\right\}$$

therefore using the transform eqn. (10 *a*) we find the ‘ noise ’ spectrum of the current

$$W(f)=4\alpha kT\left[\left\{\frac{(\omega C/\alpha)^2}{1+(\omega C/\alpha)^2}\right\}+\frac{3}{2}kTC\frac{\gamma}{\alpha}\left\{\frac{3(\omega C/3\alpha)^2}{1+(\omega C/3\alpha)^2}-\frac{(\omega C/\alpha)^2}{1+(\omega C/\alpha)^2}\right\}\right], \quad . \quad . \quad . \quad . \quad . \quad (16)$$

where $\omega\equiv 2\pi f$. These expressions, with their non-linear temperature dependence, then appear of particular interest in connection with the proposals, mentioned earlier, of using electrical 'noise' as an absolute thermometer at high temperatures.

The spectrum of the *charge* fluctuations is given, as before, by $W(f)/(2\pi f)^2$ and we may immediately verify that again the 'total' fluctuation

$$\overline{q^2}\left(=\int_0^\infty \overline{q_f^2}\,df\right)=kTC.$$

The case of *strong* non-linearity $[(\gamma/\alpha)kTC\gg 1]$ requires somewhat more detailed examination since it is evident that a^2 cannot $\to 0$ for *all* values of t. We find that for $t\ll 1/\gamma kT$

$$\overline{\Delta q_t^2}=2kTC[1-\exp(-\alpha t/C)]$$

and for $t\gg 1/\gamma kT$

$$\overline{\Delta q_t^2}=2kTC\left\{1-\frac{2\exp(-\alpha t/C)}{\{2\pi kTC(\gamma/\alpha)[1-\exp(-2\alpha t/C)]\}^{1/2}}\right\}\quad . \qquad (17)$$

These two expressions are, in fact, very nearly equal for $t=1/\pi\gamma kT$, and we may therefore expect that an excellent approximation will result by extending both to this common limit. However, the subsequent determination of the noise spectrum will not be attempted.

Finally, we may analyse readily the behaviour of an idealized 'rectifier'—a problem discussed qualitatively in the past. If we let

$$\begin{aligned}G(q)&=\alpha\,; &\quad q&>0,^{*}\\ &=\beta\,; &\quad q&<0.\end{aligned}$$

Then

$$\overline{\Delta q_t^2}=2kTC\left\{1-\frac{\exp(-\alpha t/C)+\exp(-\beta t/C)}{2}\right\}$$

therefore

$$\overline{\dot{\Delta q_t^2}}=2kT\left\{\frac{\alpha}{2}\exp(-\alpha t/C)+\frac{\beta}{2}\exp(-\beta t/C)\right\}\quad . \quad . \quad . \qquad (18)$$

Whence the spectrum of the noise current is

$$W(f)=4kT\left\{\frac{\alpha}{2}\cdot\frac{(\omega C/\alpha)^2}{1+(\omega C/\alpha)^2}+\frac{\beta}{2}\cdot\frac{(\omega C/\beta)^2}{1+(\omega C/\beta)^2}\right\}\quad . \quad . \quad . \qquad (19)$$

ACKNOWLEDGMENTS

It is a sincere pleasure to thank Dr. J. S. Dugdale for many discussions on the Brownian movement. I wish also to thank Dr. D. Polder for helpful comments.

REFERENCES

EINSTEIN, A., 1905, *Ann. Phys., Lpz.*, **17,** 549 ; 1906, *Ibid.*, **19,** 371.
KRAMERS, H. A., 1940, *Physica*, **7,** 284.
LANGEVIN, P., 1908, *Comptes Rendus (Paris)*, **146,** 530.
MACDONALD, D. K. C., 1949, *Phil. Mag.*, **40,** 561.
UHLENBECK, G. E., and ORNSTEIN, L. S., 1930, *Phys. Rev.*, **36,** 823.

---

* It will be appreciated that such an idealized model of a rectifier has been chosen deliberately for mathematical simplicity in this example, but that a strict discontinuity of such a type could not exist physically in the limit.

IX. *Note on the Theory of Brownian Motion in Non-Linear Systems*

By D. Polder
H. H. Wills Physical Laboratory, University of Bristol*

[Received October 15, 1953]

Summary

A hypothesis recently advanced by MacDonald is shown to lead to a contradiction. It is indicated how a formalism developed by Kramers may be used in this connection.

§ 1

In the preceding paper MacDonald has drawn attention to the fact that relatively little is known about the theory of the Brownian motion in non-linear systems. As an example MacDonald considered a simple *R–C* circuit in which the resistance R is a function of the charge q on the condenser C. In order to be able to work out the noise spectrum of such a circuit MacDonald advanced the following hypothesis : $\bar{q}$, the average value of q of a great number of identical systems, all starting at $t=0$ with the same value of $q=q_0$ satisfies the equation

$$R(\bar{q})\, d\bar{q}/dt+\bar{q}/C=0. \quad . \quad . \quad . \quad . \quad . \quad . \quad . \quad . \qquad (1)$$

In other words, and slightly less precisely, it was assumed that the time dependence of the average charge of the ensemble is the same as that of the charge of a single system not subject to Brownian motion.

It is obvious that for the case R is a constant hypothesis (1) is in agreement with existing theoretical ideas about the Brownian motion in linear circuits. At first sight the extension of eqn. (1) to the non-linear case seems to be a hypothesis of which the validity is no more questionable than that of any of the assumptions usually made in the theory of Brownian motion, i.e. the test of its validity depends on a detailed molecular theory of the relevant random process. However, this is not the case. It can be shown that MacDonald's hypothesis is in fact not self-consistent. This will be done in § 2. In § 3 we shall indicate how a paper by Kramers (1940) may help to illuminate the problem under discussion. We shall not discuss questions concerning the validity of the usual assumptions in the theory or the problem of the minimum number that suffices to set up the theory, though both points might be relevant to a satisfactory discussion of the problem of the noise spectrum.

§ 2

In order to test the self-consistency of MacDonald's hypothesis (1) we consider a special case in which for $q>0$ R is equal to a constant R_1, and for $q<0$ R is a constant R_2 ; $R_1>R_2$ say. If at $t=0$ all systems of the ensemble start at $q=q_0$, eqn. (1) predicts that $\bar{q}=q_0 \exp(-t/R_1C)$ since $\bar{q}$ always remains in the positive region of q. After a finite time T, however, we must expect to find in the ensemble a certain distribution of q values around $\bar{q}$. More in particular a certain fraction f of the systems will have drifted into the region $q<0$, this fraction being the larger, the larger T. Now let us split up the ensemble at $t=T$ into sub-ensembles of systems, each to be found in different intervals Δq, together covering the whole range of q-values. According to the hypothesis (1), all sub-ensembles in the positive region will again show the exponential decay $\exp(-t/R_1C)$. The sub-ensembles in the region $q<0$, however, will show a decay with the characteristic time R_2C. This means that for $t>T$ we now have

---

* Communicated by the Author.

$$\bar{q}=a \exp(-t/R_1C)-b \exp(-t/R_2C), \quad . \quad . \quad . \quad . \quad (2)$$

where a and b are certain constants >0. This obviously contradicts the previous deduction from the theory.

As to the origin of this failure, we wish to emphasize that (1) has been introduced as a purely *ad hoc* hypothesis, based on similarity rather than on existing theory. Nevertheless it may be of interest to discuss one point that should not be used as an argument against (1). It may seem surprising that the initial condition on the members of the ensemble specifies only $q=q_0$ and not the value of the current $i=dq/dt$. The answer to this is that the circuit should really be considered as one with an extremely small self-inductance L in series with R and C, with $L \rightarrow 0$. Now, whatever is the initial current i_0 of the members of the ensemble, a distribution of currents around an average $-\bar{q}/RC$ will have established itself within an extremely short time of the order L/R. It is this distribution which alternatively may be taken as the initial condition for the currents. The width of this current distribution is, of course, very wide, $\overline{(\Delta i)^2} \sim kT/L$ but the width of the q-distribution after that short time is still very small $\overline{(\Delta q)^2} \sim 2kTt/R \sim 2LkT/R^2$ as required in the hypothesis.

§ 3

It may be of interest to point out that a non-linear problem has been discussed before in a paper by Kramers (1940). In fact his treatment concerns an even more general case: a mass point subject to a frictional force $-\beta\, dq/dt$, and a systematic force K, where both β and K are functions of the coordinate q. This corresponds to an electric circuit with constant L, but R and C depending on q. Kramers soon specializes to the case of constant β and variable K, but it is not difficult to see what happens if we keep $\beta=\beta(q)$ and let $m \rightarrow 0$, thus returning to MacDonald's problem with also the capacity depending on the charge.

For details we must refer to Kramers' paper, but we mention that the fundamental assumptions in this paper are, as usual, certain statements about the integral over a small time τ of the fluctuating force acting on the particle. This time is long compared with the time scale of a molecular collision, but so small that the velocity of the particle has not substantially changed (i.e. smaller than the small time mentioned at the end of § 2). This, incidentally, means that $m \rightarrow 0$ should be considered as m is macroscopically small, not as a limiting process into the molecular region. The average of the integral, of its square, etc., over an ensemble with identical initial q and dq/dt, are supposed to be developable into a power series of τ. The terms proportional to τ involve the value of β at the initial value of q and the q-dependence of β affects only the higher order terms. Only the terms proportional to τ are of interest for setting up a differential equation for the distribution function ρ of any arbitrary ensemble in phase space. Kramers' equation for an arbitrary ensemble runs as follows:

$$\frac{\partial \rho}{dt} = -\frac{p}{m}\frac{\partial \rho}{\partial q} - \frac{\partial}{\partial p}(K\rho) + \beta\frac{\partial}{\partial p}\left(\rho\frac{p}{m}\right) + \beta kT\frac{\partial^2 \rho}{\partial p^2}. \quad . \quad . \quad . \quad (3)$$

The terms on the right-hand side describe respectively the effect of the velocity p/m, of the systematic force K, of the average of the fluctuating force or frictional force and of the Brownian motion.

Following Kramers with a minor variation, we introduce as variables Q and p instead of q and p, where

$$Q = \int^q \beta(q')\,dq' + p. \quad . \quad . \quad . \quad . \quad . \quad . \quad . \quad . \quad (4)$$

Introducing partial derivatives with respect to the new coordinates we find from (3)

$$\frac{1}{\beta}\cdot\frac{\partial \rho}{\partial t} = \frac{\partial}{\partial p}\left(\rho\frac{p}{m}\right) - \frac{\partial}{\partial p}\left(K\frac{\rho}{\beta}\right) - \frac{\partial}{\partial Q}\left(K\frac{\rho}{\beta}\right) + kT\left(\frac{\partial}{\partial p} + \frac{\partial}{\partial Q}\right)^2 \rho. \quad . \quad (5)$$

Again following Kramers we integrate over p at constant Q'. If m is very small, constant Q' means approximately the same as constant q, since the spread in p is at most of the order $\sqrt{mkT}$. Thus we have for any, not too quickly varying functions f of q, if $m \rightarrow 0$

$$\int \rho(p, Q)\,f(q)\,dp \rightarrow \sigma f \text{ at } q = q(Q, p=0) \quad . \quad . \quad . \quad . \quad (6)$$

where σ is the ensemble density in configuration space. The integration cancels the terms with $\partial/\partial p$ since $\sigma \rightarrow 0$ for large p and we have

$$\frac{1}{\beta}\cdot\frac{\partial \sigma}{\partial t} = -\frac{\partial}{\partial Q}\left(\frac{K\sigma}{\beta}\right) + kT\frac{\partial^2 \sigma}{\partial Q^2}. \quad . \quad . \quad . \quad . \quad . \quad (7)$$

Re-writing with the aid of q, we finally have

$$\frac{\partial \sigma}{\partial t} = -\frac{\partial}{\partial q}\left[\frac{1}{\beta}\left(K\sigma - kT\frac{\partial \sigma}{\partial q}\right)\right]. \quad . \quad . \quad . \quad . \quad . \quad . \quad (8)$$

This is a well-known diffusion equation in q-space. It is easily seen that the Boltzmann distribution is a stationary solution if K is a conservative force.

Equation (8) gives, in principle, the answer to all questions regarding the time-dependence of any average quantity of interest. If the initial $q=q_0$, we have to find the solution of (8) for $\sigma=\delta(q-q_0)$ at $t=0$. It is not unlikely, however, that it will be very difficult to find an explicit solution in all cases but in the well known simple ones. It is also evident, however, that a simple suggestion such as given by MacDonald does not provide the correct answer to the problem.

The author wishes to acknowledge discussions with Dr. D. K. C. MacDonald and to express his thanks for having had the opportunity to see his paper before publication.

References

MacDonald, D. K. C., 1954, *Phil. Mag.*, **45,** 63.
Kramers, H. A., 1940, *Physica*, **7,** 284.

X. *The Thermal and Electrical Conductivity of Magnesium at Low Temperatures*

By H. M. Rosenberg
The Clarendon Laboratory, Oxford*

[Received September 25, 1953]

Abstract

The electrical and thermal resistivities of the same specimen of magnesium have been measured together between 2 and 35°K. The electrical resistance had a minimum at 6°K and an effect of a similar order of magnitude occurred for the thermal resistance W. This is best demonstrated by plotting a graph of WT against T^3 which shows a marked departure from linearity in the region of the electrical resistance anomaly.

§ 1. Introduction

In some samples of certain metals a minimum is known to exist in the electrical resistance at low temperatures. The experiments to be described were designed to see whether there was a corresponding effect in the thermal resistance. An anomaly of a similar order of magnitude has indeed now been found in a batch of magnesium, which was known to exhibit a minimum in the electrical resistance (MacDonald and Mendelssohn 1950).

The only previous work on these lines is an observation by Berman and MacDonald (1952) on a copper specimen which showed an electrical resistance minimum. In this case, however, the authors stated that any deviation of the thermal resistance from its normal curve must have been considerably less than the anomalous increase in electrical resistance and that a careful analysis of the results was necessary to indicate its existence.

§ 2. Experimental Technique

Earlier work on the correspondence between electrical and thermal conductivities has on some occasions been rendered difficult of interpretation because the thermal and electrical measurements were made at different times and in some cases separate specimens have been used for each measurement. Even when the same specimen had been used for both the thermal and electrical experiments it has usually been handled between the two determinations thereby rendering it liable to a small amount of distortion which often will affect the conductivities considerably. For this reason it was decided to measure both the thermal and electrical conductivities together on the same specimen and during the same experimental run. The thermal conductivity was measured in a way similar to

---

* Communicated by Dr. K. Mendelssohn, F.R.S.

that described in our previous work (Mendelssohn and Rosenberg 1952). The accuracy of the thermal conductivity measurements over most of the experimental range was about 1%.

The electrical resistance of the specimen was measured by using a galvanometer amplifier (MacDonald 1947) to determine the potential difference between the gas thermometer contacts when a current of about 0·5 amp was passed through the specimen. The constantan potential leads were actually connected to the gas thermometers. In this way the form factors for both the electrical and thermal measurements were the same and no errors were introduced in comparing the two sets of values and, in particular, when calculating the Lorenz number. It might be thought at first that the German silver capillaries attached to the gas thermometers which are anchored together to the liquefier framework higher up in the apparatus might act as a short circuit to the potential measurement. In actual fact, however, the resistance of this ‘ short circuit ’ between the gas thermometers is about 2 ohms whereas that of the specimen is about 10^{-6} ohms. Hence no appreciable error is introduced. Since the cold end of the specimen is attached to the metal apparatus and to earth, the latter was used as one current lead whilst a 38 gauge copper wire attached to the warm end of the specimen was used as the other connection.

The specimen and the gas thermometers were mounted in a high vacuum enclosure and were surrounded by a copper radiation shield which was thermally attached to the helium container. Such an arrangement whilst being the most favourable for the measurement of the thermal resistance is not so satisfactory for the electrical measurements because the measuring current inevitably introduces a small heating both in the specimen and in the current lead which can be appreciable as the specimen is thermally isolated. Thus thermal e.m.f.'s might be produced which would lower the accuracy of the measurements. This will be appreciated when it is realized that the potentials to be measured at liquid helium temperatures were only of the order of 3×10^{-6} volts. For this reason the measuring current had to be made as small as possible and hence the relative accuracy of the electrical measurements was about 3% at liquid helium temperatures. Since the electrical measurements were undertaken mainly in order to check that this specimen did in fact exhibit an electrical resistance minimum such an accuracy was considered satisfactory.

The specimen was made from Johnson Matthey spectrographically standardized rod, JM 1703 which had a purity greater than 99·95%. The main impurities were Mn, 0·03 ; Fe, 0·0075 ; Al, 0·004. It was turned down to a diameter of 1·5 mm and was annealed *in vacuo* at 500°c for six hours. This rod was made of the same batch of metal as were two of the specimens which MacDonald and Mendelssohn (1950) used to determine the electrical resistance and since the present electrical measurements do correspond with theirs, a more detailed comparison of the thermal and electrical measurements can be made by referring to these previous electrical results.

§ 3. Results

The thermal conductivity K, and the electrical resistance R, as measured in these experiments between 2 and 35°K are shown in fig. 1. In spite of the scatter a minimum in R is clearly seen at about 6°K. At first sight the thermal conductivity curve has the appearance that one would expect from a normal fairly pure metal. There is a linear section from 2 to 10°K passing through the origin, showing electron scattering by the lattice impurities, followed by a maximum and then a decrease in K where the electrons are scattered by the lattice vibrations. A theoretical study of these mechanisms has been given by Wilson (1936), Makinson (1938) and Sondheimer (1950) and a general review of the theory by Olsen and Rosenberg (1953).

Fig. 1

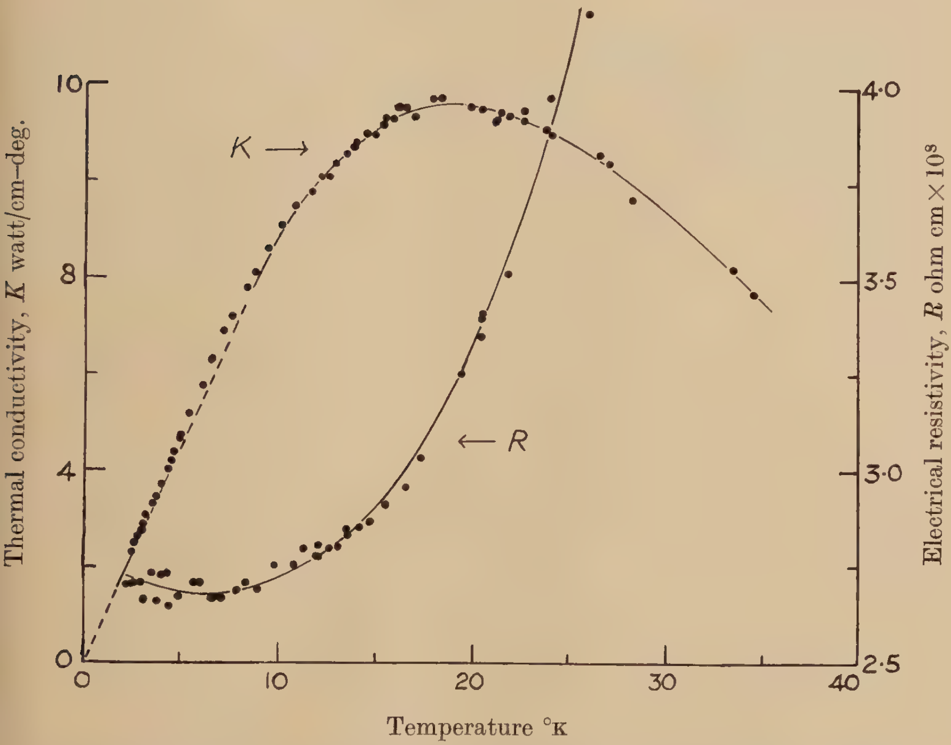

The thermal conductivity K, and the electrical resistivity R, of the magnesium specimen showing the departure of K from linearity in the region of the electrical resistance minimum.

A more careful study of the curve of K against T, however, shows that the lower temperature section is not quite linear, but that between about 4 and 9·5°K it is slightly higher than it ought to be. This departure from linearity is much better demonstrated in the following way.

The thermal resistance, W, can be written as the sum of two terms at low temperatures,

$$W = AT^2 + B/T \quad . \quad . \quad . \quad . \quad . \quad . \quad . \quad . \quad . \quad (1)$$

where, according to theory, A and B are constants of the metal and its impurity content respectively.

Thus

$$WT = AT^3 + B, \quad . \quad . \quad . \quad . \quad . \quad . \quad . \quad . \quad . \quad (2)$$

and hence a graph of WT against T^3 should be a straight line with a slope of A and an intercept on the WT axis of B. This has been found to be generally true for most metals which have been investigated and is the standard method for determining the constants A and B.

When such a plot is made for our magnesium specimen, however, as is shown in fig. 2, it is evident that there is a marked departure from a straight line below about 11°K. With falling temperature the value of WT drops below the straight line until it reaches a minimum at about 6°K and then rises again. At the lowest temperatures WT again agrees with eqn. (2). Above 11°K A and B in eqns. (1) and (2) have the values $8{\cdot}5 \times 10^{-5}$ and 1·05 respectively.

Fig. 2

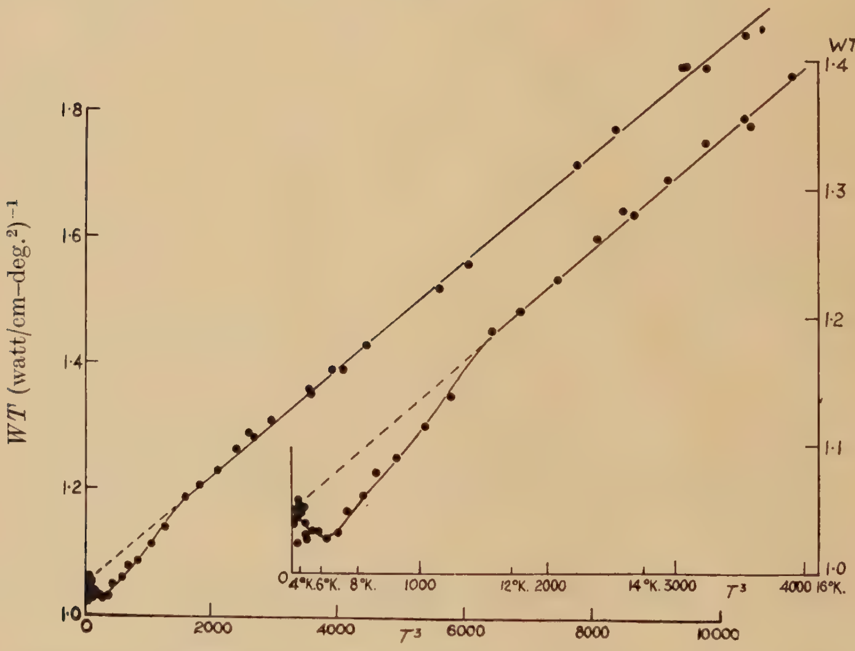

The graph of WT against T^3 showing the minimum in the value of WT. Inset, the lower half of the curve on a larger scale.

A graph of the difference between the observed WT and AT^3+B is shown in fig. 3. The scatter in the points is understandable since we are dealing with the difference of two quantities which are nearly the same and this difference is very near to the experimental accuracy. From the smoothed curve of fig. 3 a graph of ΔW, the decrease in resistance from the theoretical value of eqn. (1) against temperature is shown in fig. 4. Whilst this curve is approximately parabolic in shape a detailed analysis shows that it is not strictly so.

Fig. 3

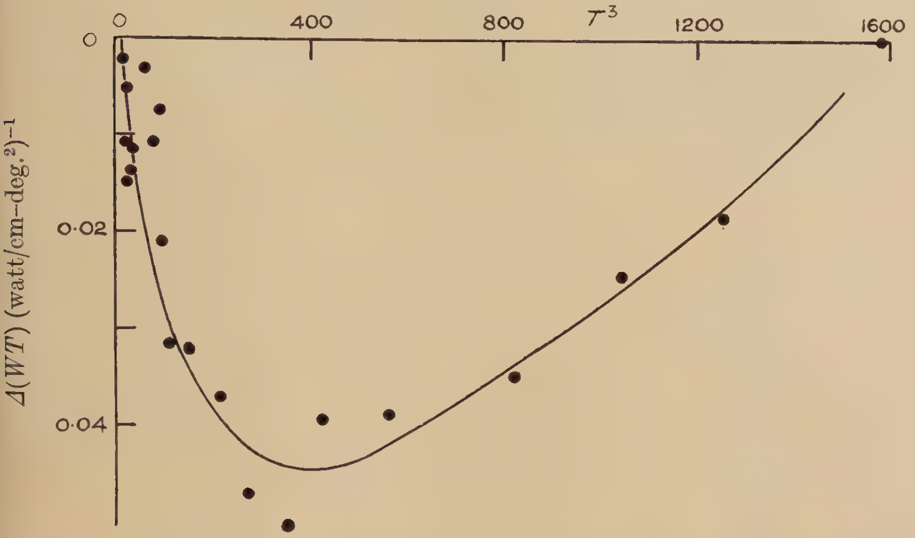

The graph of $\Delta(WT)$ against T^3, where $\Delta(WT)$ is the difference between the theoretical equation AT^3+B and the experimental results.

Fig. 4

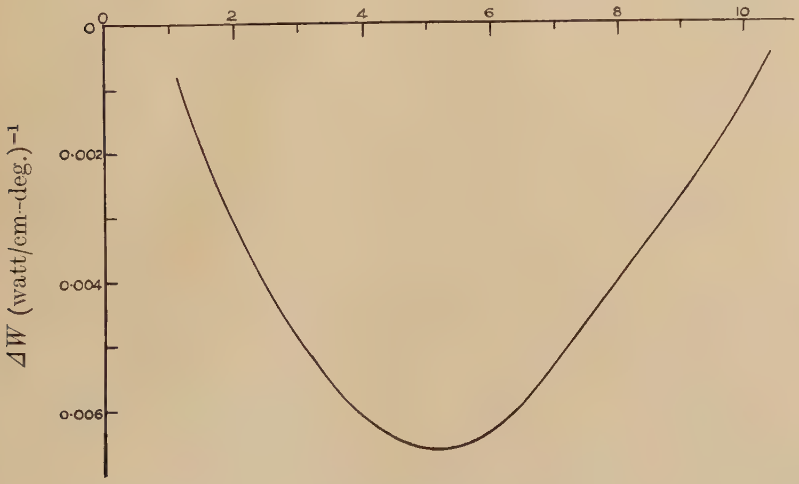

Temperature °K

The graph of ΔW against T as calculated from the smoothed curve of fig. 3.

It can be seen that the minimum in the value of ΔW occurs at 6°K which corresponds exactly to the position of the minimum in the electrical resistance both for our specimen and also for those of MacDonald and Mendelssohn. Furthermore the value of ΔW at this temperature is about 4% of the value of the absolute thermal resistance. For the electrical resistance, R, the minimum is about 3% below the residual resistance as deduced from the measured points above 10°K by plotting R against T^5. Thus whatever mechanism is producing the minimum, it seems to affect the thermal and the electrical resistances equally.

Fig. 5

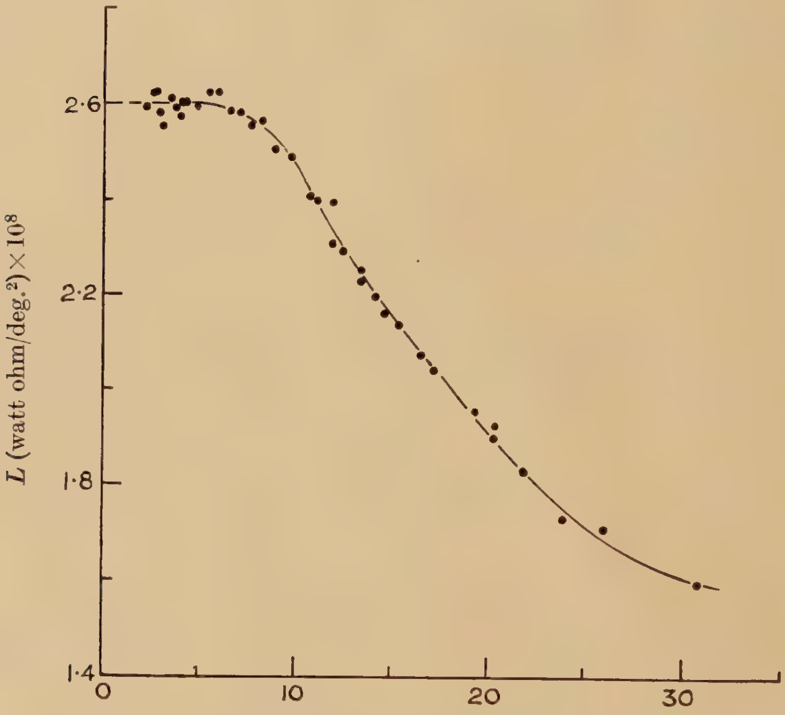

The temperature variation of the Lorenz number L, for the magnesium specimen.

It has sometimes been suggested that the rise of R below the minimum may lead to infinite resistivity at the absolute zero (cf. Gorter 1938). An indication of the low temperature behaviour of R is provided by the WT against T^3 curve of fig. 2. It will be noted that at the lowest temperatures measured the values of WT again fall on to the theoretical straight line. Since the present experiments show that W varies in a similar way with temperature as does R, they suggest that R, too, will as absolute zero is approached, return to its theoretical temperature-independent value. However, it should be noted that recent experimental work (Mendoza and

Thomas 1951, Croft, Faulkner, Hatton and Seymour 1953) still shows R increasing at the lowest temperatures reached.

As a consequence of the fact that comparable effects were found in both the electrical and thermal resistances no anomaly occurs in the curve of the Lorenz number, L, against temperature, where

$$L = R/WT.$$

In experimental range covered, the value of L, shown in fig. 5, rises with decreasing temperature, flattening off to a constant value at about 5°K, below which temperature the Wiedemann–Franz law is valid. Whilst this constant value of L is slightly higher than the theoretical value of $2{\cdot}45 \times 10^{-8}$ watt ohm/deg.^{2} this increase is not thought to be significant to this problem.

The minimum in the electrical resistance is usually very shallow and is difficult to detect. The deviation from linearity of the WT curves gives another method for showing the existence of such a minimum. It was therefore thought advisable to examine the results of thermal conductivity measurements which we have made previously on pure metals (Mendelssohn and Rosenberg 1952) to see whether any of them exhibited a slight dip in the WT against T^3 curve at low temperatures as does our magnesium specimen. In four cases such a deviation could be detected : in copper and silver (samples of which are known to exhibit a minimum) and in nickel and palladium. Further careful measurements however, would be necessary to confirm the existence of a minimum in the last two cases.

It is apparent that more data on the nature of these minima are necessary before the reason for their existence is made clear. At the moment, whilst it seems likely that their presence is connected with certain types of impurity atoms (e.g. cf. Mendelssohn 1951, MacDonald 1952) a full explanation of the phenomenon is not yet possible. The present result, that the effect is not limited to the electrical resistance, but that the thermal resistance is altered in a similar way, may widen the field of investigation.

ACKNOWLEDGMENT

I should like to thank Dr. K. Mendelssohn, F.R.S. for his constant interest during the course of this work.

REFERENCES

BERMAN, R., and MACDONALD, D. K. C., 1952, *Proc. Roy. Soc.* A, **211,** 122.

CROFT, A. J., FAULKNER, E. A., HATTON, J., and SEYMOUR, E. F. W., 1953, *Phil. Mag.*, **44,** 289.

GORTER, C. J., 1938, *Physica*, **5,** 483.

MACDONALD, D. K. C., 1947, *J. Sci. Instrum.*, **24,** 232 ; 1952, *Phys. Rev.*, **88,** 148.

MAKINSON, R. E. B., 1938, *Proc. Camb. Phil. Soc.*, **34,** 474.

MENDELSSOHN, K., 1951, *Proc. of N.B.S. Low Temp. Symposium*, 253.

MENDELSSOHN, K., and ROSENBERG, H. M., 1952, *Proc. Phys. Soc.* A, **65,** 385, 388.

MENDOZA, E., and THOMAS, J. G., 1951, *Phil. Mag.*, **42,** 291.

OLSEN, J. L., and ROSENBERG, H. M., 1953, *Advances in Physics*, **2,** 28.

SONDHEIMER, E. H., 1950, *Proc. Roy. Soc.* A, **203,** 75.

WILSON, A. H., 1936, *Theory of Metals* (Cambridge : University Press).

XI. *The Quantization of Sound Waves—I: General Theory*

By O. Penrose*
Royal Society Mond Laboratory, Cambridge, England†

[Received May 18, revised August 18, 1953]

Abstract

The theory described in this paper was developed with a view to its application to the molecular theory of helium II. This application will be discussed in a subsequent paper.

The system treated here consists of a very large number of identical interacting particles. Sound waves can be described using the Fourier components of the density operator and their time-derivatives. Approximate commutation relations for these operators are obtained, and equations of motion are deduced from the assumption that the system can propagate sound. The commutation relations are analogous to those for a set of harmonic oscillators or for a radiation field; using this analogy, creation operators, which can be said to create *phonons*, are defined. It is shown how stationary states may be constructed by adding phonons to the ground state, and that the energy or momentum of such a stationary state equals the energy or momentum of the ground state plus that of the ' phonon gas ' added to it.

The theory is illustrated by its application to three particular cases—the imperfect Bose gas, linear imperfect Fermi gas, and linear crystal. In each case the present general method leads to approximately the same creation operators as the special treatments due to other authors.

§ 1. Introduction

In his well-known treatment of the specific heats of solids, Debye (1912) introduced the approximation of treating a many-particle system as an elastic continuum. Thermal motion is represented by density and shear strain fluctuations in the continuum. This motion of the continuum can be analysed into transverse and longitudinal sound vibrations, and the system therefore has the same energy levels as an assembly of harmonic oscillators, one for each sound mode. At low temperatures, the part of the specific heat due to longitudinal modes is

$$(2\pi^2/15)\,(\kappa T/hc)^3\kappa \quad . \quad . \quad . \quad . \quad . \quad . \quad . \quad . \quad . \quad (1)$$

per unit volume, where c is the velocity of longitudinal sound waves, κ is Boltzmann's constant, and T is the temperature.

Born and von Karman (1913) justified Debye's approximation, by showing that the motion of a crystal can be analysed into normal modes of vibration, similar to sound waves, and that Debye's approximation gives

---

* Now at the English Electric Co., Luton, Beds.

† Communicated by the Author.

the correct frequencies for long wavelengths. It follows that (1) does apply to a real crystal at sufficiently low temperatures.

In his work on liquid helium II, Landau (1941) followed Debye's example and treated this many-particle system as a continuum—an ideal fluid rather than a solid. Just as in Debye's work, the irrotational part of the motion is analysed into longitudinal sound waves and gives the contribution (1) to the specific heat. The incompressible part of the motion, however, cannot be treated by Debye's method because an ideal fluid cannot support transverse vibrations. Landau claimed that the degrees of freedom associated with incompressible motion do not contribute to the specific heat at very low temperatures, so that (1) gives the entire specific heat at such temperatures. This conclusion was verified experimentally by the specific heat measurements of Kramers, Wasscher, and Gorter (1952).

A partial justification of Landau's assumptions was given by Bogolyubov (1947). Bogolyubov showed that the Hamiltonian for a degenerate imperfect Bose gas can be approximately expressed as a sum of commuting harmonic oscillator Hamiltonians. As one would expect from the application of Landau's theory at very low temperatures, the lowest frequencies are distributed as if they were the frequencies of longitudinal sound modes, and there is nothing corresponding to transverse sound modes.

Results confirming the value of Debye's point of view have been obtained for two other types of many-particle system. Tomonaga (1950) showed that the Hamiltonian for a one-dimensional imperfect Fermi gas could be expressed as a sum of commuting harmonic oscillator Hamiltonians, with the low frequencies distributed in the way suggested by Debye's theory. And Pines and Bohm (1952 a, b) showed that harmonic oscillator terms are present in the Hamiltonian for an electron gas, though other degrees of freedom are also present.

The success of Debye's method for such a variety of systems suggests the possibility that similar results would follow for any system in which sound can be propagated. This conjecture is confirmed by the general theory described in the present paper, which shows that the presence of harmonic oscillator terms in the Hamiltonian can be inferred from the periodic motions which constitute sound. The theory has been illustrated by showing that the essential results obtained for the above-mentioned special models by Born and von Karman, Tomonaga, Bogolyubov, and Pines and Bohm can also be obtained by applying this general theory.

§ 2. MICROSCOPIC DESCRIPTION OF THE SOUND FIELD

As a model of a physical system, consider a very large number, N, of interacting particles, each of mass m, with position vectors $\mathbf{q}_1, \ldots \mathbf{q}_N$, momentum vectors $\mathbf{p}_1, \ldots \mathbf{p}_N$, and Hamiltonian

$$H \equiv \sum_{j=1}^{N} p_j^2/2m + \sum_{i<j} \sum U(\mathbf{q}_i - \mathbf{q}_j). \qquad (2)$$

Dirac's notation (1947) will be used. To simulate the effect of the walls of the container, periodic boundary conditions will be imposed: that is, the coordinate representative of any permissible state or operator must be periodic in each of the $\mathbf{q}_j$'s. For example, in order for the Hamiltonian (2) to be periodic, U must be a periodic function of its argument. With these boundary conditions, each of the momentum operators $\mathbf{p}_j$ has a discrete spectrum of eigenvalues. The system is effectively confined to a volume V, where V is the repeating volume of the periodicity.

Landau (1941) defined the density operator $\rho(\mathbf{x})$ and the current density operator $\mathbf{J}(\mathbf{x})$:

$$\left.\begin{aligned} \rho(\mathbf{x}) &\equiv m \sum_j \delta(\mathbf{q}_j - \mathbf{x}), \\ \mathbf{J}(\mathbf{x}) &\equiv \sum_j \tfrac{1}{2}\{\mathbf{p}_j\, \delta(\mathbf{q}_j - \mathbf{x}) + \delta(\mathbf{q}_j - \mathbf{x})\, \mathbf{p}_j\}, \end{aligned}\right\} \qquad (3)$$

where $\delta(\mathbf{x})$ is a three-dimensional Dirac delta-function. Their expectation values are respectively the density and the current density at the point $\mathbf{x}$. They satisfy the equation of continuity

$$\dot{\rho}(\mathbf{x}) = -\operatorname{div} \mathbf{J}(\mathbf{x}), \qquad (4)$$

with Heisenberg's definition of a time-derivative

$$\dot{A} \equiv [A, H] \equiv (AH - HA)/i\hbar. \qquad (5)$$

The Fourier components of these operators,

$$\left.\begin{aligned} \rho_{\mathbf{k}} &\equiv \int_V \exp(i\mathbf{k}\cdot\mathbf{x})\rho(\mathbf{x})\, d^3\mathbf{x} = m \sum_j \exp(i\mathbf{k}\cdot\mathbf{q}_j), \\ \mathbf{J}_{\mathbf{k}} &\equiv \int_V \exp(i\mathbf{k}\cdot\mathbf{x})\mathbf{J}(\mathbf{x})\, d^3\mathbf{x} = \sum_j \tfrac{1}{2}\{\mathbf{p}_j \exp(i\mathbf{k}\cdot\mathbf{q}_j) + \exp(i\mathbf{k}\cdot\mathbf{q}_j)\mathbf{p}_j\}, \end{aligned}\right\} \qquad (6)$$

therefore satisfy the equations

$$\dot{\rho}_{\mathbf{k}} = i\mathbf{k}\cdot\mathbf{J}_{\mathbf{k}}. \qquad (7)$$

If $\mathbf{k} \neq 0$, the operators $\rho_{\mathbf{k}}$, $\rho_{-\mathbf{k}}$, $\dot{\rho}_{\mathbf{k}}$, and $\dot{\rho}_{-\mathbf{k}}$ describe the pair of longitudinal sound modes whose wave-vectors are $\pm\mathbf{k}$ (the wavelength is $2\pi/k$). Moreover, $\rho_0 = Nm$ is the mass of the system, and $\mathbf{J}_0$ is its momentum.

From (6), (7), and the fundamental commutation relations between the position and momentum variables, the following commutation relations can be deduced:

$$\left.\begin{aligned} \mathbf{J}_0\rho_{\mathbf{k}} - \rho_{\mathbf{k}}\mathbf{J}_0 &= \hbar\mathbf{k}\rho_{\mathbf{k}}, \\ \mathbf{J}_0\dot{\rho}_{\mathbf{k}} - \dot{\rho}_{\mathbf{k}}\mathbf{J}_0 &= \hbar\mathbf{k}\dot{\rho}_{\mathbf{k}}. \end{aligned}\right\} \qquad (8)$$

These will be used in discussing the momentum of sound quanta.

§ 3. THE SOUND PROPAGATION EQUATION

If sound vibrations are present in the system, $\rho_{\mathbf{k}}$ will vary approximately sinusoidally with time, with frequency $kc/2\pi$, where k is the length of the vector $\mathbf{k}$. For a system at rest, this fact can be expressed by the oscillation equation

$$\ddot{\rho}_{\mathbf{k}} + k^2c^2\rho_{\mathbf{k}} \simeq 0. \qquad (9)$$

This equation can be derived from the equations of hydrodynamics, or from the experimental fact that sound waves are observed. For the theoretical models treated in §§ 6 and 7 it will be proved directly.

If dispersion is negligible, c is independent of k and can be calculated from the adiabatic compressibility. For the present purpose, the compressibility at absolute zero will be used ; consequently (9) only applies for temperatures near absolute zero. Equation (9) neglects attenuation, fluctuations, and non-linear effects such as the coupling of different modes ; since attenuation increases rapidly with k, the approximation (9) is only permissible when

$$k<k_M. \qquad \text{. . . . .} \quad (10)$$

Here k_M is some limiting wave-number. Since disturbances of shorter wavelength than the mean separation of particles will not behave like sound waves, k_M cannot exceed $(N/V)^{1/3}$.

Since non-linear effects were neglected in (9), the amplitude of sound must be restricted to small values. That is, neither the density nor the current density may depart greatly from its value averaged over the whole volume V. Since the average velocity is

$$\mathbf{w}\equiv \mathbf{J}_0/Nm, \qquad \text{. . . . .} \quad (11)$$

this assumption can be written

$$\left.\begin{aligned} &|\,\rho(\mathbf{x})-Nm/V\,| \ll Nm/V, \\ &|\,\mathbf{J}(\mathbf{x})-\tfrac{1}{2}\{\mathbf{w}\rho(\mathbf{x})+\rho(\mathbf{x})\mathbf{w}\}\,| \ll Nmc/V. \end{aligned}\right\} \quad \text{. . . . .} \quad (12)$$

The form of the second inequality has been chosen so as to make it independent of the average velocity $\mathbf{w}$, which is irrelevant to the internal motions of the liquid. It follows from (12) that

$$\left.\begin{aligned} &|\,\rho_{\mathbf{k}}\,| = \left|\int_V \exp(i\mathbf{k}\cdot\mathbf{x})\{\rho(\mathbf{x})-Nm/V\}\,d^3\mathbf{x}\right| \ll Nm, \ldots (k\neq 0), \\ &|\,\mathbf{J}_{\mathbf{k}}-\tfrac{1}{2}\{\mathbf{w}\rho_{\mathbf{k}}+\rho_{\mathbf{k}}\mathbf{w}\}\,| \ll Nmc. \end{aligned}\right\} \quad (13)$$

The assumption (13) need only be made for $k<k_M$.

It is possible to generalize eqn. (9) to moving systems. The unitary operator

$$G_{\mathbf{u}}\equiv \exp \sum_j im\mathbf{u}\cdot\mathbf{q}_j/\hbar, \qquad \text{. . . . . . .} \quad (14)$$

transforms the variables of the system as follows :

$$G_{-\mathbf{u}}\mathbf{q}_j G_{\mathbf{u}}=\mathbf{q}_j,$$

$$G_{-\mathbf{u}}\mathbf{p}_j G_{\mathbf{u}}=\mathbf{p}_j+m\mathbf{u},$$

$$G_{-\mathbf{u}}\mathbf{J}_0 G_{\mathbf{u}}=\mathbf{J}_0+Nm\mathbf{u}, \qquad \text{. . . . .} \quad (15)$$

$$G_{-\mathbf{u}}HG_{\mathbf{u}}=H+\mathbf{u}\cdot\mathbf{J}_0+\tfrac{1}{2}Nmu^2. \qquad \text{. . . . . .} \quad (16)$$

The boundary conditions only permit values of $\mathbf{u}$ such that $m\mathbf{u}$ is a possible value of the momentum of a single particle. The transformation corresponds to changing to a frame of reference whose velocity is $-\mathbf{u}$ relative to the old one, or alternatively to increasing the velocity of every particle by $\mathbf{u}$. Neither the Hamiltonian H nor the total momentum $\mathbf{J}_0$ is invariant under this transformation, but the operator

$$\mathfrak{H} \equiv H - J_0^2/2Nm \quad . \; . \; . \; . \; . \; . \; . \; . \quad (17)$$

is so invariant. It can be regarded as the Hamiltonian referred to a frame of reference moving with the velocity $\mathbf{w}$ of the system (where $\mathbf{w}$ is given by (11)), and will be called the internal energy.

A new kind of time-derivative can now be defined :

$$\begin{aligned} \mathring{A} &\equiv [A, \mathfrak{H}] \\ &= \dot{A} - \tfrac{1}{2}\{\mathbf{w} \,.\, [A, \mathbf{J}_0] + [A, \mathbf{J}_0] \,.\, \mathbf{w}\}, \quad . \; . \; . \; . \; . \quad (18) \end{aligned}$$

e.g. $$\mathring{\rho}(\mathbf{x}) = \dot{\rho}(\mathbf{x}) + \tfrac{1}{2}\{\mathbf{w} \,.\, \operatorname{grad} \rho(\mathbf{x}) + \operatorname{grad} \rho(\mathbf{x}) \,.\, \mathbf{w}\}.$$

Since, by (12), the local velocity is approximately $\mathbf{w}$ everywhere, this last equation shows that the new time-derivative is approximately the same as the derivative following the motion of the fluid, or convective derivative, used in hydrodynamics (Lamb 1924). Equation (9) may therefore be generalized to moving systems by replacing the ordinary time-derivatives by the convective derivatives defined in (18) :

$$\mathring{\mathring{\rho}}_{\mathbf{k}} + k^2 c^2 \rho_{\mathbf{k}} \simeq 0. \quad . \; . \; . \; . \; . \; . \; . \; . \; . \quad (19)$$

Each term of this equation is invariant under transformation by $G_{\mathbf{u}}$, so that eqn. (19) is a statement of the sound propagation equation that is independent of the frame of reference.

The convective derivative of $\rho_{\mathbf{k}}$ can be found from (18), (8), (6), and (7) :

$$\mathring{\rho}_{\mathbf{k}} = i\mathbf{k} \,.\, \sum_j \tfrac{1}{2}\{(\mathbf{p}_j - m\mathbf{w}) \exp(i\mathbf{k} \,.\, \mathbf{q}_j) + \exp(i\mathbf{k} \,.\, \mathbf{q}_j)(\mathbf{p}_j - m\mathbf{w})\}. \quad (20)$$

The sets of operators $\rho_{\mathbf{k}}$ and $\mathring{\rho}_{\mathbf{k}}$, being invariant under transformation by any $G_{\mathbf{u}}$, are suitable for a description of the sound field that is independent of the velocity of the system. Their commutation relations, which follow from (6), (20), (11), (8), and the fundamental quantum conditions, are

$$\begin{aligned} &\rho_{\mathbf{a}}\rho_{\mathbf{b}} - \rho_{\mathbf{b}}\rho_{\mathbf{a}} = 0, \\ &\rho_{\mathbf{a}}\mathring{\rho}_{\mathbf{b}} - \mathring{\rho}_{\mathbf{b}}\rho_{\mathbf{a}} = -i\hbar(\mathbf{a} \,.\, \mathbf{b})\{\rho_{\mathbf{a}+\mathbf{b}} - \rho_{\mathbf{a}}\rho_{\mathbf{b}}/Nm\}, \\ &\mathring{\rho}_{\mathbf{a}}\mathring{\rho}_{\mathbf{b}} - \mathring{\rho}_{\mathbf{b}}\mathring{\rho}_{\mathbf{a}} = \hbar(\mathbf{a} \,.\, \mathbf{b})(\mathbf{a} - \mathbf{b}) \,.\, (\mathbf{J}_{\mathbf{a}+\mathbf{b}} - \tfrac{1}{2}\{\mathbf{w}\rho_{\mathbf{a}+\mathbf{b}} + \rho_{\mathbf{a}+\mathbf{b}}\mathbf{w}\}) \\ &\qquad\qquad + i\hbar(\mathbf{a} \,.\, \mathbf{b})(\mathring{\rho}_{\mathbf{a}}\rho_{\mathbf{b}} - \mathring{\rho}_{\mathbf{b}}\rho_{\mathbf{a}})/Nm. \end{aligned}$$

On account of (13), these simplify to

$$\left.\begin{aligned} &\rho_{\mathbf{a}}\rho_{\mathbf{b}} - \rho_{\mathbf{b}}\rho_{\mathbf{a}} = 0, \\ &\rho_{\mathbf{a}}\mathring{\rho}_{-\mathbf{a}} - \mathring{\rho}_{-\mathbf{a}}\rho_{\mathbf{a}} \simeq i\hbar N m a^2. \\ &|\rho_{\mathbf{a}}\mathring{\rho}_{\mathbf{b}} - \mathring{\rho}_{\mathbf{b}}\rho_{\mathbf{a}}| \ll \hbar N m a b \quad \text{if} \quad \mathbf{a} + \mathbf{b} \neq 0, \\ &|\mathring{\rho}_{\mathbf{a}}\mathring{\rho}_{\mathbf{b}} - \mathring{\rho}_{\mathbf{b}}\mathring{\rho}_{\mathbf{a}}| \ll \hbar N m a b(a+b)c. \end{aligned}\right\} \quad . \; . \; . \; . \quad (21)$$

Thus, $\mathring{\rho}_{-\mathbf{k}}/Nmk^2$ is an approximate canonical conjugate variable to $\rho_{\mathbf{k}}$. This is analogous to the situation for a harmonic oscillator, where the canonical conjugate of either the position or the momentum variable is proportional to the time-derivative of this variable.

Kronig and Thellung (1952) have given a field-theoretical treatment of the irrotational motion of a perfect fluid. Their treatment shows that the density field possesses an exact canonical conjugate—the velocity potential. The canonical conjugates of the $\rho_{\mathbf{k}}$'s are therefore the Fourier components of the velocity potential. These are indeed proportional to the approximate time-derivatives of the $\rho_{\mathbf{k}}$'s obtained from the approximate Hamiltonian which contains only terms of the second order in the $\rho_{\mathbf{k}}$'s and their conjugates (eqn. (39) of Kronig and Thellung's paper). Since the number of $\rho_{\mathbf{k}}$'s is infinite, the fact that canonical conjugates can be found for all of them simultaneously means that the ideal fluid has an infinite number of degrees of freedom.

The system of particles considered in the present paper has only a finite number ($3N$) of degrees of freedom. Consequently it is not possible to find exact canonical conjugates for all the $\rho_{\mathbf{k}}$'s simultaneously. Thus, the approximate nature of the commutation relations (21) can be thought of as resulting from the attempt to describe a discrete system of particles in a way more appropriate for the description of a continuous fluid.

§ 4. The Creation and Destruction Operators

Using the analogy between a sound mode and a harmonic oscillator, mentioned above, a quantum theory of sound waves can be built up, similar to Dirac's treatment of the harmonic oscillator (1947 a). Dirac's treatment is based on ' creation ' and ' destruction ' operators, which transfer the system from one stationary state to another. It will be shown here that the corresponding operators for a sound mode are

$$\left.\begin{aligned}\eta_{\mathbf{k}} &\equiv (2Nm\hbar k^3c)^{-1/2}(\mathring{\rho}_{\mathbf{k}}+ikc\rho_{\mathbf{k}}),\\ \bar{\eta}_{\mathbf{k}} &\equiv (2Nm\hbar k^3c)^{-1/2}(\mathring{\rho}_{-\mathbf{k}}-ikc\rho_{-\mathbf{k}}).\end{aligned}\right\}\ldots(k<k_M). \quad . \quad . \quad (22)$$

Very similar operators have already been given by Akhieser and Pomeranchuk (1945).

Because of (19), the $\eta_{\mathbf{k}}$'s and $\bar{\eta}_{\mathbf{k}}$'s have the equations of motion

$$\mathring{\eta}_{\mathbf{k}} \simeq ikc\eta_{\mathbf{k}}; \quad \mathring{\bar{\eta}}_{\mathbf{k}} \simeq -ikc\bar{\eta}_{\mathbf{k}}, \quad . \quad . \quad . \quad . \quad . \quad . \quad (23)$$

and, because of (21), they satisfy the commutation relations

$$\left.\begin{aligned}\eta_{\mathbf{a}}\eta_{\mathbf{b}}-\eta_{\mathbf{b}}\eta_{\mathbf{a}} &\simeq 0,\\ \eta_{\mathbf{a}}\bar{\eta}_{\mathbf{b}}-\bar{\eta}_{\mathbf{b}}\eta_{\mathbf{a}} &\simeq -\delta_{\mathbf{ab}}.\end{aligned}\right\} \quad . \quad . \quad . \quad . \quad . \quad . \quad . \quad (24)$$

Thus the $\eta_{\mathbf{k}}$'s and $\bar{\eta}_{\mathbf{k}}$'s approximately satisfy the commutation relations characteristic of the creation and destruction operators for a set of harmonic oscillators or for a set of Bose–Einstein particles (Dirac 1947 b). These operators $\eta_{\mathbf{k}}$ and $\bar{\eta}_{\mathbf{k}}$ may therefore be said respectively to create and destroy sound quanta or *phonons* in the mode **k**.

The operators defined by

$$\nu_{\mathbf{k}} \equiv \eta_{\mathbf{k}}\eta_{\mathbf{k}} \quad . \quad . \quad . \quad . \quad . \quad . \quad . \quad . \quad . \quad (25)$$

satisfy, by (24), the relations

$$\left.\begin{aligned} \nu_{\mathbf{k}}\eta_{\mathbf{a}} &\simeq \eta_{\mathbf{a}}(\nu_{\mathbf{k}}+\delta_{\mathbf{ak}}), \\ \nu_{\mathbf{k}}\bar{\eta}_{\mathbf{a}} &\simeq \bar{\eta}_{\mathbf{a}}(\nu_{\mathbf{k}}-\delta_{\mathbf{ak}}). \end{aligned}\right\} \quad . \; . \; . \; . \; . \; . \; . \; . \quad (26)$$

Equation (26) means that if a state $|\nu'\rangle$ is simultaneously an approximate eigenstate of all the ν's, corresponding to the set of eigenvalues $\ldots\nu_{\mathbf{a}}'\ldots\nu_{\mathbf{b}}'\ldots\nu_{\mathbf{k}}'\ldots$ (this is possible because the ν's commute), then $\eta_{\mathbf{k}}|\nu'\rangle$ and $\bar{\eta}_{\mathbf{k}}|\nu'\rangle$ are also eigenstates of all the ν's, corresponding to the sets of eigenvalues $\ldots\nu_{\mathbf{a}}'\ldots\nu_{\mathbf{b}}'\ldots(\nu_{\mathbf{k}}'+1)\ldots$ and $\ldots\nu_{\mathbf{a}}'\ldots\nu_{\mathbf{b}}'\ldots(\nu_{\mathbf{k}}'-1)\ldots$ respectively. The form of eqn. (25) shows that the expectation of $\nu_{\mathbf{k}}$ cannot be negative, so that $\nu_{\mathbf{k}}$ has no negative eigenvalues. Consequently, the sequence $|\nu'\rangle$, $\bar{\eta}_{\mathbf{k}}|\nu'\rangle$, $\bar{\eta}_{\mathbf{k}}^2|\nu'\rangle\ldots$ cannot continue indefinitely; it must end with some state that is annihilated by $\bar{\eta}_{\mathbf{k}}$. By (25), such a state must be an eigenstate of $\nu_{\mathbf{k}}$, with the eigenvalue zero, and therefore $\nu_{\mathbf{k}}'$ can only take the values 0, 1, 2, 3. . . . (This proof is due to Dirac (1947 a).) It is therefore natural to interpret $\nu_{\mathbf{k}}$ as the number of phonons in the mode **k**. The interpretation of $\eta_{\mathbf{k}}$ and $\bar{\eta}_{\mathbf{k}}$ as operators creating and destroying one phonon in the mode **k** is confirmed by this discussion.

Quanta of energy and momentum may be associated with each phonon in the following way: eqn. (23) is equivalent to

$$\mathfrak{H}\eta_{\mathbf{k}} \simeq \eta_{\mathbf{k}}(\mathfrak{H}+\hbar kc). \quad . \; . \; . \; . \; . \; . \; . \; . \quad (27)$$

Thus, if $|\mathfrak{H}'\rangle$ is an eigenstate of the internal energy operator $\mathfrak{H}$, corresponding to the eigenvalue $\mathfrak{H}'$, then $\eta_{\mathbf{k}}|\mathfrak{H}'\rangle$ is also an eigenstate of $\mathfrak{H}$, corresponding to the eigenvalue $\mathfrak{H}'+\hbar kc$. In this way, the addition of a phonon in the mode **k** is accompanied by an increase of energy $\hbar kc$, which may be called the energy of that phonon. Similarly, the equation

$$\mathbf{J}_0\eta_{\mathbf{k}} = \eta_{\mathbf{k}}(\mathbf{J}_0+\hbar\mathbf{k}), \quad . \; . \; . \; . \; . \; . \; . \; . \quad (28)$$

which follows from (8) and (22), can be interpreted to mean that a phonon in the mode **k** has the momentum $\hbar\mathbf{k}$. This momentum of a phonon is related to the Doppler effect: by (18) and (28),

$$\mathring{\eta}_{\mathbf{k}} = \dot{\eta}_{\mathbf{k}} - \tfrac{1}{2}i\mathbf{k}\,.\,\{\mathbf{w}\eta_{\mathbf{k}}+\eta_{\mathbf{k}}\mathbf{w}\},$$

and therefore, by (23),

$$\dot{\eta}_{\mathbf{k}} = \tfrac{1}{2}i\{(kc+\mathbf{k}\,.\,\mathbf{w})\eta_{\mathbf{k}}+\eta_{\mathbf{k}}(kc+\mathbf{k}\,.\,\mathbf{w})\}. \quad . \; . \; . \; . \quad (29)$$

Thus, the frequency of sound in the mode **k**, when the velocity of the system is **w**, is $(kc+\mathbf{k}\,.\,\mathbf{w})/2\pi$. This value agrees with the Doppler effect formula.

The creation operators can be used to construct stationary states from the ground state. The ground state $|0\rangle$ is defined as the eigenstate of H corresponding to the lowest eigenvalue, E_0. For simplicity this energy level is assumed non-degenerate. Since H commutes with the momentum $\mathbf{J}_0$, $|0\rangle$ is also an eigenstate of $\mathbf{J}_0$; the corresponding eigenvalue must be zero because the properties of the system are unaltered by reflections. Consequently $|0\rangle$ corresponds to the eigenvalue E_0 of the internal energy operator $\mathfrak{H}$.

One may also define ‘ moving ground states ’, as follows :

$$|\mathbf{u}\rangle \equiv G_{\mathbf{u}}|0\rangle,$$

where $G_{\mathbf{u}}$ is defined by (14). Because $G_{\mathbf{u}}$ commutes with $\mathfrak{H}$, while $\mathbf{J}_0$ is transformed by it according to (15), $|\mathbf{u}\rangle$ is an eigenstate of $\mathfrak{H}$ and of $\mathbf{J}_0$, corresponding to the eigenvalues E_0 and $Nm\mathbf{u}$ respectively.

Now, consider the state $\bar{\eta}_{\mathbf{k}}|0\rangle$. Equations (27) and (28) apparently indicate that this is an eigenstate of $\mathfrak{H}$ and of $\mathbf{J}_0$ corresponding to the eigenvalues $E_0-\hbar kc$ and $-\hbar\mathbf{k}$ respectively, and hence of H corresponding to the eigenvalue $E_0-\hbar kc+\hbar^2k^2/2Nm$. This quantity, however, cannot be an eigenvalue of H because it is less than E_0 ; consequently, $\bar{\eta}_{\mathbf{k}}|0\rangle \simeq 0$ must hold. Since $G_{\mathbf{u}}$ commutes with the $\rho_{\mathbf{k}}$'s and $\mathring{\rho}_{\mathbf{k}}$'s, and therefore with the $\eta_{\mathbf{k}}$'s, it follows that

$$\bar{\eta}_{\mathbf{k}}|\mathbf{u}\rangle \simeq 0. \tag{30}$$

This implies that $|\mathbf{u}\rangle$ is an eigenstate of all the $\nu_{\mathbf{k}}$'s, corresponding to the eigenvalue zero ; that is, no phonons are present when the system is in a moving ground state.

By operating on any moving ground state $|\mathbf{u}\rangle$ with a succession of $\eta_{\mathbf{k}}$'s, a state may be constructed which is an eigenstate of $\mathbf{J}_0$ and an approximate eigenstate of $\mathfrak{H}$, H and all the $\nu_{\mathbf{k}}$'s. By virtue of (26), (27), and (28), the corresponding eigenvalues will satisfy

$$\mathfrak{H}' \simeq E_0 + \sum_{\mathbf{k}} \hbar kc\nu_{\mathbf{k}}', \tag{31}$$

$$\mathbf{J}_0' = Nm\mathbf{u} + \sum_{\mathbf{k}} \hbar\mathbf{k}\nu_{\mathbf{k}}'. \tag{32}$$

These equations mean that the energy of a state constructed by adding phonons to a moving ground state can be regarded as the sum of the energy of the ground state and the energy of a ‘ phonon gas ’, and the momentum similarly.

§ 5. STATISTICAL THERMODYNAMICS OF THE SYSTEM

For some systems, the method of constructing stationary states by adding phonons to the various moving ground states, described above, is sufficient to construct approximations to nearly all the low-energy stationary states. In other words, longitudinal sound vibrations are the only degrees of freedom effective at very low temperatures. If this is so, the specific heat at such low temperatures will be that for the equivalent assembly of harmonic oscillators, as given by (1).

The mean number of phonons in the mode $\mathbf{k}$ will be

$$\langle\nu_{\mathbf{k}}\rangle = (\exp \hbar kc/\kappa T - 1)^{-1} \tag{33}$$

(cf. Fowler 1936). Since the right-hand side is independent of N, it follows from (25) and (22) that $\rho_{\mathbf{k}}$ and $\mathring{\rho}_{\mathbf{k}}$ have the order of magnitude $N^{1/2}$. Therefore the approximation (13) is justified for this application. The approximation (19) will be justified if $\nu_{k_M} \ll 1$. This will be so if

$$T \ll \hbar k_M c/\kappa. \tag{34}$$

For helium II, if we take $k_M=(N/V)^{1/3}$, the right-hand side of (34) is about 5°K.

If there are low-energy states which cannot be constructed by adding phonons to moving ground states, one may say that the system has extra degrees of freedom, other than longitudinal sound modes. In this case, the specific heat must be *greater* than (1). For example, in a crystal, transverse vibrations are extra degrees of freedom, which give an extra contribution to the specific heat, comparable with the contribution of longitudinal vibrations.

In this way, the theory of phonons gives a lower limit to the specific heat, and whether or not the lower limit is achieved shows whether or not all the low-energy stationary states can be constructed by the method described in the last section. I am grateful to Professor Lars Onsager for pointing this out.

§ 6. THE LINEAR CRYSTAL

In this and the next section it will be verified that the present theory gives correct results for some simple models whose low-energy stationary states are known. The first of these is the linear crystal. Equation (19) does not apply to a real crystal because it ignores the coupling between longitudinal and transverse vibrations. However, the theory can be applied to a linear crystal, where transverse vibrations are excluded by confining all the particles to a straight line.

Consider the part of configuration space where all the quantities $q_{j+1}-q_j-L/N$ $(j=1, 2, \ldots N-1)$ are small (L being the repeating distance of the periodic boundary conditions). This means that the particles are approximately equally spaced and are arranged in the order in which they are numbered. The deviations of the particles from the equally spaced positions are

$$r_j \equiv q_j - jL/N - Q_0, \qquad (35)$$

where $Q_0 \equiv \sum_j q_j/N - \frac{1}{2}(N+1)L/N$. (This choice of 'equally spaced positions' serves to make $\sum_j r_j$ equal to zero.)

A good approximation to the Hamiltonian for the part of configuration space where all the r_j's are small is obtained by Born and von Karman's method—neglecting third and higher order terms in a Taylor expansion of the potential energy:

$$H \simeq \sum_j p_j^2/2m + (mc^2N^2/2L^2)\left\{\sum_{j=1}^{N-1} (r_{j+1}-r_j)^2 + (r_N-r_1)^2\right\} + \text{const.} \qquad (36)$$

The interaction between the first and N'th particles arises from the mathematical device of making the Hamiltonian periodic, mentioned in § 2.

The canonical transformation

$$\left.\begin{aligned} P_k &\equiv \sum_j \exp(ikjL/N)p_j, && (\text{all } k) \\ Q_k &\equiv \sum_j \exp(ikjL/N)r_j/N, && (k\neq 0) \end{aligned}\right\} \cdot \qquad (37)$$

where k takes the values

$$-(N-1)\pi/L,\ -(N-3)\pi/L,\ \ldots\ -2\pi/L,\ 0,\ \ldots\ (N-1)\pi/L \quad (N \text{ odd}),$$

$$-(N-2)\pi/L,\ -(N-4)\pi/L,\ \ldots\ -2\pi/L,\ 0,\ \ldots\ N\pi/L \quad (N \text{ even}),$$

transforms (36) into a sum of harmonic oscillator Hamiltonians :

$$\begin{aligned} H &\simeq \tfrac{1}{2}\sum_k (P_kP_{-k}/Nm + Nm\omega_k{}^2Q_kQ_{-k}) + \text{const.} \\ &= J_0{}^2/2Nm + \sum_{k\neq 0} \hbar\omega_k\xi_k\bar{\xi}_k + \text{const.}, \end{aligned}$$

where

$$\omega_k \equiv (2cN/L)\sin|k|L/2N \simeq c|k|,$$

$$\xi_k \equiv (2Nm\hbar\omega_kk^2)^{-1/2}ik(P_k + iNm\omega_kQ_k).$$

The creation operators ξ_k are due to Peierls (1929). In terms of P_k's and Q_k's, the Fourier components of density become

$$\begin{aligned} \rho_k &= m\sum_j \exp(ikq_j) \\ &= m\sum_j \exp(ikjL/N)\{1 + ikr_j + O(k^2r_j{}^2)\}\exp(ikQ_0) \\ &\simeq ikNmQ_k \exp(ikQ_0). \ldots \quad (k \neq 0). \end{aligned}$$

Now, the equations of motion for Q_k and P_k following from the Hamiltonian (36) are, for $k\neq 0$,

$$\mathring{Q}_k = \dot{Q}_k = P_k/Nm,$$

$$\mathring{P}_k = \dot{P}_k \simeq Nm\omega_k{}^2Q_k,$$

and hence

$$\mathring{\rho}_k \simeq ikP_k \exp(ikQ_0),$$

$$\overset{\circ\circ}{\rho}_k \simeq -ikNm\omega_k{}^2Q_k \exp(ikQ_0) \simeq -k^2c^2\rho_k$$

(since $\mathring{Q}_0 = 0$). Thus the sound propagation eqn. (19) holds, and consequently approximate stationary states may be constructed using the creation operators

$$\eta_k \simeq \xi_k \exp(ikQ_0). \quad . \ . \ . \ . \ . \ . \ . \ . \quad (38)$$

For small values of k, the η_k's differ from Peierls' creation operators ξ_k only in the factor $\exp(ikQ_0)$. This factor is analogous to the operator $G_{\mathbf{u}}$ of (14), and changes the momentum of the system but not its internal energy, while ξ_k changes the energy but not the momentum. Although either factor can be used separately to construct eigenfunctions of the approximate Hamiltonian (36), these functions will be approximations to eigenfunctions of the true Hamiltonian only if the two factors are combined as in (38). If they are not so combined, the boundary conditions cannot be satisfied. For example, $\exp(ikQ_0)$ by itself does not obey the periodic boundary conditions unless k either vanishes or is outside the range of values enumerated in (37).

This discussion shows why Peierls' theory apparently leads to the incorrect result that a phonon has no momentum.

§ 7. Imperfect Gases

To compare the present theory with the known results for imperfect Bose and Fermi gases, the expressions for $\rho_{\mathbf{k}}$ and its time-derivatives in the formalism of second quantization (Dirac 1947 b, c, Fock 1932) are necessary. These are (Tomonaga 1950, Nishiyama 1951)

$$\rho_{\mathbf{k}}=m\sum_{\mathbf{a}}\bar{\psi}_{\mathbf{a}+\frac{1}{2}\mathbf{k}}\psi_{\mathbf{a}-\frac{1}{2}\mathbf{k}}, \quad . \quad . \quad . \quad . \quad . \quad . \quad . \quad . \quad (39)$$

$$\dot{\rho}_{\mathbf{k}}=i\hbar\sum_{\mathbf{a}}(\mathbf{a}\,.\,\mathbf{k})\bar{\psi}_{\mathbf{a}+\frac{1}{2}\mathbf{k}}\psi_{\mathbf{a}-\frac{1}{2}\mathbf{k}}, \quad . \quad . \quad . \quad . \quad . \quad . \quad . \quad (40)$$

$$\ddot{\rho}_{\mathbf{k}}=-(\hbar^2/m)\sum_{\mathbf{a}}(\mathbf{a}\,.\,\mathbf{k})^2\bar{\psi}_{\mathbf{a}+\frac{1}{2}\mathbf{k}}\psi_{\mathbf{a}-\frac{1}{2}\mathbf{k}}-\sum_{\mathbf{a}}(\mathbf{a}\,.\,\mathbf{k})\rho_{\mathbf{a}}\rho_{\mathbf{k}-\mathbf{a}}U_{\mathbf{a}}/m^2V,$$

where $U_{\mathbf{a}}\equiv\int_V \exp(i\mathbf{a}\,.\,\mathbf{x})U(\mathbf{x})\,d^3\mathbf{x}$, and $\bar{\psi}_{\mathbf{k}}$ and $\psi_{\mathbf{k}}$ are respectively the creation and destruction operators for a particle with momentum $\hbar\mathbf{k}$. In the sum which forms the second term in the expression for $\ddot{\rho}_{\mathbf{k}}$, the term containing ρ_0 is overwhelmingly the largest because (13) applies to only one of its factors instead of to two. Therefore, if $U_{\mathbf{k}}$ decreases rapidly enough as $k\rightarrow\infty$, only this term need be retained :

$$\ddot{\rho}_{\mathbf{k}}\simeq-(\hbar^2/m)\sum_{\mathbf{a}}(\mathbf{a}\,.\,\mathbf{k})^2\bar{\psi}_{\mathbf{a}+\frac{1}{2}\mathbf{k}}\psi_{\mathbf{a}-\frac{1}{2}\mathbf{k}}-k^2N\rho_{\mathbf{k}}U_{\mathbf{k}}/mV. \quad . \quad . \quad . \quad (41)$$

This is equivalent to Pines and Bohm's approximation of random phase (1952 a).

In an imperfect Bose gas at low temperatures, nearly all the particles are assumed to be in the zero-momentum single-particle state. Since the number of particles with momentum $\hbar\mathbf{k}$ is

$$n_{\mathbf{k}}\equiv\bar{\psi}_{\mathbf{k}}\psi_{\mathbf{k}}, \quad . \quad . \quad . \quad . \quad . \quad . \quad . \quad . \quad (42)$$

this assumption may be written

$$\bar{\psi}_0\psi_0\gg\sum_{\mathbf{k}\neq 0}\bar{\psi}_{\mathbf{k}}\psi_{\mathbf{k}}, \quad \text{or} \quad \psi_0\gg\psi_{\mathbf{k}}.$$

Bogolyubov's approximation (1947) is to neglect $\psi_{\mathbf{k}}$ in comparison with ψ_0. Applied to (39), (40), and (41), this gives

$$\left.\begin{aligned}\rho_{\mathbf{k}}&\simeq m(\bar{\psi}_{\mathbf{k}}\psi_0+\bar{\psi}_0\psi_{-\mathbf{k}}),\\ \dot{\rho}_{\mathbf{k}}&\simeq\tfrac{1}{2}ihk^2(\psi_{\mathbf{k}}\psi_0-\bar{\psi}_0\psi_{-\mathbf{k}}),\end{aligned}\right\} \quad . \quad . \quad . \quad . \quad . \quad (43)$$

$$\begin{aligned}\ddot{\rho}_{\mathbf{k}}&\simeq-(\hbar^2k^4/4m)(\bar{\psi}_{\mathbf{k}}\psi_0+\bar{\psi}_0\psi_{-\mathbf{k}})-k^2N\rho_{\mathbf{k}}U_{\mathbf{k}}/mV\\ &\simeq-k^2\{(\hbar k/2m)^2+U_{\mathbf{k}}N/mV\}\rho_{\mathbf{k}}. \quad . \quad . \quad . \quad . \quad . \quad . \quad (44)\end{aligned}$$

Therefore the oscillation eqn. (9) is satisfied, with

$$c^2=(\hbar k/2m)^2+U_kN/mV.$$

If the velocity $\mathbf{w}$ of the system is negligible, so that $\mathring{\rho}_{\mathbf{k}}\simeq\dot{\rho}_{\mathbf{k}}$, (44) is equivalent to (19), so that the present theory is applicable. Indeed, Bogolyubov showed that all the low-energy stationary states could be constructed from the ground state by means of certain creation operators. These are just the $\eta_{\mathbf{k}}$'s of the present theory, with the approximations (43) and $\mathring{\rho}_{\mathbf{k}}\simeq\dot{\rho}_{\mathbf{k}}$. Bogolyubov also showed that the velocity of sound as calculated from the compressibility is $(U_0 N/mV)^{1/2}$; hence (44) is a genuine sound propagation equation for small enough values of k.

In an imperfect Fermi gas at low temperatures, it may be assumed that all the single-particle levels with momenta $\ll \hbar k_F$, where k_F is the Fermi maximum, are full, while all those with momenta $\gg \hbar k_F$ are empty. That is, $n_{\mathbf{k}} = \bar{\psi}_{\mathbf{k}} \psi_{\mathbf{k}} \simeq 0$ and $\psi_{\mathbf{k}} \simeq 0$ if $k \gg k_F$, while $1 - n_{\mathbf{k}} = \psi_{\mathbf{k}} \bar{\psi}_{\mathbf{k}} \simeq 0$ and $\bar{\psi}_{\mathbf{k}} \simeq 0$ if $k \ll k_F$. Hence either $\psi_{\mathbf{k}}$ or $\bar{\psi}_{\mathbf{k}}$ is negligible unless $k \simeq k_F$. The sums in (39), (40), and (41) accordingly become, for $k \neq 0$ and $k \ll k_F$,

$$\left.\begin{aligned} \rho_{\mathbf{k}} &\simeq m \sum_{a \simeq k_F} \bar{\psi}_{\mathbf{a}+\frac{1}{2}\mathbf{k}} \psi_{\mathbf{a}-\frac{1}{2}\mathbf{k}}, \\ \dot{\rho}_{\mathbf{k}} &\simeq i\hbar \sum_{a \simeq k_F} (\mathbf{a} \cdot \mathbf{k}) \bar{\psi}_{\mathbf{a}+\frac{1}{2}\mathbf{k}} \psi_{\mathbf{a}-\frac{1}{2}\mathbf{k}}, \end{aligned}\right\} \quad . \quad . \quad . \quad . \quad (45)$$

$$\ddot{\rho}_{\mathbf{k}} \simeq -(\hbar^2/m) \sum_{a \simeq k_F} (\mathbf{a} \cdot \mathbf{k})^2 \bar{\psi}_{\mathbf{a}+\frac{1}{2}\mathbf{k}} \psi_{\mathbf{a}-\frac{1}{2}\mathbf{k}} - k^2 U_{\mathbf{k}} \rho_{\mathbf{k}} N/mV. \quad . \quad . \quad (46)$$

For one dimension, (9) follows at once, with

$$c^2 = (\hbar k_F/m)^2 + U_k N/mV.$$

Just as for the Bose gas, the theory of §§ 3 and 4 is applicable if the velocity of the system is small.

Tomonaga (1950) has shown that the Hamiltonian for this system can be expressed as a sum of harmonic oscillator Hamiltonians. The creation operators for these harmonic oscillators are, with the approximations (45) and $\mathring{\rho}_{\mathbf{k}} \simeq \dot{\rho}_{\mathbf{k}}$, just the $\eta_{\mathbf{k}}$'s defined in (22). A perturbation calculation of the energy of the ground state can again be made ; the resulting value of the velocity of sound agrees at long wavelengths with the expression given above.

For three dimensions, $(\mathbf{k} \cdot \mathbf{a})^2$ in the expression (46) for $\ddot{\rho}_{\mathbf{k}}$ may be replaced by its value averaged over all directions of $\mathbf{a}$ and $\mathbf{k}$, which is $\frac{1}{3}k^2a^2$. Then (9) follows, with

$$c^2 = \tfrac{1}{3}(\hbar k_F/m)^2 + U_k N/mV.$$

As before, the theory described in this paper is applicable if the velocity is small, and the perturbation calculation verifies the formula for the velocity of sound in the limit of long wavelengths. However, even without interactions formula (1) will give a specific heat proportional to T^3, while the true specific heat is known to be proportional to T. Therefore, there must be extra degrees of freedom, and the phonon theory is not very useful in this case.

For Coulomb interactions, $U_k = 4\pi\epsilon^2/k^2$, where ϵ is the charge on each particle, and therefore (41) is approximately

$$\ddot{\rho}_{\mathbf{k}} + (4\pi\epsilon^2 N/mV)\rho_{\mathbf{k}} \simeq 0$$

for small k. This corresponds to plasma oscillations (Tomonaga 1950, Pines and Bohm 1952 a). In this case, it is not clear whether or not extra degrees of freedom are effective at low temperatures.

The application of the theory developed here to the problem of liquid helium II will be considered in part II of this paper.

ACKNOWLEDGMENTS

I am indebted to Mr. H. N. V. Temperley for supervising this work, to Professor Lars Onsager and Dr. P. J. Price for helpful discussions, to many of my colleagues for painstaking criticism of the manuscript, and to King's College, Cambridge, for the award of the R. J. Smith Memorial Studentship, which I held when this work was begun.

REFERENCES

AKHIESER, A., and POMERANCHUK, I., 1945, *J. Phys. USSR*, **9,** 461.
BOGOLYUBOV, N. N., 1947, *J. Phys. USSR*, **11,** 23.
BORN, M., and VON KARMAN, TH., 1913, *Phys. Zeits.*, **14,** 15.
DEBYE, P., 1912, *Ann. der Phys.*, **39,** 789.
DIRAC, P. A. M., 1947 a, *Principles of Quantum Mechanics* (Third Edition : Oxford), p. 136 ; 1947 b, *Ibid.*, pp. 225–239 ; 1947 c, *Ibid.*, pp. 248–251.
FOCK, V., 1932, *Zeits. f. Phys.*, **75,** 622.
FOWLER, R. H., 1936, *Statistical Mechanics* (Second Edition : Cambridge) pp. 117–8.
KRAMERS, H. C., WASSCHER, J. D., and GORTER, C. J., 1952, *Physica*, **18,** 329.
KRONIG, R., and THELLUNG, A., 1952, *Physica*, **18,** 749.
LAMB, H., 1924, *Hydrodynamics* (Fifth Edition: Cambridge) p. 3.
LANDAU, L. D., 1941, *J. Phys. USSR*, **5,** 71.
NISHIYAMA, T., 1951, *Prog. Theor. Phys.*, **6,** 366.
PEIERLS, R., 1929, *Ann. Phys.*, **3,** 1055.
PINES, D., and BOHM, D., 1952 a, *Phys. Rev.*, **85,** 338 ; 1952 b. private communication.
TOMONAGA, S., 1950, *Prog. Theor. Phys.*, **5,** 544.

XII. *A Variation Principle for Electronic Wave Functions in Crystals*

By D. P. Jenkins and L. Pincherle
Radar Research Establishment, Ministry of Supply

[Received September 19, 1953]

ABSTRACT

A variation principle giving the energy levels of electrons in polyatomic lattices is presented. When used in conjunction with the cellular method it includes the matching of the wave functions across cell boundaries without the need of making *ad hoc* assumptions. Values of $\nabla_{\mathbf{k}} E(\mathbf{k})$ can be obtained from quantities used to determine $E(\mathbf{k})$ without carrying out any numerical differentiation. The results of some calculations on the valency bands of lead sulphide are reported.

§ 1. INTRODUCTION

It is often found that a convenient method of dealing with problems in mathematical physics is to set up a variation principle which is equivalent to the more obvious equations. It is then possible to approximate to some function associated with the problem by a convenient expression containing parameters which are varied to give the best answer possible. However the Ritz variational form of the Schrödinger equation can only be used to determine the energy levels of electrons in crystals if a very restricted class of trial wave function is used (as in the tight binding method and in the method of orthogonalized plane waves). Such functions and their variations must satisfy the correct boundary conditions on the surface enclosing the volume of integration, and the condition appropriate to Bloch functions in crystals gives little freedom of choice.

Kohn (1952) has removed this restriction by formulating a variation principle which includes the Bloch condition as well as the Schrödinger equation. As usual, the latter is expressed by a volume integral, but the Bloch condition gives a new term, a surface integral over the boundary of the volume (which need only be one unit cell of the crystal). However, when trial wave functions are obtained by the cellular method, Kohn's form of the principle applies only to crystals with one atom in the unit cell. The present paper extends his variation functional to polyatomic crystals and also shows that it is closely related to an expression giving the gradient of the energy in momentum space.

The technique has been used to redetermine some of the energy levels of lead sulphide giving results in agreement with those previously obtained by other methods (Bell *et al.* 1953).

---

* Communicated by the Authors.

§ 2. THE VARIATION PRINCIPLE

The total electronic wave function of a crystal can be written as a determinantal product of one-electron Bloch functions $\psi(\mathbf{k}, \mathbf{r})$, satisfying the approximate equation (in atomic units)

$$[-\tfrac{1}{2}\nabla^2+V(\mathbf{r})-E(\mathbf{k})]\,\psi(\mathbf{k}, \mathbf{r})=0. \quad . \quad . \quad . \quad . \quad . \quad . \quad (1)$$

The potential $V(\mathbf{r})$ has the periodicity of the lattice and will be assumed to be independent of the form of $\psi(\mathbf{k}, \mathbf{r})$.

When each unit cell of the lattice is divided into N polyhedra it becomes convenient to change the phase of ψ in each polyhedron and define

$$\psi_p(\mathbf{k}, \mathbf{r})=\exp\,(-i\mathbf{k}\,.\,\mathbf{p})\,\psi\,(\mathbf{k}, \mathbf{r}) \quad . \quad . \quad . \quad . \quad . \quad . \quad (2)$$

where $\mathbf{p}$ locates an origin in the pth polyhedron. Because of the Bloch condition, the ψ_p will have the same value at corresponding points in equivalent polyhedra in different unit cells. Clearly they will satisfy (1), and for $\psi\,(\mathbf{k}, \mathbf{r})$ to be continuous

$$\psi_p\,(\mathbf{k}, \mathbf{r})=\exp\,[i\mathbf{k}\,.\,(\mathbf{q}-\mathbf{p})]\,\psi_q\,(\mathbf{k}, \mathbf{r})\,;\ \nabla\psi_p\,(\mathbf{k}, \mathbf{r})=\exp\,[i\mathbf{k}\,.\,(\mathbf{q}-\mathbf{p})]\,\nabla\psi_q\,(\mathbf{k},\mathbf{r}) \quad . \quad . \quad . \quad (3)$$

for all points on the boundary between the polyhedra p and q.

When Kohn's analysis is applied to these conditions on the ψ_p, it is found that the generalization of his formula (5.8) is that the functional

$$J(\psi_p)=\text{Real}\sum_{p=1}^{N}\left\{\int_{\tau_p}\bar{\psi}_p[-\tfrac{1}{2}\nabla^2+V-E(\mathbf{k})]\psi_p\,d\tau+\tfrac{1}{2}\sum_q\exp\,[i\mathbf{k}\,.\,(\mathbf{q}-\mathbf{p})]\right.$$
$$\left.\times\int_{\sigma_{pq}}\psi_q\nabla\bar{\psi}_p\,.\,d\mathbf{S}_p\right\} \quad . \quad . \quad . \quad . \quad . \quad . \quad (4)$$

must be stationary for all variations of the ψ_p. In (4), $\bar{\psi}$ denotes the complex conjugate of ψ, p goes over all the polyhedra in one unit cell, τ_p being the volume of the pth polyhedron, while the q summation is over all polyhedra having a surface σ_{pq} in common with polyhedron p. As well as being stationary, J vanishes for the correct wave function and energy. However, the $E(\mathbf{k})$ found from the principle is not an upper bound for the correct value (Kohn, *loc. cit.*).

The application of the variation principle will depend on the form of the approximation to the wave function, but a very convenient technique is based on the conventional cellular method. Each polyhedron is chosen to have an atom at its centre which is taken as the origin, so that over a large volume it is reasonable to approximate to the potential by a spherically symmetric function, $V(r_p)$. Equation (1) is then separable and the wave function in each polyhedron can be approximated to by the expansion

$$\psi_p(\mathbf{r})=\sum_s A_{ps}\,\phi_{ps}(\mathbf{r}_p, \lambda)\,;\ \phi_{ps}(\mathbf{r}_p, \lambda)=L_s(\theta_p, \phi_p)\,P_s\,(r_p, \lambda) \quad . \quad . \quad (5)$$

where r_p, θ_p and ϕ_p are spherical polar coordinates, the L_s are angular functions depending on $\mathbf{k}$ and completely determined by symmetry, and the P_s are solutions of a radial equation such that

$$[-\tfrac{1}{2}\nabla^2+V(r_p)-\lambda]\phi_{ps}(\mathbf{r}_p, \lambda)=0. \quad . \quad . \quad . \quad . \quad . \quad . \quad (6)$$

The coefficients A_{ps} (in general complex) and the parameter λ are to be determined by the condition that the functional J shall be stationary when they are varied. For this type of trial function, the functional can be written in the real form

$$J(A_{ps}, \lambda)=[\lambda-E(\mathbf{k})]\sum_{p,s}\bar{A}_{ps}A_{ps}+\sum_{p,s}\sum_{q,u}\bar{A}_{ps}A_{qu}K_{ps,\,qu}(\mathbf{k},\lambda) \quad . \quad . \quad (7)$$

$$\begin{aligned}K_{ps,\,qu}(\mathbf{k},\lambda)&=\tfrac{1}{4}\exp[i\mathbf{k}\,.\,(\mathbf{q}-\mathbf{p})]\int_{\sigma_{pq}}[\phi_{qu}(\lambda)\nabla\bar{\phi}_{ps}(\lambda)-\bar{\phi}_{ps}(\lambda)\nabla\phi_{qu}(\lambda)]\,.\,d\mathbf{S}_p\\&=\bar{K}_{qu,\,ps}(\mathbf{k},\lambda)\end{aligned}$$

when, as is always possible, the base functions ϕ_{ps} are chosen to be orthonormal in their own polyhedra :

$$\int_{\tau_p}\bar{\phi}_{ps}\phi_{pt}\,d\tau=\delta_{st}.$$

Equation (7) neglects any lack of spherical symmetry in the potential function in each polyhedron ; if a more exact potential is available, the ϕ_{ps} can still be used as reasonable base functions, but the volume integral will contribute another term to (7).

From the condition that J shall be stationary the following equations are obtained :

$$\frac{\partial J}{\partial\bar{A}_{ps}}=[\lambda-E(\mathbf{k})]A_{ps}+\sum_{q,u}A_{qu}K_{ps,\,qu}(\mathbf{k},\lambda)=0 \quad . \quad . \quad . \quad (8)$$

for all ps ;

$$\frac{\partial J}{\partial\lambda}=\sum_{p,s}\bar{A}_{ps}A_{ps}+\sum_{p,s}\sum_{q,u}\bar{A}_{ps}A_{qu}\left[\frac{\partial K_{ps,\,qu}}{\partial\lambda}\right]=0. \quad . \quad . \quad . \quad (9)$$

The eqns. (8) are of familiar latent root form and, together with (9) and a normalization condition, are just enough to give those values of λ and the A_{ps} from which the best $E(\mathbf{k})$ can be obtained.

In principle this may be done by solving (8) for trial values of λ and then substituting the coefficients in (9) until a value of λ which satisfies it is found ; in practice this is a very tedious procedure. However, if an infinite number of terms could be included in the expansion (5), the value obtained for λ would be $E(\mathbf{k})$; it is only the use of a finite number of terms that makes the variation of λ necessary. This suggests that choosing $\lambda=E(\mathbf{k})$ will be a good approximation even for a finite number of terms. Equations (8) then become

$$\sum_{q,u}A_{qu}K_{ps,\,qu}(\mathbf{k},\lambda)=0 \quad . \quad . \quad . \quad . \quad . \quad . \quad . \quad (10)$$

and for these equations to be consistent the determinant of the $K_{ps,\,qu}$ must vanish : the value of λ for which this happens is the required energy, $E(\mathbf{k})$. This simplifies computation enormously but sacrifices an important aspect of the variation principle : the compromise between a mismatch at the boundaries and a poor solution of the differential equation (1).

However, this is a minor approximation compared with others implicit in the cellular method.

The use of (10) introduces an ambiguity for it can be shown that, when (10) is satisfied, the cellular functions must obey one of the two continuity conditions

$$\psi_p = \pm \exp[i\mathbf{k}\,.\,(\mathbf{q}-\mathbf{p})]\psi_q \quad . \quad . \quad . \quad . \quad . \quad . \quad . \qquad (11)$$

and, in general, only one of these gives the Bloch function required. The other gives spurious solutions derived from a variation functional which differs from J of (4) by having a negative sign between the volume integral and the surface integrals. This fact makes it possible to recognize them. But suppose that all the polyhedra in the crystal can be divided into two sets such that no polyhedra in the same set have a common surface (for instance, crystals with NaCl structure when the two polyhedra are taken to be of equal size). Then both continuity conditions in (11) correspond to a Bloch function of wave vector **k** obtained by taking

$$\psi(\mathbf{k},\mathbf{r}) = \quad \exp(i\mathbf{k}\,.\,\mathbf{p})\psi_p \text{ for polyhedra in one set,}$$

$$\psi(\mathbf{k},\mathbf{r}) = \pm\exp(i\mathbf{k}\,.\,\mathbf{q})\psi_q \text{ for polyhedra in the other set,}$$

(the sign used for the second set depending on the sign in the continuity conditions) and the determinant has no spurious zeros. Now, however (10) gives no relation between the coefficients in the two different sets of polyhedra. The latent root eqn. (8) does not solve this difficulty because it can be partitioned by putting together all elements associated with polyhedra of the same set

$$\left|\begin{array}{c:c} [\lambda - E(\mathbf{k})]I_M & K_{ps,\,qu} \\ \hdashline K_{qv,\,pt} & [\lambda - E(\mathbf{k})]I_M \end{array}\right| = 0 \quad . \quad . \quad . \qquad (12)$$

where I_M is the unit matrix of order M, the total number of base functions in one set; it is assumed that the total number of functions in each set is the same. It is easily seen that at $\lambda = E(\mathbf{k})$ the matrix has two degenerate eigenvectors which may be taken in any linear combination. No limiting procedure is possible because the coefficients obtained from (12) for $\lambda \neq E(\mathbf{k})$ satisfy

$$\sum_{\substack{p \text{ in one}\\ \text{set}}} \sum_{s} \bar{A}_{ps} A_{ps} = \sum_{\substack{q \text{ in other}\\ \text{set}}} \sum_{u} \bar{A}_{qu} A_{qu} = \frac{\sum\limits_{p,s}\sum\limits_{q,u} \bar{A}_{ps} A_{qu} K_{ps,\,qu}(\lambda)}{2(E(\mathbf{k})-\lambda)} \quad . \qquad (13)$$

which implies that for any electron the total charge in all polyhedra of the p set is equal to that in all the q polyhedra, a physically absurd conclusion. Hence for this class of crystals (10), rather than (8), must be considered to be the correct equation, while (9) supplies the required relation between the coefficients in the two sets of polyhedra.

§ 3. THE GRADIENT OF $E(\mathbf{k})$ IN $\mathbf{k}$ SPACE

The variation principle of eqn. (4) can be used to obtain a convenient formula for the vector $\nabla_{\mathbf{k}}E(\mathbf{k})$. Since J vanishes for the correct ψ_p and is stationary for their variations, a first order error in ψ_p only introduces a second order error in the energy obtained by equating J to zero. Hence it is permissible to assume the ψ_p to be independent of $\mathbf{k}$ when calculating $\nabla_{\mathbf{k}}E(\mathbf{k})$. This leads to

$$\sum_{p=1}^{N}\int_{\tau_p}\bar{\psi}_p[\nabla_{\mathbf{k}}E(\mathbf{k})-\nabla_{\mathbf{k}}V]\psi_p\,d\tau$$
$$=-\tfrac{1}{2}\,\text{Imag.}\sum_{p=1}^{N}\sum_{q}(\mathbf{q}-\mathbf{p})\exp[i\mathbf{k}\,.\,(\mathbf{q}-\mathbf{p})]\int_{\sigma_{pq}}\psi_q\nabla\bar{\psi}_p\,.\,d\mathbf{S}_p. \quad . \quad . \quad . \qquad (14)$$

It is generally assumed that V is independent of $\mathbf{k}$ so that $\nabla_{\mathbf{k}}E(\mathbf{k})$ can be found in terms of surface integrals which are evaluated when $E(\mathbf{k})$ is determined. This is much simpler and more accurate than obtaining $\nabla_{\mathbf{k}}E$ by numerical differentiation of $E(\mathbf{k})$ and is a very convenient feature of this method of finding crystal energy levels. The frequency with which $\nabla_{\mathbf{k}}E(\mathbf{k})$ appears in formulae relating to the properties of electrons in crystals, e.g. the density of states, makes it very desirable to have a simple method of calculating this quantity.

Table 1. Energy Levels of the Valency Band of PbS

Symmetry	Angular Functions	Energy (arbitrary zero)	
		Variation procedure	Matching conditions (Legendre matching)
Γ_1	α_0, α_4, α_6	—0·048	—0·049
X_1	α_0, $(\gamma_2)_1$, α_4	—0·111	—0·11
X'_4	δ_1, δ_3	—0·179	—0·18
Γ'_4	δ_1	—0·039	—
	δ_1, δ_3	—0·005	—0·004
	δ_1, δ_3, δ_5	—0·005	—0·010
	δ_1, δ_3, δ'_5	+0·007	+0·016
	δ_1, δ_3, δ_5, δ'_5	+0·005	+0·007

§ 4. APPLICATION TO LEAD SULPHIDE

Lead sulphide is a crystal of NaCl type so that its energy levels and wave functions can be obtained by using eqns. (9) and (10). Values of the ϕ_{ps} (eqn. (6)) obtained in an earlier calculation (Bell *et al.* 1953) have been used to redetermine some energy levels in the valency bands giving the values shown in table 1 (notation as in Bouckaert, Smoluchowski and Wigner (1936)). The energy of the Γ'_4 level was calculated with varying numbers of terms in the expansion of the wave functions in the two cells, the notation for the angular functions being as in Von der Lage and Bethe (1947).

When the coefficients in the expansions were calculated it was found that (9) did not give a reasonable value for the relation between the coefficients in the two polyhedra, lead and sulphur, with the limited number of terms used, possibly because the orthonormal relations for the ϕ_{ps} were satisfied over equal volume spheres (this approximation has no effect on the energy calculated from (10)). Also, because of the symmetry of (9) in the two polyhedra, there seems to be no way of deciding between two sets of coefficients which give opposite total charges to the two cells. To overcome these difficulties a semi-empirical procedure was adopted, and the relation between the coefficients in the two cells obtained by matching the average values of the wave function and of its normal derivative over each face in a unit cell. In general, this gives twelve different values for the ratio, one each for function and derivative on each of six faces, and deviations among these values give some estimate of the accuracy. This is illustrated in table 2 which gives the coefficients for the level Γ'_4 with varying numbers of terms in the expansion of ψ in each cell.

Table 2. Coefficients of Base Functions for Γ'_4 Level

	Pb-cell				S-cell			
	δ_1	δ_3	δ_5	δ'_5	δ_1	δ_3	δ_5	δ'_5
Variation Procedure	0·473	0·233			—0·847	—0·075		
	0·472	0·228	—0·003		—0·848	—0·075	0·005	
	0·425	0·254		—0·046	—0·864	—0·077		0·027
	0·431	0·285	0·020	—0·035	—0·849*	—0·099	—0·012	0·027
Legendre Matching	0·465	0·222			—0·852	—0·094		
	0·475	0·225	0·007		—0·845	—0·103	—0·009	
	0·401	0·255		—0·039	—0·874	—0·094		0·028
	0·429	0·259	0·013	—0·037	—0·857	—0·110	—0·011	0·027

* There are only two non-equivalent faces for this value of **k**, and the ratio given between the δ_1 coefficients in the two cells is the mean of

equating the average of ψ on x=constant : —1·962,
equating the average of ψ_n on x=constant : —1·986,
equating the average of ψ on y=constant or z=constant : —1·998,
equating the average of ψ_n on y=constant or z=constant : —1·947.

It is clear from tables 1 and 2 that the matching conditions employed in previous work (in this case matching of Legendre coefficients, see Bell *et al.*, *loc. cit.*, p. 82) and the variation procedure lead to practically the same results; it appears that the variation procedure converges more rapidly to the correct energy. It should be mentioned that if very few terms are included in the wave function, the determinant of eqn. (10) may not vanish for any value of λ.

As an illustration of the calculation of the slope of the $E-\mathbf{k}$ curves by eqn. (14), table 3 gives some values of $dE(k)/dk_x$ for the Δ_1 valency band at various points in the (α, 0, 0) direction.

Table 3. Values of $\partial E/\partial k_x$

PbS—Valency band. $\mathbf{k}=(\alpha, 0, 0)$. Δ_1 symmetry

$\lvert S-L\rvert\,\alpha$	0	0·74	1·151	1·341	1·596	1·81	π
E	−0·004	0·03	0·06	0·06	0·03	0	−0·11
From eqn. (14)	0	0·37	0·14	−0·53	−0·77	−0·74	0
From E–k curve	0	0·4	0·2	−0·3	−0·8	−0·8	0

§ 5 CONCLUSION

The variation principle discussed in this paper throws some light on the method used by Howarth and Jones (1952) in their calculation of the energy levels of sodium. They obtain their best values of λ and A_{ps} by point matching conditions on the boundaries of the unit cell, and then substitute in what is effectively (7) to determine $E(\mathbf{k})$ by the condition that J shall vanish. The difference between λ and $E(\mathbf{k})$ is used as a criterion for the accuracy of the wave function. In the present paper it is suggested that the stationary property of J gives a better method of obtaining the energy and coefficients than any necessarily arbitrary matching conditions. With the same number of terms in the expansion of ψ, the numerical labour is greater than that required in point matching: it has been found, however, that a smaller number of terms is necessary to obtain the same degree of approximation. Because of this and of the ease of obtaining $\nabla_{\mathbf{k}}E(\mathbf{k})$, the variation procedure, besides being more general and rigorous, appears to be of considerable practical value.

The authors would like to thank Dr. G. G. Hall of St. John's College, Cambridge, for a very illuminating discussion on the variation principle, and colleagues at R. R. E. for helpful comments. Acknowledgment is also made to the Chief Scientist, Ministry of Supply, and the Controller of Her Majesty's Stationery Office, for permission to publish this paper. Crown copyright reserved.

REFERENCES

BELL, D. G., HUM, D. M., PINCHERLE, L., SCIAMA, D. W., and WOODWARD, P. M., 1953, *Proc. Roy. Soc.* A, **217,** 71.

BOUCKAERT, L. P., SMOLUCHOWSKI, R., and WIGNER, E., 1936, *Phys. Rev.*, **50,** 58.

HOWARTH, D. J., and JONES, H., 1952, *Proc. Phys. Soc.* A, **65,** 355.

KOHN, W., 1952, *Phys. Rev.*, **87,** 472.

VON DER LAGE, F. C., and BETHE, H., 1947, *Phys. Rev.*, **71,** 612.

XIII. CORRESPONDENCE

The Propagation of Heat in Liquid Helium

By J. M. Ziman
Clarendon Laboratory, Oxford*

[Received October 30, 1953]

The results of experiments to measure the velocity of second sound in He II below about 0·5°K have not proved easy to interpret. It has been suggested (Gorter 1952, de Klerk, Hudson and Pellam 1953, Atkins 1953, Mayper and Herlin 1953) that true second sound does not exist at the very lowest temperatures in pure ^{4}He, and that the observed propagation of heat pulses is due to the scattering of phonons by the walls of the apparatus. There does not, however, seem to have been any quantitative consideration of the effects to be expected if this interpretation is correct, for comparison with experiment. This may be because of the mathematical complexity of the problem, and the labour required to obtain a general exact solution. But it may not be generally realized that a reasonable approximate solution can be obtained very simply for the case of a tube which is long compared with its diameter.

The essence of the argument is that we may neglect those processes in which the phonons reaching the detector have made few collisions with the walls of the apparatus. Since their wavelengths are small, the phonons will presumably be scattered at random, and the problem can be reduced to a complicated variant of the problem of the ' random walk ', with the appropriate probability distribution functions. But it is known (Chandrasekhar 1943) that, in the limit of many collisions, this problem may be reduced to the solution of a diffusion equation,

$$\frac{\partial T}{\partial t} = D\frac{\partial^2 T}{\partial x^2},$$

for the temperature T, which is equivalent to the phonon flux, at any point of the surface of the tube. This equation may evidently be identified with the equation of heat conduction, and comparison with Casimir's analysis (1938) for the boundary scattering thermal resistance of a cylinder of radius R, shows that $D=2vR/3$, where v is the mean phonon velocity in the medium. Again, as a reasonable approximation, to avoid mathematical complications, we consider an infinite tube, ignoring the end effects which would presumably correspond to scattering of the phonons back and forth along the length of the tube, i.e. reflection of the received pulse.

---

* Communicated by M. H. L. Pryce.

It is then easy to show (e.g. Sneddon 1951) that the temperature $T(x, t)$ at time t at a point distant x from the origin is given by

$$T(x, t) = \frac{2}{\sqrt{\pi}} \int_{x/\sqrt{(4Dt)}}^{\infty} T(0, t - x^2/4D\eta^2)\, e^{-\eta^2}\, d\eta,$$

where $T(0, t)$ is the temperature at the origin at time t (>0) and the tube is initially at zero temperature throughout. For a square pulse, of height T_0 and length t_0, applied at the end of a section of length L, we have

$$T(L, t) = T_0[\operatorname{erf}\{(\tau - \tau_0)^{-1/2}\} - \operatorname{erf}\{\tau^{-1/2}\}],$$

where $\tau = 8Rvt/3L^2$ and $\tau_0 = 8Rvt_0/3L^2$. In the limiting case of a very short pulse, we obtain

$$T(L, t) \propto \tau^{-3/2} \exp(-1/\tau).$$

It will be seen from the figure, in which the cases $\tau_0 \to 0$ and $\tau_0 = 0{\cdot}2$, $0{\cdot}5$ have been plotted, that the pulses are similar in shape (having been reduced to the same maximum ordinate).

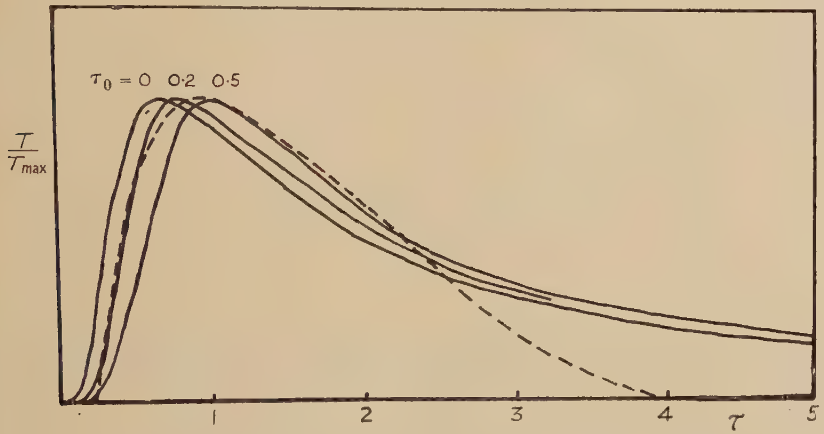

——— Pulse shape calculated for $\tau_0 \to 0$, $\tau_0 = 0{\cdot}2$, $\tau_0 = 0{\cdot}5$
– – – – Observed pulse shape (Atkins and Osborne).

For comparison, the shape of the pulse observed by Atkins and Osborne (1950) is also plotted on the same scale, and it will be seen that it agrees quite closely with that predicted with the present theory. In their case we have $L = 3{\cdot}4$ cm, $2R = 0{\cdot}5$ cm, and $t_0 = 100\,\mu$sec, so that $\tau_0 = 0{\cdot}14$ (taking v equal to $2{\cdot}37 \times 10^4$ cm sec^{-1}). The leading edge lies very close to the curve which has been plotted for $\tau_0 = 0{\cdot}2$, but there is a considerable discrepancy in the shape of the tail, although here the experimental curve is difficult to measure against the background of noise.

The approximation is valid only when $2R/L$ is rather small; otherwise the main contribution to the observed pulse comes from phonons which have made very few collisions, and their arrival times are no longer governed mainly by the random scattering process. In this case, also, the replacement of the exact binomial distribution in the solution of the random walk problem by continuous functions derived from Stirling's approximation tends to bring the leading edge too far forward. An alternative approximation is easily obtained for the other limiting case, in which the tube is very short compared with its diameter, so that most of the phonons pass directly between the source and the detector, but this configuration does not seem to have been used in any of the experiments.

This note arose out of discussions with Professor H. A. Fairbank and Dr. J. Wilks.

References

Atkins, K. R., 1953, *Phys. Rev.*, **89,** 526.
Atkins, K. R., and Osborne, D. V., 1950, *Phil. Mag.*, **41,** 1078.
Casimir, H. B. G., 1938, *Physica*, **5,** 495.
Chandrasekhar, S., 1943, *Rev. Mod. Phys.*, **15,** 1.
de Klerk, D., Hudson, R. P., and Pellam, J. R., 1953, *Phys. Rev.*, **89,** 326.
Gorter, C. J., 1952, *Phys. Rev.*, **88,** 681.
Mayper, V., and Herlin, M. A., 1953, *Phys. Rev.*, **89,** 523.
Sneddon, I. N., 1951, *Fourier Transforms* (New York : McGraw-Hill), p. 167.

Optical Determination of the Thickness of the Unsaturated Helium II Film

By N. G. McCrum and K. Mendelssohn, F.R.S.
Clarendon Laboratory, Oxford *

[Received November 12, 1953]

The thickness of the saturated helium film has been measured by Burge and Jackson (1951) using an optical method based on the influence of surface layers on metallic reflection. In this laboratory volumetric experiments have recently been made on the isothermal formation on glass surfaces of the unsaturated film with increasing pressure (Brewer and Mendelssohn 1953). These have now been supplemented by optical measurements with percentage saturations varying between 60 and 100%.

The method used was essentially similar to that of Burge and Jackson† (*loc. cit.*), but required certain modifications in our case. In order to study the formation of the film, the mirror had to be enclosed in a separate adsorption chamber which in turn was immersed in a bath of liquid helium II of constant temperature. Since the unsaturated film is considerably thinner than the saturated, great care had to be taken to screen it, when under measurement, from extraneous light. The beam was admitted to the apparatus by means of a small shutter in short bursts usually of less than two seconds duration. Balances were always finally checked by observing the instantaneous half field matching on opening the shutter. This procedure was repeated several times for each point, the experimental scatter in the analyser nicol reading being usually under ±2′ of arc. The illuminated portion of the mirror was moreover only a small fraction ($\sim 10^{-3}$) of the total surface carrying the film. Thus any evaporation of film from the observation area could be made good rapidly by superflow from the unilluminated part. Since the percentage saturation in the adsorption chamber is a rapidly varying function of temperature, the latter had to be kept accurately constant.

---

* Communicated by the Authors.

† We are greatly indebted to Dr. L. C. Jackson and Dr. E. J. Burge for much advice.

Fig. 1

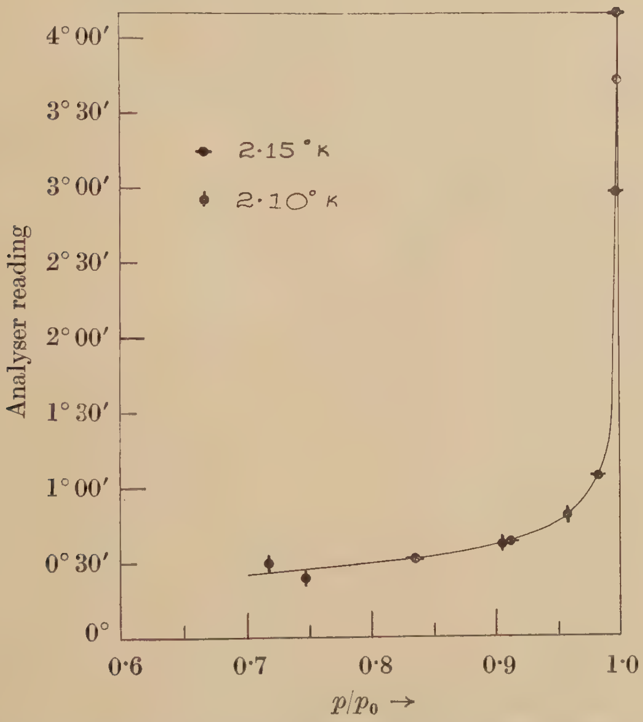

The difference between the analyser reading and an arbitrary fixed position against relative saturation. The quarter wave plate fast axis orientation with respect to the vertical was 134° 33′ at 1·84°K and 127° 10′ at 1·87°K.

This was particularly essential close to saturation where the film thickness is strongly dependent on pressure. By keeping the temperature constant to better than 0·0005°K during all observations leading to an experimental point, reproducible results were obtained.

The results for four different temperatures expressed in nicol rotation, are plotted in figs. 1 and 2. As these graphs show, the thickness was found to be a rapidly increasing function of relative saturation (p/p_0) for $0{\cdot}95 < p/p_0 < 1{\cdot}0$. This is in good agreement with the volumetric adsorption measurements (Long and Meyer 1949, Frederikse and Gorter 1950, Brewer and Mendelssohn 1953, Strauss 1953 (cf. Long and Meyer 1953)), which though differing in other respects all give a very steep increase in coverage just below saturation. The same behaviour was found by Bowers (1953), using a gravimetric method. It is interesting to note that measurements of superflow of the unsaturated film (Bowers, Brewer and Mendelssohn 1951) indicate that even at the lowest temperatures measured (1·37°K) the ratio of the unsaturated to the saturated flow rate is less than 0·1 for $p/p_0 < \sim 0{\cdot}9$. Any temperature dependence for $p/p_0 < 1{\cdot}0$ for values of $T < T_\lambda$ was too small to be resolved in these experiments. A more detailed account of the work which is being continued will be given at a later date.

Fig. 2

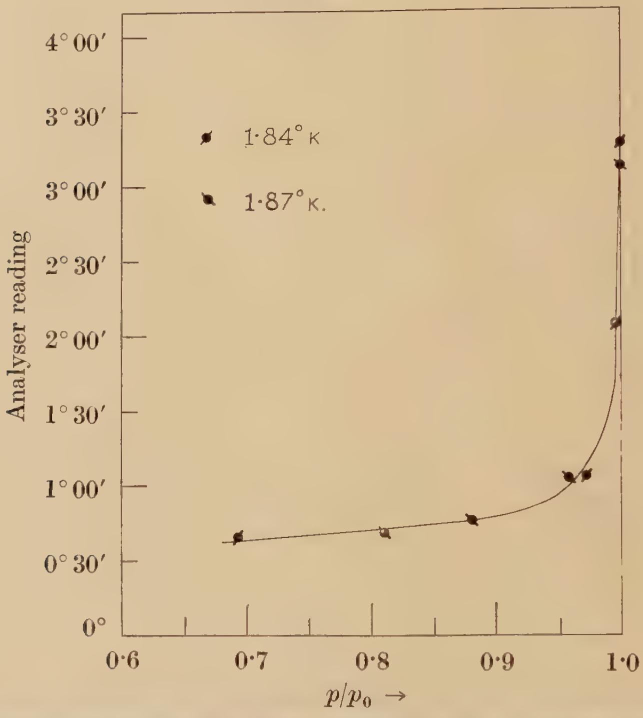

The difference between the analyser reading and an arbitrary fixed position against relative saturation. The quarter wave plate fast axis orientation with respect to the vertical was 133° 27′ at 2·1°K and 130° 00′ at 2·15°K.

REFERENCES

BREWER, D. F., and MENDELSSOHN, K., 1953, *Phil. Mag.*, **44,** 340.
BOWERS, R., 1953, *Phil. Mag.*, **44,** 485.
BOWERS, R., BREWER, D. F., and MENDELSSOHN, K., 1951, *Phil. Mag.*, **42,** 1445.
BURGE, E. J., and JACKSON, L., 1951, *Proc. Roy. Soc.* A, **205,** 270.
FREDERIKSE, H. P. R., and GORTER, C. J., 1950, *Physica*, **16,** 402.
LONG, E. A., and MEYER, L., 1949, *Phys. Rev.*, **76,** 440; 1953, *Advances in Physics*, **2,** 1.

Fig. 1

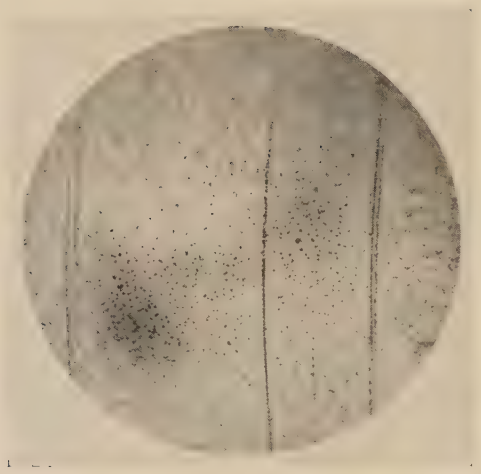

×200

Fig. 2

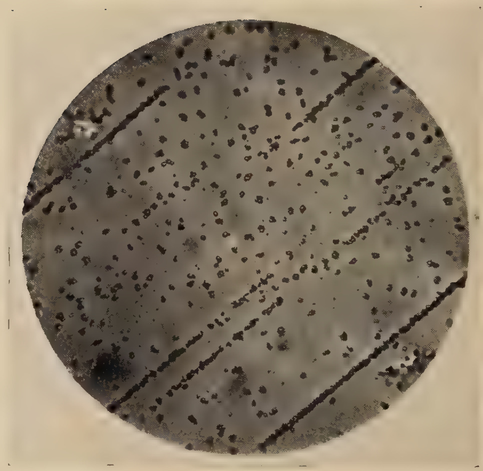

×400

Fig. 3

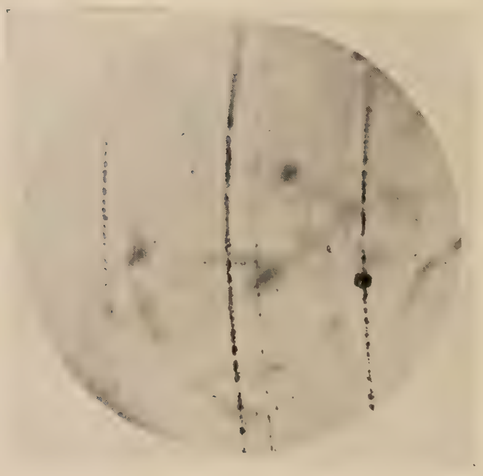

×1000

Fig. 4

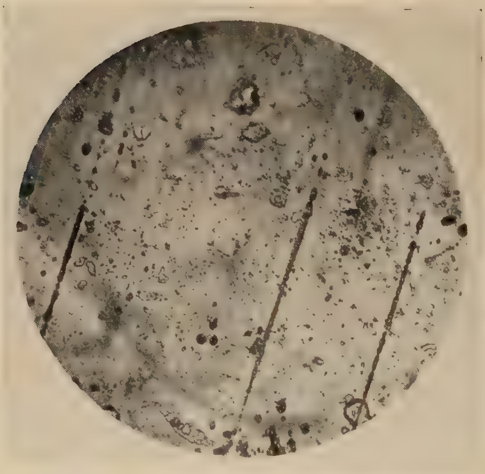

×200

Slip Lines, Etchpits and Corrosion-pits

By A. H. Abdou
Department of Metallurgy, Sir John Cass College, London, E.C.3*

[Received October 29, 1953]

It has been shown recently that by rapid etching of crystals the centre of each isolated spiral growth arising from an independent screw dislocation is replaced by an etchpit (Horn 1952). This technique for revealing dislocations in crystals depends on the differential rates of chemical attack of a dislocation and good crystal.

Before this relation between a dislocation and an etchpit was discovered, the grouping of etchpits was used to reveal crystallite boundaries (Lacombe 1948) and polygonization walls (Cahn 1949). Amelinckx (1953) was the first to attempt the use of this technique in finding correlation between dislocations and slip lines in aluminium. He found that etchpits grouped themselves preferentially along slip lines and certain grain boundaries in addition to a general random distribution.

Similar observations have been made by the writer on single crystals of high purity zinc (99·99%) grown from the melt. These were electrolytically polished in 20% chromic acid and then deformed in tension. Some crystals were left in the laboratory atmosphere and others were etched in 20% chromic acid for various periods. In the first case it was found that corrosion pits rapidly developed on the surface and their positions can be distinguished along slip lines and at random. Figure 1 (figs. 1-4, Pl. 1) is of a crystal left for 12 hours in the laboratory atmosphere and fig. 2 is of another crystal after 36 hours.

In the case of etching, however, it was found that if the attack is rapid enough etchpits group themselves along slip lines *only* leaving the rest of the surface free of them as shown in fig. 3. Figure 4 shows the effect of prolonged etching ; existing etchpits on slip lines are deepened while new ones develop at random.

This work is now being extended to find a correlation between the distribution of etchpits and the slip displacement and to investigate whether slip originates near the surface or in the interior of the crystal.

References

Amelinckx, S., 1953, *Phil. Mag.*, **44,** 1048.
Cahn, R. W., 1949, *J. Inst. Metals*, **76,** 121.
Horn, F. H., 1952, *Phil. Mag.*, **43,** 1210.
Lacombe, P., 1948, *Report on the Strength of Solids* (London : Physical Society), p. 91.

---

* Communicated by the Author.

XIV. *Notices of New Books and Periodicals received*

Crystal Growth and Dislocations. By Ajit Ram Verma. (London Butterworths Scientific Publications, 1953.) [Pp. 182.] Price 30*s*. net.

Errors and omissions excepted, this is a valuable and timely little book. It is based on a Ph.D. thesis, and displays the merits and demerits of such works. The portions of the subject with which the author was most intimately concerned are generally well presented. The remainder is compiled from the best authorities, and usually condensed merely by the omission of steps, which does not introduce error, but may leave the reader uncertain about the degree of reliability of a conclusion. When the author adds or substitutes his own arguments, the result can be disastrous. Like others before him (Wulff included), he devises a short ' proof ' of Wulff's theorem which is no proof at all. His particular fallacy is the assumption that two n-dimensional vectors orthogonal to a third are necessarily parallel to each other. There is fortunately a reference to the correct treatment by von Laue (1943). Minor errors of argument occur not infrequently: however the statement on page 28 that a left-handed screw can be changed into a right-handed screw by a rotation should serve as a sufficient reminder that critical reading is necessary. The main point is that there has recently been a decisive advance in the understanding of crystal growth, and that silicon carbide, the principal material of Dr. Verma's researches, exhibits a greater variety of the newly comprehended phenomena than any other substance, together with a few that have yet to be understood. This documentation of the subject should be of real value to all for whom crystal growth or crystal surfaces are of importance.

The principal blemish of the book appears to be accidental. It contains a considerable number of photographs and drawings provided by other authors. With one exception their names do not appear in the legends, and they cannot in general be easily discovered from the text.* The preface states that a complete list of acknowledgments will be found on p. xii. On examining this page (which carries no names) it appears that it is a list of Journal references for the author's own re-published illustrations, with the addition of only two references to the work of others. Presumably the wrong list has been printed. Publisher and author must both be held to blame for allowing this very regrettable lapse to occur.

F.C.F.

The Mathematical Theory of Non-uniform Gases. By S. Chapman and T. G. Cowling. 2nd edition. (Cambridge: University Press.) [Pp. 431.] Price 60*s*.

The second edition of this standard text book in theoretical physics is almost identical with the 1939 edition, apart from 25 pages of added material to account for more recent developments. The added pages deal with the viscosity on the basis of the r^{-7}, r^{-13} model, with various aspects of diffusion and thermo-diffusion, with a third order approximation of the velocity distribution function. They also contain some consideration of the work of Kirkwood and Born and Green on the theory of liquids.

D.P.

Radioactivity and Radioactive Substances. By Sir James Chadwick. [Pp. 120.] (Isaac Pitman.) Price 12*s*. 6*d*.

This is the fourth edition of a simple, concise and accurate statement of the main facts and theories of the subject. It first appeared in 1921, but has now been revised and supplemented by Professor J. Rotblat.

---

* *Publisher's Note.*—This error was noticed and the necessary correction slip has been printed for insertion in the book.

Scintillation Counters. By J. B. Birks. (Pergamon Press Ltd., London.) [Pp. viii+142+index; 59 diagrams, 4 plates.] Price 21*s*.

On the jacket it is claimed that this book forms a complete review, that all factors are discussed, that a new theory is presented in detail, that every major application is reviewed, that the references are exhaustive and completely up to date and that the treatment is wholly new. However, the reader will be relieved, on proceeding further, to find that the book takes the normally expected form, except perhaps in a limited number of respects. Thus it is possible that the phrase "wholly new" refers to the author's advocacy in chapters 6 and 7 of the so-called photon exchange mechanism of energy migration in the fluorescence of organic substances. Here the author's intention is to propagate vigorously the view that this mechanism (one of four recognized mechanisms of migration) and no other is involved. The possibility that two or more of the mechanisms might occur simultaneously in the rather complex phenomena of fluorescence apparently is not considered. It is difficult to agree that the author's views are established. He dismisses rather too readily work which does not fit into the proposed scheme. He has given a detailed account of his own experiments, performed and to be performed.

Where the author is not concerned with photon exchange the book is well and concisely written with numerous, but not exhaustive, references. The first five chapters constitute a good condensed account of the main factors involved in scintillation technique. There are, however, dangers to the uninitiated in this condensation as for example in the diagrams for the energy distributions of secondary ionizing particles produced in scintillators by γ-rays and fast neutrons. These depend greatly on the size of the scintillator which may range in practice from a few mm^3 to several cubic feet. Just over three pages are specifically devoted to consideration of the luminescence process in inorganic phosphors, a difficult and extensive field meriting longer discussion. Information on crystal growing is scanty and there is no separate treatment of circuitry problems arising in the use of very fast crystals and liquids. It is doubtful if the somewhat controversial treatment of energy migration can be justified in view of such brevity.

The book is for the most part a useful and compact survey of much of the field of scintillation technique and its presentation of factual material is sound if somewhat over-condensed. When the author departs from such presentation to suggest improvement in the work of others the result is less happy as on page 117 where it appears that he misunderstands the method of fast neutron spectrometry under discussion.

"The miraculous speed of publication" is contrasted with that of certain scientific journals but such a criticism of the journals will appear unwarranted to most readers at this time. In any case the problems are rather different in the two cases and comparison will be valid only if each member of the series of monographs appears equally speedily.

The book is likely to prove useful to nuclear physicists rather than to those in other sciences where the chief task, generally speaking, consists in using the technique to its best advantage in a particular set of circumstances.

S. C. C.

Methods of Mathematical Physics. Vol. I. By R. Courant and D. Hilbert. (Interscience Publishers, Inc.) [Pp. 561.] Price $9.50.

This is a very welcome translation (and slight revision) of the well-known German book. It treats such topics as Linear Integral Equations, the Calculus of Variations, and Eigenvalue Problems in a manner which is useful to both the mathematician and the physicist. It is to be hoped that the translation of Volume II will also be available soon.

R. W.

The Theory of Metals. By A. H. Wilson. 2nd edition. (Cambridge: University Press.) [Pp. 346.] Price 45*s*.

This book looks altogether different from the first edition dating from 1936. A great number of recent developments in the theory have been incorporated, causing a considerable increase in size of the volume. The chapters on the formal theory of conduction and the mechanism of conductivity have benefited from Dr. Sondheimer's contributions to the theory. Conduction in semiconductors receives due attention. A chapter on ferromagnetism gives an account of the collective electron theory of ferromagnetism. The diamagnetism of free electrons is dealt with in a new way, but one has to consult the first edition for the expressions for the diamagnetism of electrons in a periodic field. A minor point for criticism in this part of the book is that no mention is made of the importance of the 'thermodynamics of irreversible processes' in connection with certain symmetry relations and the derivation of the Kelvin relations in thermoelectricity.

Since the emphasis in Wilson's book is on the formal rather than the physical aspect of the theory, it is somewhat disappointing that no great improvements have been made in the chapters dealing with the band theory of solids. The systematic discussion of the zone-theory of three-dimensional lattices on the basis of the reduced zone picture is completely absent. Brillioun zones are discussed with reference to structure factors, but it is not clearly pointed out that this is only significant for those solids in which the free electron approximation is a good one. Strictly speaking the discussion of the diamond structure is incorrect, while the suggestion implied in the information on the (non integral) number of electrons in the first zone of more complicated structures is very misleading.

The optical properties of metals are not discussed in the second edition and superconductivity is also left out. This is in line with the apparent intention of the author, not to touch upon subjects of which the present theory is still highly unsatisfactory. There is no doubt that the edition will be a most useful textbook, especially for the detailed theory of conductivity. D.P.

Chemical Constitution. An Introduction to the Theory of the Chemical Bond. By J. A. A. Ketelaar. [Pp. 398.] (London: Elsevier Publishing Co.) Price 40*s*.

This book is a very good translation by Dr. L. C. Jackson of the second Dutch edition (1952). Although the contributions of the Dutch school of physical chemistry to the study of chemical combination has most notably been concerned with ionic bonding, the present book is not overweighted in this direction. The nature of ionic bonding is, of course, well treated, and covers a variety of topics, including ionic complex formation, volatility, hardness and solubility. Quantitative illustrations are largely restricted to those instances where the bonds may reasonably be regarded as purely ionic.

The chapters on covalent bonding are rather more conventional and include a discussion of colour, free radicals, and chemical reactivity with a brief mention of recent work on electron deficient structures.

The last two sections of the book are concerned with metallic and van der Waals binding. The former is briefly but clearly treated with some reference both to alloys and to semi-conductors. The latter is discussed very well and is related to the subjects of molecular compound formation, melting and boiling points, miscibility and solubility. Hydrogen bonding is included in this section.

In general the presentation is likely to stimulate the reader to further thought and, at a not excessive price, the book can be recommended to both honours students and research workers. G. E. C.

Introduction to Solid State Physics. By C. KITTELL. [Pp. 396.] (London: Chapman and Hall.) Price 50*s*.

THE scope of this book can best be illustrated by a summary of its contents. The first 90 pages deal with crystal structure, lattice energies and thermal capacities; 110 pages follow on dielectric and magnetic properties of crystals; 100 on electrical properties; 50 on imperfections in solids, including firstly Frenkel defects and related topics, and secondly dislocations and mechanical properties. Finally there are 50 pages of Appendices elaborating some of the more mathematical points.

In his preface, the author gives an impressive list of seventeen topics that have been omitted, and explains that those subjects have been favoured which can be discussed in terms of simple, concrete, and well-developed models. Even so, the result is a highly condensed piece of writing which can be called an ‘ Introduction ’ only in virtue of an excess of modesty on the part of the author. Lack of space has prevented the inclusion of the experimental details relating to the phenomena dealt with. But further than this, it is assumed that the reader has a fair knowledge of the results of such experiments, and the discussion proceeds almost immediately to a consideration of models which will account for these results. The emphasis here is rather on the mathematical development, than the underlying physical concepts.

The book is clearly written and well documented; it will prove invaluable to many readers—not least to those who have to prepare lectures on its subject matter. But to imply, as is done in the preface, that it constitutes a text-book suitable for students, either just before or just after graduation, is to suggest a standard of attainment in American Universities a good deal higher than in their British counterparts—a conclusion which could not be supported by most people in a position to judge. N.T.

The Outer Layers of a Star. By R. v. d. R. WOOLLEY and D. W. N. STIBBS. [Pp. xi+303.] (Oxford: Clarendon Press, 1953.) 40*s*. net.

A CONSIDERABLE body of knowledge has grown up, especially during the past thirty years, about those outer layers of the stars which we can see. The subject shares most of the complications of meteorology, as well as the characteristic difficulties of astronomy, but there is by now general agreement on much observational material and on the usefulness of a substantial body of theory, although most workers in this field would readily admit that the real stellar atmospheres are far more complicated than our present pictures or models. For many years there has been a need for a general book in English on the subject, not too difficult or specialized, and this volume may go some way towards meeting the demand.

The mathematical techniques involved in the theory of stellar atmospheres have already been thoroughly treated in two other of the Oxford Monographs on Physics, those by Chandrasekhar and by Kourganoff and Busbridge respectively. Although *The Outer Layers of a Star* pays more attention to the physical problem than these other books, the general emphasis in my opinion could with profit have been shifted still more in this direction. Important progress in this subject during the past twenty years has come predominantly from new physical methods and ideas, and the big obstacles to further advances are still essentially physical. The book deals with a great many of the standard problems, although certain irregular phenomena such as sun-spots, flares, prominences, etc. have been specifically excluded. There is surprisingly little attention paid to the question of the chemical composition of stars, although spectrum analysis of their outer layers is our chief source of extra-terrestrial information. The style of writing is clear and there are sufficient references to guide the reader to the more important literature. The printing is excellent.

R. O. R.

Experimental Nuclear Physics, Vol. II. Edited by E. Segré. (Chapman and Hall.) [Pp. 600.] Price 96*s*.

This is the second volume of a comprehensive treatise aiming to bring the experimentalist up to date in techniques, and indicate the broad lines of theoretical interpretation. Its bibliography is complete up to the end of 1952 in the two fields with which this volume is concerned, namely (i) a survey of nuclear reactions, and (ii) the neutron. The third volume is announced to be in preparation.

Flames, their Structure, Radiation and Temperature. By A. G. Gaydon and H. G. Wolfhard. (Chapman & Hall, 1953.) [Pp. 352.] Price 55*s*.

Flames are regions where energy changes form as rapidly as Proteus, and they are equally fascinating to the scientist and the engineer. The chemist wants to know the steps in the reactions, the intermediate products and the degree to which equilibrium is reached, the physicist wants to understand the way energy is released and distributed and the effects of the flame on flow. The engineer on the other hand wants to be able to produce a given heat release in a certain space which may be large or small, and to give the resulting flame certain heat transfer characteristics which may be high or low emissivity coupled with high or low convection coefficients. Gaydon and Wolfhard look at flames primarily as physicists, secondarily as chemists and tertiarily as engineers. For this reason they are most interested in the stationary non-turbulent premix flame typified by the Bunsen burner, because it can be most readily explored by physical techniques. Of these techniques, spectroscopy has in their hands made an outstanding contribution to the physical understanding of the energy release processes, especially when applied to premix flames at low pressures which have a much thicker flame front than those at atmospheric temperatures. Laminar diffusion flames have a chapter and the effect of turbulence on both premix and diffusion flames are considered, but clearly the difficulties in the way of obtaining fundamental understanding of the physical and chemical processes are much greater in these cases than with the simple premix flame, which has a characteristic burning velocity. Propagating and explosion flames are not covered at all except where they are of interest as providing another method of measuring burning velocity.

An illustration of the authors viewpoint is provided by the fact that the combustion of powdered coal which is responsible for a large and increasing proportion of all the electricity made in this country, is mentioned (p. 310) under the heading "Some unusual flames". Nevertheless, no engineer can afford to ignore the very real progress in understanding which is coming from the study of the simple Bunsen flame, while physicists must welcome the fact that flames are emerging from the natural history stage and becoming regions to which physical formulae can be applied as instructively as they were applied to simple gases at very low pressures in the first decades of this century.

Gaydon and Wolfhard's book can be strongly recommended as an excellent review of our present state of knowledge in its chosen field, both describing in fair detail the experimental methods used for producing the flames, measuring flow temperature (two chapters), spectral radiation characteristics, and ion concentrations and the theories for flame shape, reaction stages, flame propagation, soot formation, and energy liberations. The experimental evidence is carefully studied and wherever possible conclusions are drawn as to which theory gives the best agreement with this evidence, although naturally, in such a developing subject many rival theories remain in the field. M. W. T.

[*The Editors do not hold themselves responsible for the views expressed by their correspondents.*]